EFFECTS OF CURTAIN WALL FAÇADE ON THE DYNAMIC PROPERTIES OF A BUILDING

by

Nusret Sözüer

B.S., Civil Engineering, Dokuz Eylül University, 2012

Submitted to Kandilli Observatory and Earthquake Research Institute
in partial fulfillment of the requirements for the degree of
Master of Science

Graduate Program in Earthquake Engineering

Boğaziçi University

2017

ACKNOWLEDGEMENTS

I would like to express my sincere thanks to my thesis supervisors Prof. Dr. Erdal Şafak and Assoc.Prof.Dr. S. Ümit Dikmen for their guidance through the study and their assistance in preparing my thesis.

In addition, I would like express my gratitude and appreciation to the owners of the building for allowing me to instrument their building for the purposes of my research. In that respect, I would also like to thank Mr. Murat Sönmez (MSc), project manager of the building construction, for his assistance and support in placing the recording instruments. I also like to express my deep appreciation and gratitude to Mr. Ahmet Korkmaz of KOERI for his endless energy and meticulous work in instrumenting the building without which this study could not be realized.

ABSTRACT

EFFECTS OF CURTAIN WALL FAÇADE ON THE DYNAMIC PROPERTIES OF A BUILDING

In recent decades the number of high-rise buildings in Turkey has increased considerably and still growing in number at a high pace. However, there is very limited research on the in-situ behavior of these buildings in Turkey. On the other hand, the emergence of system identification techniques developed especially in the second half the last century provides the possibility of identification of the dynamic properties of buildings through the use of seismic noise recording. The objective of this study is the determination of dynamic parameters of a high-rise building at Maslak, Istanbul prior to and after the installation of the curtain wall façade and interior finishes.

In the study, the dynamic characteristics (natural frequencies and mode shapes) were identified using well-known spectral analyses and Frequency Domain Decomposition (FDD) methods. The real-time modal frequencies are estimated by using basic signal processing tools such as baseline correction, band-pass filtering, windowing, FFT, smoothing and decimation. The real-time damping is estimated with half-power bandwidth technique. For this purpose, data validation is done through a series of MATLAB codes developed to perform the main signal processing. The developed MATLAB codes have been tested with the ambient vibration data set recorded from the monitoring structure. Modal properties of the structure have been identified successfully in real-time. Results of the monitoring building test have been compared with finite element model. This study underlines how fundamental and torsional frequencies as well as damping properties vary for the different stages of construction mentioned above.

ÖZET

CAM GİYDİRME CEPHENİN BİNANIN DİNAMİK ÖZELİKLERİ ÜZERİNDEKİ ETKİLERİ

Son on yılda Türkiye'de yüksek binaların sayısı önemli ölçüde artmış ve sayıları gittikçe artmıştır. Bununla birlikte, Türkiye'de bu binaların yerinde davranışı üzerine çok sınırlı araştırma bulunmaktadır. Diğer yandan, geçen yüzyılın ikinci yarısında özellikle geliştirilen sistem tanımlama tekniklerinin ortaya çıkışı, sismik gürültü kaydı kullanarak binaların dinamik özelliklerinin belirlenmesi imkânı sağlıyor. Bu çalışmanın amacı, Maslak'taki bir yüksek katlı binanın cam giydirme cephesinin kurulumundan önce ve sonrasında dinamik parametrelerinin belirlenmesidir.

Çalışmada, dinamik özellikler (doğal frekanslar ve mod şekilleri) iyi bilinen spektral analizler ve FDD (Frequency Domain Decomposition) yöntemleri kullanılarak tanımlandı. Gerçek zamanlı mod frekansları, taban çizgisi düzeltme, bant-geçirgen filtreleme, Fourier dönüşümü, düzleştirme ve azaltma gibi temel sinyal işleme araçlarını kullanarak tahmin edildi. Ayrıca, ivme verileri belli örtüşme oranıyla pencerelere bölündü ve frekansa bağlı olarak her pencere için hızlı Fourier dönüşümü uygulanarak her pencere için Fourier genlik spektrumları oluşturuldu. Gerçek zamanlı sönüm, half-power bandwidth tekniği ile tahmin edilmiştir. Bu amaçla, veri doğrulama, ana sinyal işlemeyi gerçekleştirmek için geliştirilen bir dizi MATLAB kodu vasıtasıyla yapıldı. Geliştirilen MATLAB kodları, incelenen yapıdan kaydedilen ortam titreşim veri seti ile test edilmiştir. Yapının modal özellikleri gerçek zamanlı olarak tespit edilmiştir. İncelenen yapı testinin sonuçları sonlu elemanlar modeli ile karşılaştırılmıştır. Bu çalışma, yukarıda sözü edilen yapının farklı aşamalarında temel ve burulma frekanslarının ve sönümleme özelliklerinin nasıl değiştiğini göstermektedir.

TABLE OF CONTENTS

LIST OF FIGURES

LIST OF TABLES

LIST OF SYMBOLS/ABBREVIATIONS

E	Young's modulus of elasticity
EW	East-west
FAS	Fourier Amplitude Spectra
FDD	Frequency Domain Decomposition
f_n	Natural cyclic frequency
f_{res}	Resonant frequency
FRF	Frequency Response Function
G_{xx}	Power Spectral Density matrix of the input
G_{yy}	Power Spectral Density matrix of the output
H	Complex conjugate
K	Stiffness matrix
M	Mass matrix
n	Mode number
NS	North-south
PSD	Power Spectral Density
R_k	Residue matrix
SFAS	Smoothed Fourier Amplitude Spectra
SNR	Signal-to-noise ratio
SVD	Singular Value Decomposition
S_{xx}	The Power Spectral Density of the signal x
S_{yy}	The Power Spectral Density of the signal y
S_{xy}	The Cross-spectrum Density of x and y
t	Time
T_n	Natural period of vibration
UBC	Uniform building code
UD	Up-down (vertical)
ω	Circular frequency
ω_n	n^{th} natural circular frequency
ϕ_n	n^{th} mode shape
ξ	Damping ratio

1. INTRODUCTION

1.1. Objectives of the Study

In recent decades, the number of high-rise buildings in Turkey has increased considerably and still growing in number at a high pace. These types of civil structures compared to ordinary buildings often times constitute landmarks of the city. However, there is very limited research on the in-situ behavior of these buildings in Turkey. Yet, for the advancement of design techniques, as well as the codes and regulatory provisions, it is important to have study the real life behavior of the constructed structures. This topic is further important for cities like Istanbul where high seismic risks exist.

On the other hand, the advancement of system identification methods and techniques, as well as the development of more sensitive instruments, in the last decades of the 20th century provides the opportunity of identification of the dynamic characteristics of buildings with ambient seismic noise recordings. Using the ambient vibration recordings, one can obtain the dynamic properties of a building. The basic characteristics in which case will be natural frequencies and corresponding mode shapes. Furthermore inter-story drifts and damping ratios can also be estimated.

Subsequently, these techniques are used in "Structural Health Monitoring" (SHM). In this respect, SHM is broadly defined as the process of establishment of a damage detection strategy for engineering structures. Hence, it provides the means for increasing safety, as well as the optimization of operational and maintenance related actions of complex structures. In this respect, SHM is considered to deliver information on the current state of structures by measuring the vibrations of the structure caused mostly by wind and traffic loads and other environmental factors, such as temperature. Thus, for a proper SHM system, there is a need for monitoring the structure continuously by instruments such as acceleration sensors and/or recorders. Since, the dynamic properties, especially the natural frequencies, of structures are associated to their rigidity, it is reasonable to use the alterations in the natural frequencies as a damage detection. In this

respect, the dynamic characteristics determined from in-situ tests can further be used to identify the emergence, as well as the possible location of the damage in the structures. This is usually based on the fact that the damage will cause a loss in the stiffness/rigidity properties of the structure. Consequently, the main objective of the SHM system is to monitor the of changes in the dynamic properties in order to identify and decide if the damage caused is at beyond a predefined threshold for the structure. Thus, for ample reasons the ambient vibration testing is preferred especially for the large structures, instead of the other non-destructive techniques such as forced vibration measurements. Another advantage of the use of ambient forces is that the infrequent occurrence of extreme loads. Hence, the ambient vibration data is useful and appropriate for the identification of the dynamic characteristics in the linear range. The natural frequencies, damping ratios, mode shapes and torsional motion are named by the dynamic characteristics of the structure.

The objective of this study is the determination of dynamic parameters of a high-rise building at Maslak, Istanbul prior to and after the installation of the curtain wall façade and interior finishes. The scope of this study covers the description of the structure and the monitoring system, complimented by a detailed investigation of the dynamic performance of the building as derived from analyses of ambient vibration recordings. Also, the analyses of mathematical models (FEA) were made to compare the dynamic properties with those of the properties using the ambient vibration data analysis.

In the study, the dynamic properties, namely natural frequencies, mode shapes and damping ratios were obtained spectral analyses and Frequency Domain Decomposition (FDD) methods. Studies were conducted for three different stages of the construction separately. This study demonstrates how fundamental and torsional frequencies as well as damping vary for different stages of construction. Subsequently, the frequency variation of building is compared with the variation of construction stages. The real-time modal frequencies are estimated through use of baseline correction, band-pass filtering, windowing, FFT, smoothing and decimation, namely elementary signal processing tools modal frequencies were calculated. The modal damping ratios corresponding to the first transitional and torsional modes were estimated using half-power bandwidth method. The developed MATLAB codes have been checked with the ambient vibration data set recordings. As mentioned earlier, the results obtained have been also compared with FE

model analyses. A good result is acquired with the comparison between the results of the ambient vibration test and the analytical study.

1.2. Scope of the Study

As mentioned above, in this thesis, a study was performed to determine the modal parameters of a 23-storey office building in Maslak, Istanbul using ambient vibration testing techniques. The dynamic properties of the monitored building are estimated by Fourier Amplitude Spectra, Frequency Domain Decomposition, and Spectral Ratio approach.

Acceleration records are divided into one minute segments and the Fourier amplitude spectra of each segment are calculated using windowing. To observe the time dependent properties of the signals, equal length hamming windows with an overlap are used. The data in every window is calculated individually. The sequential analysis results are then averaged to form an output for each running window. This averaging process reduces the effect of noise in the output. The calculated FAS are then smoothed by using running Hamming smoothing windows with optimum lengths. Smoothed Fourier amplitude spectra were computed and plotted for all channels for each data set. In addition, spectral analyses including the computation of cross-spectra, phase and coherence were performed on selected pairs of channels for data sets. Channel pairs were selected to examine repeatability in identification of translational modal frequencies.

The ambient vibration tests were conducted on March 27, 2015, September 13, 2015 and March 16, 2016 by a group of investigators from the Boğaziçi University. These dates also represent the three different stages of the construction. The building was instrumented stations at the third and first basement, the 7^{th} floor, and the roof. The fundamental natural frequencies and mode shapes are the modal parameters studied. The frequency variation of the monitored building is compared with the variation of construction stages and the results are assessed individually. The modal parameters and mode shapes of the structure are determined.

Also, to identify natural frequencies associated the mode shapes and vibration direction, the mode shapes of the first spectral eigenvector at selected natural frequencies are computed using the FDD technique. The results were compared with the results of the FEM analyses. Damping ratios are also estimated using half-power technique and these results are also presented.

Finite element model of the building is developed with SAP 2000 version 16.0 to compare the results obtained from the real data and Finite Element Analysis (FEA). The fundamental frequencies and mode shapes determined are discussed in comparison with those from the real data analysis.

1.3. Organization of the Study

Chapter 2 presents a short assessment of the literature on subjects of structural health monitoring and the development of system identification from vibration records.

Chapter 3 will present the basic methodology carried out in this study for monitoring structures and analyzing the data collected. Brief information about Fourier transformation, natural frequency and eigenvector analysis will also be given.

Chapter 4 will cover a comprehensive presentation of the architecture and the general outline of case study building. Moreover, instrumentation and sensor locations of ambient response measurements at the monitoring building are presented for different construction stages.

Chapter 5 will present and discuss the findings of the study performed on the subject building.

Chapter 6 presents the conclusions of the study.

2. EARLIER STUDIES ON STRUCTURAL SYSTEM IDENTIFICATION USING AMBIENT VIBRATION DATA

System identification techniques using the ambient vibration data has been applied in civil engineering since early 1980's. The methods primarily emerged as tools to identify the dynamic properties of structures by one time data sets. The techniques then got extended to structural health monitoring systems through the use of continuous data recordings. Hence Structural Health Monitoring systems constitute an extended version of the system identification techniques utilizing ambient vibration data.

Doebling *et al*, (1996), primarily on fundamental structural health monitoring subject, presented a comprehensive literature review, summarizing a large number of publications published till 1995. They reviewed and discussed the technical publications covering the detection, location, and characterization of structural damage using techniques examining changes in the vibration response. Furthermore, they categorized the methods according to required measured data and analysis technique that contains changes in modal frequencies and in measured deformation shapes.

Brincker *et al.*, (2000) have presented a novel FDD technique for the system identification of output-only systems. The classical frequency domain including Peak Picking technique provided that the modes are well separated, yields a reasonable approximation of mode shapes and natural frequencies. Yet otherwise, it is difficult to identify the close modes. However, authors' study showed that the response spectrum can be divided into a set of single degree of freedom (SDOF) systems. Then each SDOF will correspond to an individual mode, thus allowing to identify the close modes with high accuracy by frequency domain decomposition technique.

Şafak *et al.,* (2001) studied a number of earthquake records made at different. Their publication demonstrates a summary of the techniques that are generally used to analyze seismic records. The authors stated that a typical study in this respect covers basic data processing, modal identification as well as damage indicator. The authors also explained

that band-pass filter, de-trending and decimation techniques are used during data processing to decrease the effects of noise on the records.

Ventura *et al.,* (2002) presented a general review of the experimental and finite element analysis done a 48-storey reinforced concrete building. The building had an oval-shaped floor plan with a core structure and tuned liquid column dampers placed on the top floor of the building. In their study, authors performed ambient vibration testing on the building and determined the dynamic characteristics such as the translational and torsional natural frequencies of the structure and modal damping ratios. They also computed the fundamental frequencies and mode shapes using two finite element models and compared to the ambient vibration results. For modal identification, they used the FDD technique. Fourier Amplitude Spectra (FAS) were also calculated and frequencies were identified in vertical, lateral, longitudinal directions.

Zhang *et al.,* (2002) performed a system identification study of a 15-storey office structure built in Tokyo using ambient vibration test. Authors used the FDD technique for modal identification. The authors concluded that the FDD technique is a powerful technique for the studies on dynamic response estimation and real time monitoring. They also concluded that the modal characteristics obtained from the ambient response test are in correlation with the finite element model.

Şafak *et al.,* (2005) in their study on the steel-frame UCLA Factor Building have concentrated on the earthquake and ambient vibration monitoring. The main objective of the authors was the development of a database of measurements prior to the occurrence of a large future earthquake. Furthermore, they aimed to predict the response of the building under earthquake, which later will be compared with actual earthquake responses. They also aimed to detect the soil-structure interactions during large earthquakes. Another, goal in their study was to determine significant nonlinearities in the system response under large earthquakes with an aim to improve the building model and predictions of strong earthquake.

Kaya *et al.,* (2011) present the effects of different traffic conditions on the vibration response of Fatih Sultan Mehmet suspension bridge in Istanbul, Turkey. The authors

discussed of the vibration effects of heavy-traffic conditions on the bridge and the effects of the vibrations obtained from light and no traffic conditions on the free vibration characteristics of the bridge. Free vibration differences were discussed with comparison of the vibrations of the bridge obtained from heavy traffic condition and the vibrations obtained from light and no traffic conditions. In their work, the authors explained that, in order to characterize the effect of the traffic and vibration differences between heavy traffic, light traffic and no traffic conditions, Fourier Amplitude Spectra (FAS) were calculated and frequencies and displacements were identified in vertical, lateral, longitudinal directions.

Çelebi *et al.,* (2013) have presented an investigation on the ambient response of a tall building. The building has a unique performance-based design which included buckling-restrained braces and tuned liquid sloshing dampers as dynamic response identification properties. The building consisted of 64 stories with reinforced concrete core shear walls. It was instrumented by an array of accelerometers having a total of 72 channels. The dynamic responses of the building to ambient vibrations both from ground were recorded and calculated. The modes and the related natural frequencies as well as modal damping were determined through modal identification analysis by obtaining experimental data sets. The results were compared with those determined by spectral analyses. For the first five modes the results showed high level of similarity, both for the spectral analyses and modal identification techniques.

Şafak *et al.,* (2014) presented a review, which focused on the real-time analysis including the explanation of continuous data from structural health monitoring systems. The paper includes a method for signal processing and analysis of real-time structural health monitoring data from building-type structures. The authors also present REC_MIDS, which is based on Matlab software for the real-time system identification and damage detection. The authors in their publication, also presented techniques for the real-time analysis and noise decrease in the ambient vibration data. These techniques are widely employed in this study. A detail presentation of them will be given in Chapter 5.

Petrovic *et al.,* (2015) in their paper have presented an investigation on two buildings on the use of ambient vibration analysis. Authors employed the FDD technique is used for all data sets from all the instrumentation up to obtain the natural frequencies and corresponding to the mode shapes.

3. METHODOLOGY

This chapter will briefly present the techniques used in this study for the analysis of the selected structure.

3.1. Fourier Transformation and Power Spectral Density

The common approach for system identification is to use Fourier transform of the signals in applying the so called frequency-domain techniques to the analysis of random signals. Fourier amplitude spectrum of an ambient vibration expresses the frequency content of a motion very clearly. The simplest way to identify modal frequencies is to inspect Fourier Amplitude Spectra (FAS) of the records. FAS reach peak values at natural frequencies and modal frequencies due to resonant effects. The vibration data obtained from structural monitoring systems are in discrete-time domain. The Fourier transform provides the same information in frequency domain. Fourier transformation produces a sinusoidal output for a sinusoidal input to a system. The frequency and wave shape must remain the same while the phase and amplitude of the signal can change. Therefore, sinusoids are the only waveform that has these beneficial properties.

If *x(t)* denotes an N-point discrete-time vibration record with sampling interval Δt, its discrete Fourier transform, *X(f)*, is expressed by the following equation (Şafak and Çaktı, 2014). For any function $x(t_j)$ which is continuous signal, the Fourier transform can be denoted as $X(f_k)$ and the frequency array f_k is unique and set by the number of points in the record, *N*, and the sampling interval, Δt as defined in the equation below.

$$X(f_k) = \frac{1}{\sqrt{N}} \sum_{j=0}^{N-1} x(t_j)\, e^{-i2\pi kj/N} \qquad (3.1.a)$$

$$t_j = j\Delta t; \quad f_k = \frac{k-1}{N\Delta t}; \quad j = 0, \ldots\ldots, (N-1); \quad k = 1, \ldots\ldots, \left(\frac{N}{2}+1\right); \quad i = \sqrt{-1} \qquad (3.1.b)$$

As seen from the equation, $X(f_k)$ is a complex-valued quantity. Its amplitude and phase, $A(f_k)$ and $\emptyset(f_k)$, are obtained by the following equations:

$$A(f_k) = \sqrt{X(f_k)X^*(f_k)} \qquad and \qquad \emptyset(f_k) = \tan^{-1}\left(\frac{Im[X(f_k)]}{Re[X(f_k)]}\right) \qquad (3.2)$$

Here, $X^*(f_k)$ is the complex-conjugate of $X(f_k)$, and Im[…] and Re[…] denote the complex and real parts. Taking the Fourier transform of a record is equivalent to expressing it as a sum of harmonics. $A(f_k)$ denotes the amplitude of the sinusoid at frequency f_k in the sum, and $\phi(f_k)$ its phase (i.e., the time shift of the sinusoid with respect to *t=0* axis) (Şafak and Çaktı, 2014).

The plot of absolute value of the Fourier transfer versus frequency is known as a Fourier amplitude spectrum. Similarly, the plot of Fourier phase angle versus frequency gives the Fourier phase spectrum.

Power spectral density function (PSD) shows the strength of the energy as a function of frequency and can describe the frequency content of a ground motion. Power spectral density obtained through the Fourier transform of the signal's auto-correlation function is more often used. The frequency content of the signal does not alter by taking the autocorrelation. Subsequently, the signal to noise ratio in the autocorrelation of a signal is higher than that of the original signal. This is why taking the autocorrelation amplifies the amplitudes of any periodic components in the data. Thus, using the autocorrelation functions of the records is more advantageous than the original records while calculating Fourier spectrum of ambient vibration. The Fourier spectrum of auto correlation function is named the power spectral density (PSD) function. Cross power spectral density is also the Fourier transform of cross correlation.

3.2. Natural Frequencies

Natural frequency is the frequency at which a system vibrates between its original position and its displaced position without having an applied force on it. In other words, the natural frequency is equal to the number of times per second that the structure will

vibrate back and forth. The word 'natural' is used to describe these factors since they are natural properties of the structure when it is allowed to vibrate freely without any external excitation (Chopra, 1981).

The natural period of vibration is to complete one cycle of free vibration the required time for the undamped system. It is symbolized as T_n, in units of seconds. The natural period of vibration, the natural circular frequency of vibration, ω_n, in units of radians per second, and the natural cyclic frequency of vibration f_n, in units of cycles/sec or Hz are related as follows;

$$\mathrm{T_n} = \frac{2\pi}{\omega_n} \qquad (3.3.a)$$

$$f_n = \frac{1}{T_n} \qquad (3.3.b)$$

$$f_n = \frac{\omega_n}{2\pi} = \frac{1}{2\pi}\sqrt{\frac{k}{m}} \qquad (3.3.c)$$

Per these equations, the natural vibration characteristics ω_n, T_n, and f_n based only on the mass and stiffness of the structure.

3.3. Free Vibration Characteristics

3.3.1. Eigenvector Analysis

Eigenvector analysis determines the free vibrations of structural indicators including natural frequencies and mode shapes of the system. The dynamic behavior of the structures can be explained by means of natural modes. Eigenvector analysis includes the result of the generalized eigenvalue problem;

$$[K - \omega^2 \mathrm{M}]\emptyset = 0 \qquad (3.4)$$

Equation 3.4 caused an equation in ω^2 called the polynomial of the system. The solutions of this equation are the eigenvalues of $[K - \omega^2 \mathrm{M}]$. Physical vibrating system is a set of N eigenvalues ranging from $\omega_1^2, \omega_2^2, \ldots\ldots, \omega_N^2$, where N is the number of degrees of freedom. For each ω_N^2 substituted back into Equation 3.4, we will get a certain amplitude vector ϕ_N. Each eigenvalue or natural frequency has an associated eigenvector. This eigenvector expresses the mode shapes of the system. This means that mode shape is described the geometrical shape of the vibration within a given resonant frequency. The magnitude of the eigenvectors is not expressed in physical coordinates.

3.4. Frequency Domain Decomposition Theory Background

The Frequency Domain Decomposition (FDD) technique is based on the fact that modes can be determined from the spectral densities. However, this requires that the input has white noise characteristics and the structure does not have high damping capacity. The technique is a nonparametric method estimating the modal parameters directly from signal processing calculations (Brincker *et al.*, 2000, Andersen *et al.*, 2000). Hence, the method uses spectral representation from the Singular Value Decomposition. Thus in turn the method is capable to obtain the natural frequencies, as well as the relevant mode shapes of the structure under study (Brincker *et al.*, 2001). The decomposition process, for each singular value determines a Single Degree of Freedom (SDOF). Hence, the correlation between the input x(t), and the output y(t) is formulated as follows;

$$\left[G_{yy}(\omega)\right] = [H(\omega)]^* \, [G_{xx}(\omega)] \, [H(\omega)]^T \tag{3.5}$$

where $[G_{xx}(\omega)]$ is the (r x r) Power Spectral Density (PSD) matrix of the input, r being the number of input channels. $[G_{yy}(\omega)]$ is the (m x m) PSD matrix of the output, m being the number of output signals, and $[H(\omega)]$ is the (m x r) Frequency Response function (FRF) matrix, and * and superscript T denote complex conjugate and transpose, respectively. $[G_{xx}(\omega)]$ and $[G_{yy}(\omega)]$ matrices derive from Finite Fourier Transforms for the PSD evaluation (Bendat et.al.,1986). The FRF matrix can be written in a typical partial fraction form, in terms of poles (in complex conjugate pairs), λ and residues matrices (m x r), R_k

$$[H(\omega)] = \frac{[Y(\omega)]}{[X(\omega)]} = \sum_{k=1}^{m} \frac{[R_k]}{j\omega - \lambda_k} + \frac{[R_k]^*}{j\omega - [\lambda_k]^*} \tag{3.6}$$

with

$$\lambda_k = -\sigma_k + j\omega_{dk} \tag{3.7}$$

where m is the total number of modes of interest, λ_k is the pole of the k^{th} mode, σ_k is the modal damping (decay constant) that is minus the real part of the pole and ω_{dk} is the damped natural frequency of the k^{th} mode which can be expressed as Equation (3.8)

$$\omega_{dk} = \omega_{ok}\sqrt{1 - \xi_k^2} \tag{3.8}$$

$$\xi_k = \frac{\sigma_k}{\omega_{ok}} \tag{3.9}$$

In Equation (3.8), ζ_k is the damping ratio for the mode and ω_{ok} is the undamped natural frequency for the k^{th} mode. $[R_k]$ in Equation (3.6) is given as:

$$[R_k] = \{\varphi_k\}\{\gamma_k\} \tag{3.10}$$

In the expression (3.10), φ_k is the mode shape of the k^{th} mode and γ_k is the modal participation vector of the k^{th} mode. If the input to the system is considered as the white noise, power spectral density matrix can be taken as a constant matrix $[G_{xx}(\omega)] = [C]$ and Equation (3.5) takes the following form.

$$\left[G_{yy}(\omega)\right] = \sum_{k=1}^{m}\sum_{s=1}^{m}\left(\frac{[R_k]}{j\omega - \lambda_k} + \frac{[R_k]^*}{j\omega - \lambda_k{}^*}\right) C \left(\frac{[R_s]^T}{j\omega - \lambda_s} + \frac{[R_s]^H}{j\omega - \lambda_s{}^*}\right) \tag{3.11}$$

Where superscript H represents the complex conjugate transpose. With using the expression $[G_{yy}(\omega)]$ in Equation (3.5) and with some mathematical operations, output power spectrum matrix can be written as:

$$\left[G_{yy}(\omega)\right] = \sum_{k=1}^{m} \frac{[A_k]}{j\omega - \lambda_k} + \frac{[A_k]^*}{j\omega - \lambda_k{}^*} + \frac{[B_k]}{-j\omega - \lambda_k} + \frac{[B_k]^*}{-j\omega - \lambda_k{}^*} \tag{3.12}$$

where A_k is the k^{th} residue matrix of the output PSD.$\left[G_{yy}\right]$ matrix is a Hermitian matrix (they are complex conjugate symmetric, meaning that they have complex conjugate elements around the diagonal) and can be expressed as;

$$[A_k] = [R_k]\, C \sum_{s=1}^{m} \frac{[R_s]^H}{-\lambda_k - \lambda_s{}^*} + \frac{[R_s]^T}{-\lambda_k - \lambda_s} \tag{3.13}$$

The contribution of the residue for the k^{th} mode has the following expression;

$$[A_k] = \frac{[R_k]C[R_s]^H}{2\sigma_k} \tag{3.14}$$

Where σ_k is the negative of the real part of the pole as $\lambda_k = -\sigma_k + j\omega_{dk}$. If this term is dominating, the damping is light. In the case of light damping, modal contribution matrix is proportional to the mode shape vector and can be written as:

$$\lim_{damping \to light} [A_k] = [R_k]C[R_k]^T = \{\varphi_k\}\{\gamma_k\}^T C\{\gamma_k\}\{\varphi_k\}^T = d_k\{\varphi_k\}\{\varphi_k\}^T \tag{3.15}$$

A lightly damped model (small damping ratios ζ_k << 1) and that the contribution of the modes at a curtain frequency is restricted to a finite number. This set of modes are signified by *Sub(ω)*. A lightly damped structure the response spectral density matrix can be written as:

$$\left[G_{yy}(\omega)\right] = \sum_{k \epsilon Sub(\omega)} \frac{d_k\{\varphi_k\}\{\varphi_k\}^T}{j\omega - \lambda_k} + \frac{d_k{}^* \varphi_k{}^* \varphi_k{}^{*T}}{j\omega - \lambda_k{}^*} \tag{3.16}$$

where $k \in Sub(\omega)$ is the set of modes that contribute at the particular frequency and where

φ_k is the mode shape and d_k is a scaling factor for the k^{th} mode. This is a modal decomposition of the spectral matrix.

This final form of the $[G_{yy}(\omega)]$ matrix is then decomposed, using the singular value decomposition technique, into a set of singular values and their corresponding singular vectors, the singular vectors is an approximation to the mode shapes. This decomposition is performed to obtain dynamic characteristics of the system.

As can be mentioned above, singular value decomposition technique is carried out at each frequency $\omega = \omega_i$. Then, it is decomposed by taking the Singular Value Decomposition (SVD) of the matrix:

$$G_{yy}{}^{T}(\omega_i) = U_i S_i U_i{}^{H} \tag{3.17}$$

where S_i is the singular value diagonal matrix including the n singular values s_{ij} with $j=1,\ldots..,n$ and $[U_i=u_{i1,}\ u_{i2,\ldots..,}\ u_{in}]$ is the orthogonal matrix of the singular vectors, which (the columns in $[U]$) are orthogonal to each.

Spectral eigenvalue contains full information of dominant frequencies to be used for extracting the natural frequencies and spectral eigenvector brings information of mode shapes at each dominant frequency. The i_{th} mode shape can be estimated from the first spectral eigenvector at certain dominant frequencies as follows:

$$\hat{\varphi} = u_{i1} \tag{3.18}$$

4. DESCRIPTIONS OF THE BUILDING AND THE DATA ACQUISITION SYSTEM

4.1. Architectural and Structural Systems

The building used in the study is a high-rise building which has been recently constructed at Istanbul's developing business district Maslak. The total height of the tower is 92.84 m from the surface of slab at parking level 4 to the roof of the tower. The total height underground is 26.0 m. The building was designed and constructed to be an office building.

The floor area for floors first basement through ground, ground through first and first through two decreases by approximate 29.8%, 18% and 61.5%, respectively. The floor plan for the second through fifteenth levels is rectangular with near-perfect symmetry. The foundation area of the building is 5527.52 m^2 and the overall elevation above ground level is about 66.84m. A photo of the tower at the time of testing is shown in Figure 4.1.

The 23-story high-rise building's structural system is a concrete structure, consisting of four structural walls in the center and columns. There are seven basement levels and one level partly above grade. These cores where are located at center of the building enclose two stairways and two lift shafts and. The structural system joins these shear walls with reinforcement concrete frames with longitudinal beams bearing the full reinforcement concrete floors. The building is made up of a central reinforced concrete core whose walls are up to 50 cm thick at the base. The thickness of the shear walls in the center of the structure in the NS direction from first level (basement level) to the 17^{th} floor is 40 cm and from the 17^{th} floor from the 23^{th} story to the top of the building is 30.0 cm. The thickness of the core shear walls in the EW direction at all floors is 50 cm. The ratio of curtain walls to floor areas is between 2.32% and 2.82%. This ratio indicates that the structural earthquake forces will be mainly covered by the core curtains. Along the perimeter of the building at the underground parking levels and lobby levels, continuous basement walls have the double function of carrying vertical and lateral loads as well as working as

retaining walls for the soil surrounding the construction. Four central structural cores placed approximately at the center of the tower define the lateral system. The foundation is a raft foundation bearing directly on the subsoil.

Figure 4.1. The tall building monitored in the study

The floor height is 4 meters for all the for the office floors. The floor heights of the parking are 3.20 and 4.25 meters. The basement floors three through seven consist of a 25 cm concrete slab. The thickness of second basement floor is 30 cm. floors. The first basement floor through 15th floor consists of a 20 cm concrete slab. Story heights and cumulative height, as well as the slab types are listed in Table 4.1. The first six basement floors are flat slab with drop panels, and the other floors are two-way beam supported. All the slabs are supported by columns distributed along the edge of the building.

Table 4.1. Floor heights and slab types of the Building

Floor	Story Height(m)	Cumulative Height(m)	The Type of Slab
15	4	59.85	Two-Way Beam-Supported
14	4	55.85	Two-Way Beam-Supported
13	4	51.85	Two-Way Beam-Supported
12	4	47.85	Two-Way Beam-Supported
11	4	43.85	Two-Way Beam-Supported
10	4	39.85	Two-Way Beam-Supported
9	4	35.85	Two-Way Beam-Supported
8	4	31.85	Two-Way Beam-Supported
7	4	27.85	Two-Way Beam-Supported
6	4	23.85	Two-Way Beam-Supported
5	4	19.85	Two-Way Beam-Supported
4	4	15.85	Two-Way Beam-Supported
3	4	11.85	Two-Way Beam-Supported
2	4	7.85	Two-Way Beam-Supported
1	4	3.85	Two-Way Beam-Supported
0	4	-0.15	Two-Way Beam-Supported
-1	4	-4.15	Two-Way Beam-Supported
-2	4	-8.15	Flat Slab With Drop Panels
-3	4	-12.15	Flat Slab With Drop Panels
-4	4.25	-16.4	Flat Slab With Drop Panels
-5	3.2	-19.6	Flat Slab With Drop Panels
-6	3.2	-22.8	Flat Slab With Drop Panels
-7	3.2	-26.0	Flat Slab With Drop Panels

4.2. Instrumentation and Sensor Locations

The instruments which are force balance type accelerometers of GURALP Systems type CMG-5T. The CMG-5T Accelerometer System consists of 4 components: Sensor (Transducer), Digitizer/Recorder, Communication Module, Timing Module (GPS) and

Power Supply and in addition a laptop computer for the data acquisition and data storage were used for the dynamic measurements of the building. The properties of the system components are available at the web page of Kandilli Observatory and Earthquake Institute of Bogazici University.

The ambient vibrations were recorded in horizontal, longitudinal and vertical directions at five different locations for each test. Five GURALP CMG-5T accelerometer sensors with +/- 2g range and with total of 15 channels were used for the tests and data was recorded at 100 sampling rate synchronously.

Figure 4.2. Strong motion accelerometer and transducer

The experimental set-up located on structure is performed with five accelerometers to measure the ambient vibration response at 3 different floors compatible per the recommendations of Uniform Building Code (UBC, 1997). UBC recommendation is illustrated in Figure 4.3.

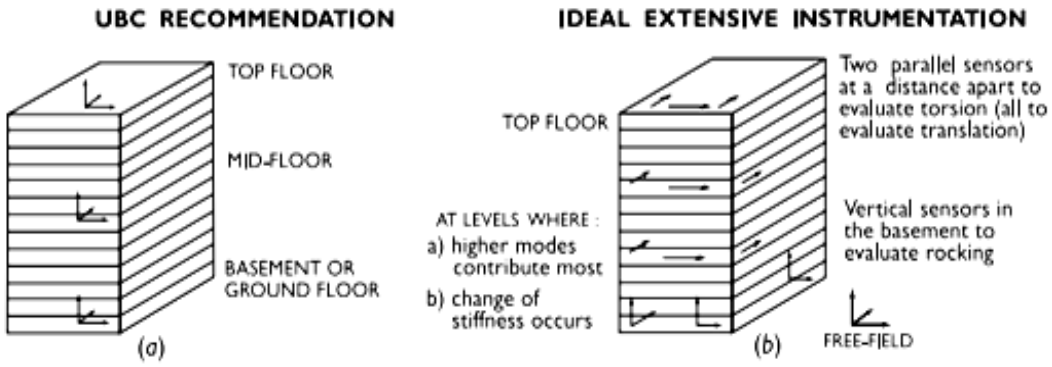

Figure 4.3. UBC recommendation and ideal extensive instrumentation

In this study, ambient vibration response recordings of the structure monitored at various construction steps were planned in order to obtain the difference of its dynamic properties. These are named as Case 1, Case 2, and Case 3, respectively. This was done in order to examine the separate contributions of the only structural elements, in addition glass curtain wall façade, and complete building to the dynamic characteristics of the structure.

The first test was carried out on March 27, 2015 just after the completion of structural works but before any finishing works in the building achieved. The data collection has started at 10:30 am and ended at 11:30 am.

The second test was done to collect data and the real-time vibration data is starting 11:30 and the end time is 12:30, 13th of September, 2015. At that date the building had the glass curtain façade wall installed and screed was laid at floors.

The last instrumentation was done between 10:20 and 10:50 on March 2016 when the building was completed and ready for commissioning. In that respect, all the finishing works at the common spaces of floors were completed and all the mechanical and electrical systems were installed.

Figure 4.4. Experimental set-up located on the first basement, 7th and 15th story (Case 2)

Figure 4.4 shows the sensors and the recorder located on the first and third basements, 7th and 15th stories. Five stations were installed at five locations at four different floors. The sensor systems for Case 1 and Case 2 consist of 15 channels of acceleration sensors and they are installed to different level floors of the structure. In specific, sensors were located on first basement level, on 7th level floor and on top level. The last sensor system of building consists of nine channels of acceleration sensors for Case 3 and they are installed to different level floors of the structure. The sensors were located at third basement level and top level. Table 4.2 shows the specific locations and the directions of the strong motion instrumentation. Figures 4.5, 4.6, 4.7 and 4.8 show the layout of the strong motion instrumentation installed on the case study state building.

The position of sensors is determined to obtain the most of the lateral and torsional modes. Also, it is done to visualize the mode shapes of the relevant modes appropriately. Experimental set-up located on the third basement, first basement, 7^{th} and 15^{th} floors. For each story, acceleration-time histories in EW, NS, and vertical directions are recorded at a location close to the center. Three stations whose names are KND01, KND04 and KND05 were placed at almost similar location at different stories and at a position close to the center in the corridor. The instruments were synchronized by receiving the GPS signal. On the top floor, additional accelerometers whose names are KND02 and KND06 are placed on the lateral *x*-direction and on the *y*-direction, approximately 13.5 and 18.5 meters away from the center so as to monitor the torsional motions of the monitored structure, respectively. The motion of the apexes of the building was generated assuming that the floor slab behaved as a rigid diaphragm. The accelerometer coordinates with respect to the reference point conveniently selected in figures, are presented in Table 4.2.

Table 4.2. Locations of sensors

Floor	**Instrument ID**	**Direction**	**y(m)**	**x(m)**
First and Third Basement Level	KND05-5533	EW	0	0
	KND05-5533	NS		
	KND05-5533	Z		
7^{th}	KND04-5540	EW	0	0
	KND04-5540	NS		
	KND04-5540	Z		
15^{th}	KND01-5497	EW	0	0
	KND01-5497	NS		
	KND01-5497	Z		
	KND02-5329	EW	18.5	0
	KND02-5329	NS		
	KND02-5329	Z		
	KND06-5444	EW	0	13.5
	KND06-5444	NS		
	KND06-5444	Z		

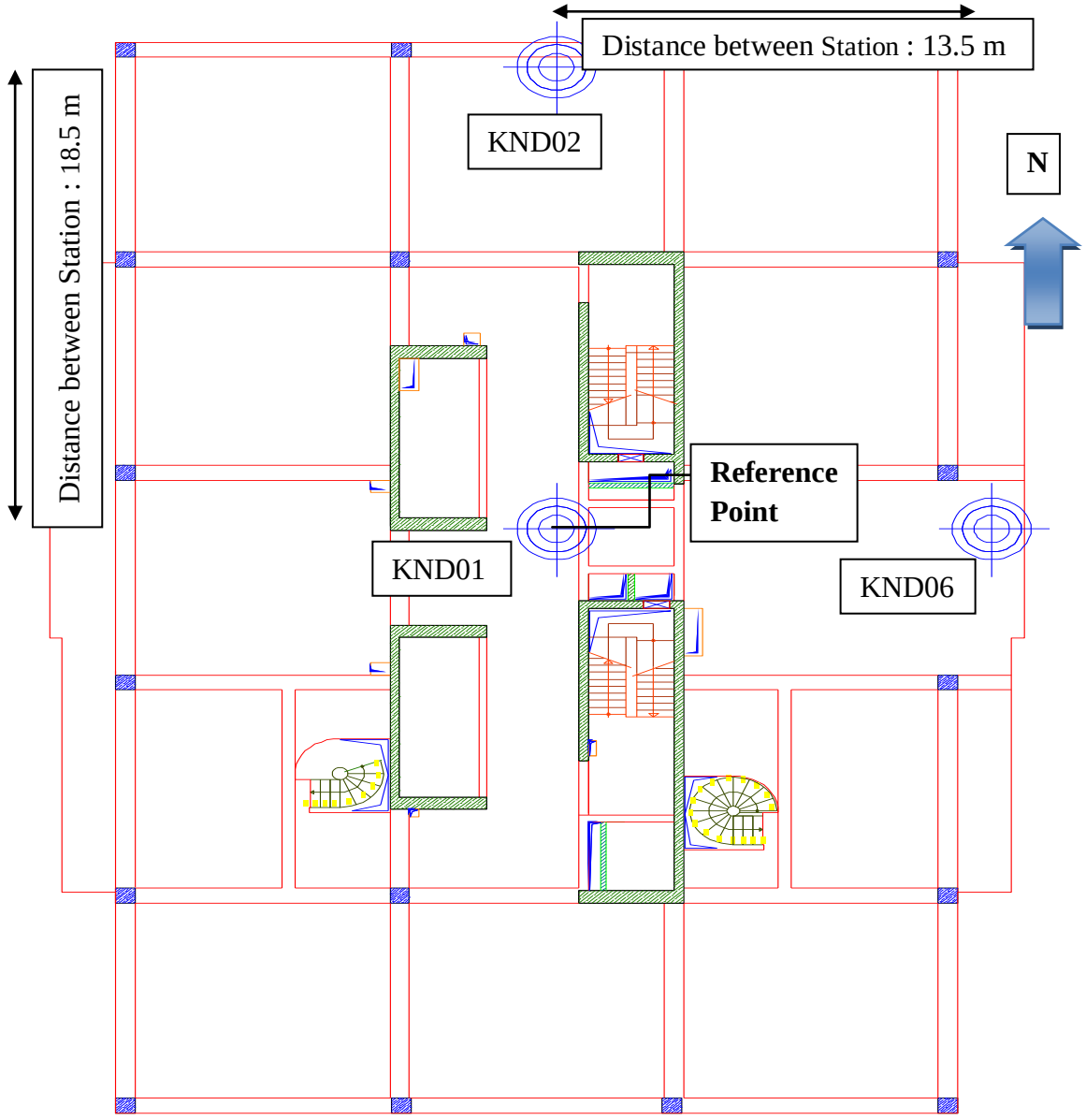

Figure 4.5. Location of the sensors (blue target marks) at the 15th floor level

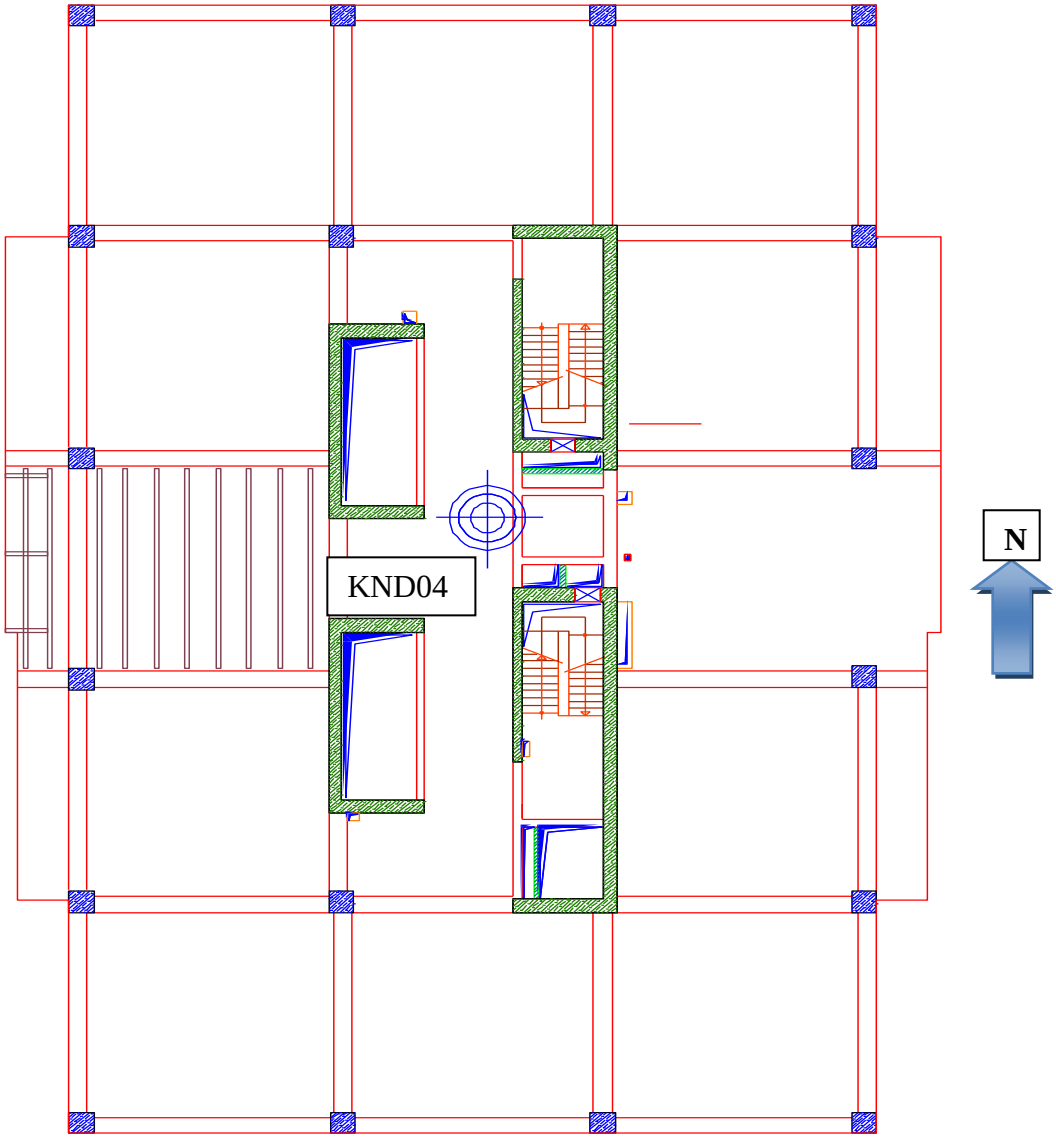

Figure 4.6. Location of the sensor (blue target mark) at the 7th floor level

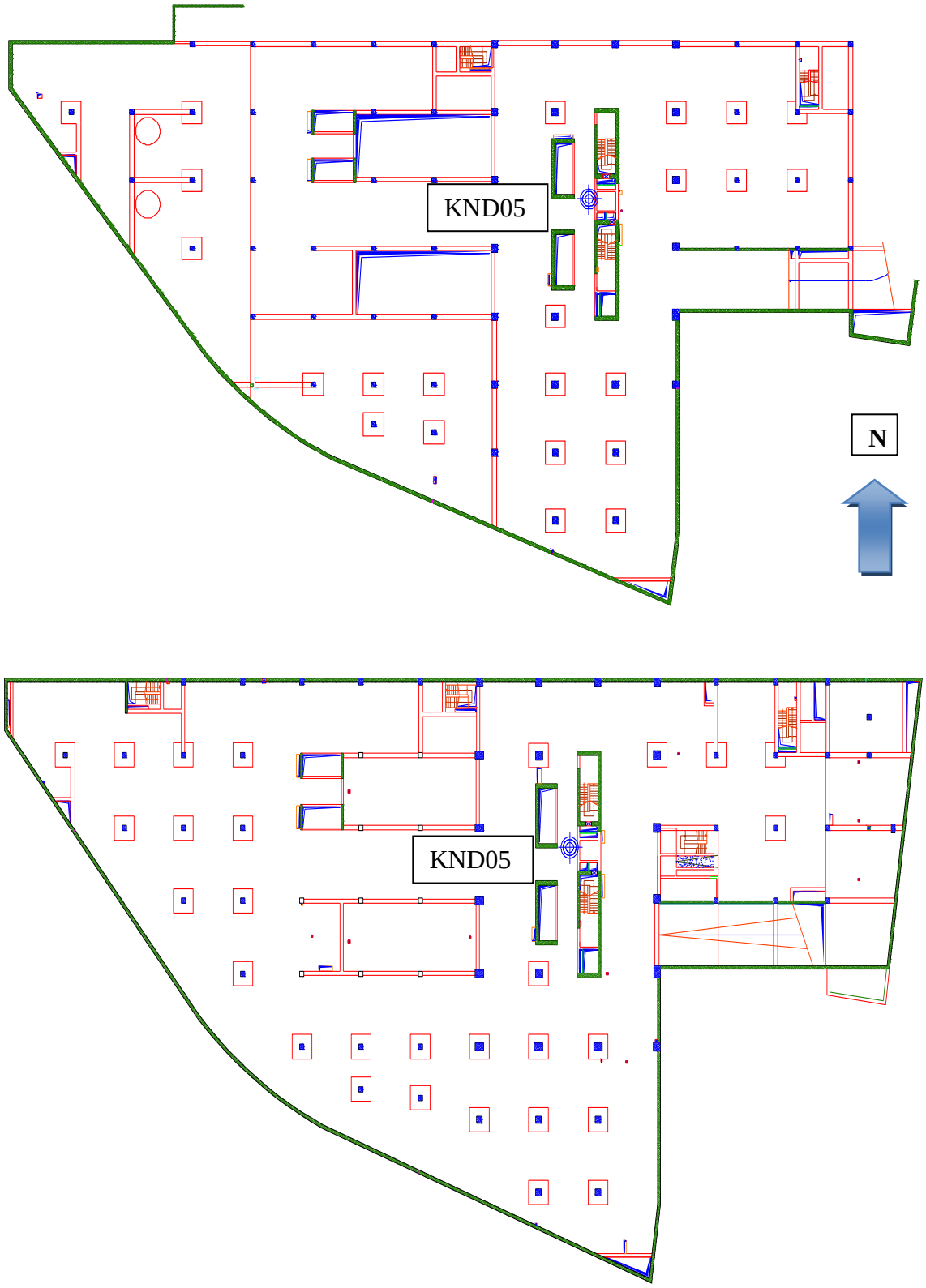

Figure 4.7. Location of the sensors (blue target mark) at the basement levels. (a) First Basement level (b) Third Basement level.

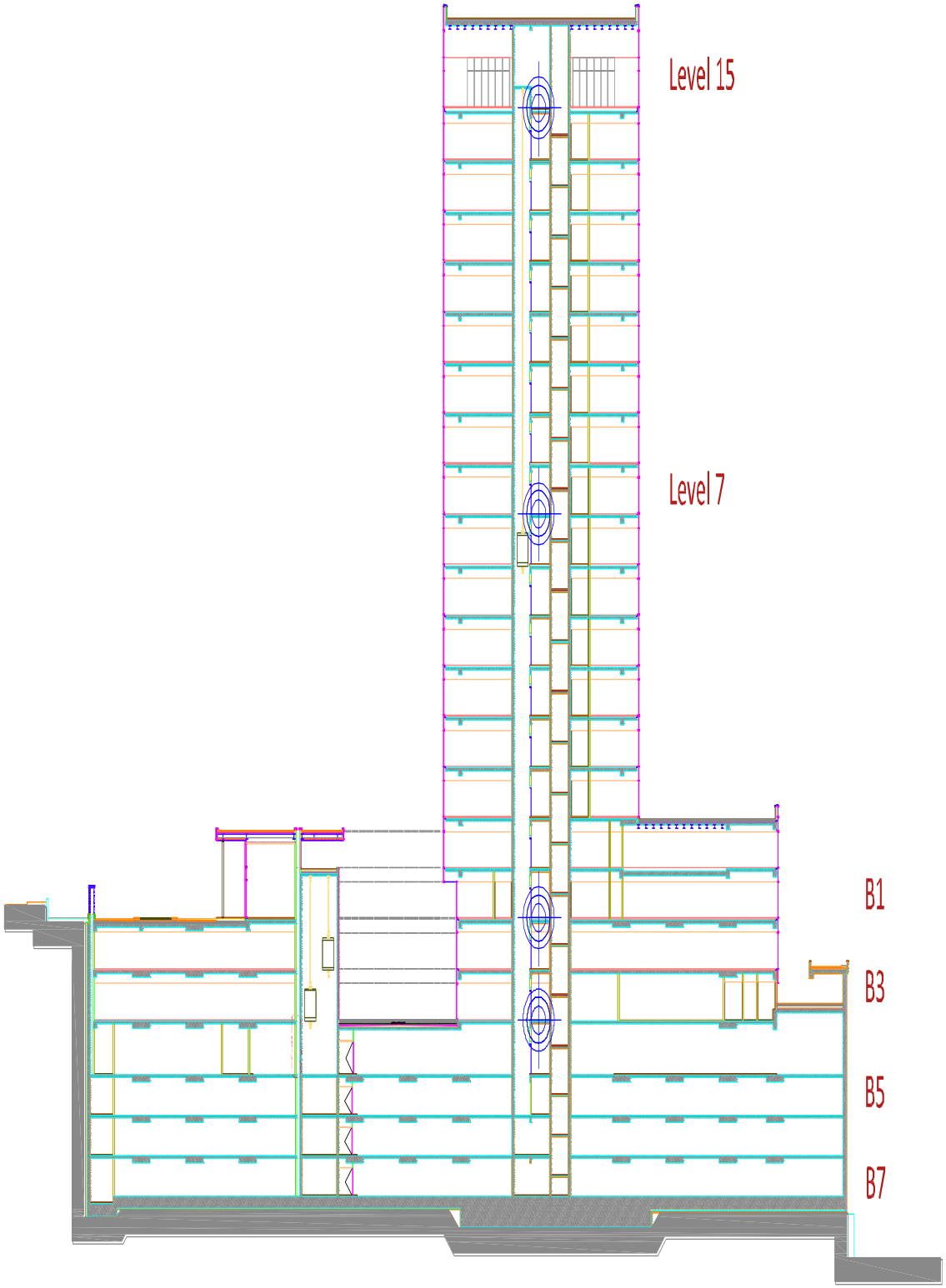

Figure 4.8. The locations of the instrumentations (blue target mark) along the height of the structure monitored

4.3. Data Collected

The recording intervals and length of the data obtained were demonstrated Table 4.3. The biggest peak amplitude of acceleration among all the ambient vibration data sets is smaller than 20 cm/s^2. Some parts of the data set exhibited some discontinuities. Two instruments, namely 270320151130 and 130920161050 had some gap in their recordings however 20 and 30 minutes continuous data could be extracted from the records. Consequently sufficient amount of synchronized data were extracted from four data sets for about 60 minutes.

Table 4.3 The recording intervals and length of the data.

Date (DDMMYYYY) Time (HHMM)	**Length of recorded data (s)**	**Length of data windows (s)**
27032015 1030	360000	6000
27032015 1130	120000	6000
13092015 1130	360000	6000
16032016 1050	180000	6000

5. ANALYSIS AND DISCUSSION OF RESULTS

Due to the combined existence of ambient and instrument noise in the data recordings, raw form of data usually do not provide the possibility for a good identification of the dynamic properties of the structure. Some of the main reasons for this can be the environmental conditions, instrument noise in the recorded signal, possible low-frequency drifts in the data (mainly due to mechanical imperfections in the force-balanced accelerometers), installation process, and other flaws in the sensors. To minimize the undesirable effects of such factors on the modal identification, the recorded data should be processed first before using it. Hence, data processing may involve removal of mean, removal of linear trends (i.e., baseline correction), windowing, smoothing, decimation, and band-pass filtering.

The first step in data processing is to track and remove the mean value. The mean value of a vibration record represents the static component of the structure's response. The mean value of records should be zero. Due to various external factors, the mean value of the records usually fluctuate around zero. Environmental factors and the loading are usually the affecting parameters. Among the environmental factors one can mention wind and rain. Thus, the change in the mean value of a record is a critical parameter that should be tracked accurately (Kaya and Şafak, 2014).

Afterwards as a second step, linear trends in the data need to be eliminated. This process often times named as “de-trending” or “baseline correction”. The process simply performs a straight line fitting to the record, which then afterwards the difference is subtracted.

Third step in data processing is filtering. Filtering is used in data-processing to remove the short or long period noise and other unwanted components from the raw data to obtain the clear waveforms. In general, band-pass filter that is required to reduce noise and eliminate unwanted frequency components in records is used for filtering process. The low- and high-frequency ends of the spectrum define the corner frequencies of the band-pass filter. An important point is that the phase of the signal during filtering should not be

distorted and to ensure this, band-pass filters with zero-phase (Kaya and Şafak, 2014). It should be noted that some of the digital filters distort the data by changing the phase of the signal. To overcome this problem, either zero phase filters (e.g. Ombsy filter) should be used, or the signal should be filtered twice, first in forward and then in backward directions (e.g., Butterworth filters). In this study, Butterworth filter is preferred in data processing since it has non-zero phase.

It should be kept in mind that the band-pass filtering might not completely remove the low-frequency errors in the record although band-pass filters remove mean value from recorded data and eliminate the components dominated by noise. Low frequency in the data usually create an offset in the output following integration. Namely, for instance this offset will result in a curvy displacement or velocity time history (Şafak, 2004).

These errors will demonstrate in the form of linear trends in the calculated velocity and displacement time histories. A straight line to the accelerations and velocities should be fit and subtracted this line from the records to eliminate linear trends. The low-frequency errors and low-frequency corner will remove static component. More details on the data processing can be found in Hudson, 1979. Therefore, low corner frequency was used as 0.20 Hz in this study.

The last point about data processing is that decimating reduces the data to a more manageable size and the effects of unavoidable noise as well as filters out high frequency content. Decimation involves reducing the sampling rate by an integer factor. Decimation involves two procedures: low-pass filter the original signal at or below the Nyquist frequency and generating the decimated signal by skipping appropriate number of data points.

In this study, data processing is done through a series of developed MATLAB codes so as to perform the basic signal processing, modal identification, and the mode shape validation for the monitoring structure.

5.1. Data Processing for Spectral Analysis

Fourier spectral analysis is a widely used approach for vibration analysis of structures when data is available. However as mentioned above, raw data in general is contaminated by noise induced by environmental factors. Hence the signal-to-noise ratio (SNR) of the record can be very low. Subsequently, the SNR, in the difference of the signals will be much lower than the original signals.

Obviously in this case, the presence of noise in the records does affect the amplitudes and the frequency content of Fourier spectra. Therefore, the noise in the recordings, especially in case of the real time data analysis poses a problem. To overcome this problem the data is split into two windows, namely truncated window and running window (Figure 5.1).

Analysis window runs inside the running window, as shown in Figure 5.1. The running window moves through the truncated data segment to a predefined overlap ratio. Finally, each window is analyzed individually. Afterwards the outputs of all the windows are averaged to obtain the final output for the record.

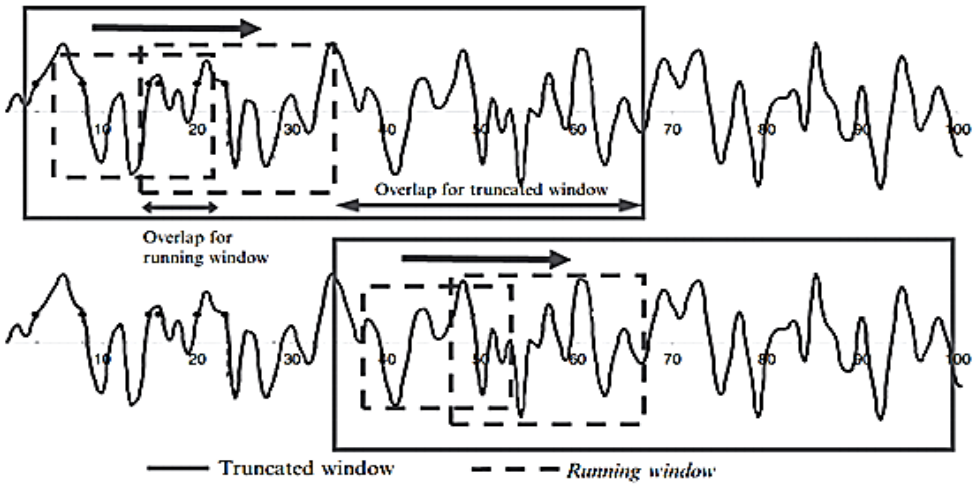

Figure 5.1. Running window moves within the truncated widow by a predefined overlap ratio.

The effect of noise in the truncated data segment is reduced by averaging the outputs of running windows. The averaging the outputs of every running window reduces the effect of the noise in the all output of data segment. Increasing the overlap ratio also increases the number of running windows in the truncated data segment. Therefore, if the number of running window is increased, the accuracy in the all output increases and the effect of noise in the overall output of the truncated data segment will decrease.

Another stage processing the data for spectral analysis is the smoothing of the Fourier amplitude spectra. Şafak et al., (2014) recommends that to select the optimum window size, one should collect a set of experimental data, namely ambient vibration data in this case and analyze them for different window sizes.

The distortions may demonstrate in FAS when high amplitude noise is often observed in ambient vibration records, which results in low signal-to-noise ratios. As a result, the points of the peaks in FAS may not be observed clearly. The smoothing windows are used to decrease the effect of noise in FAS in order to solve this problem. There are different techniques and approaches to select a smoothing window. The results are obviously sensitive to the size of the window. While short windows cannot eliminate the noise, long windows may chop off the peaks.

Safak (1997) proposed a simple method for the determination of the optimal window size. The method determines the window length by plotting the area under the power spectrum, namely the square of the Fourier amplitude spectrum. The optimal window is obtained where the decay of this curve slows down significantly. A demonstration of the method is given in Figure 5.2 (Safak *et al*., 2014).

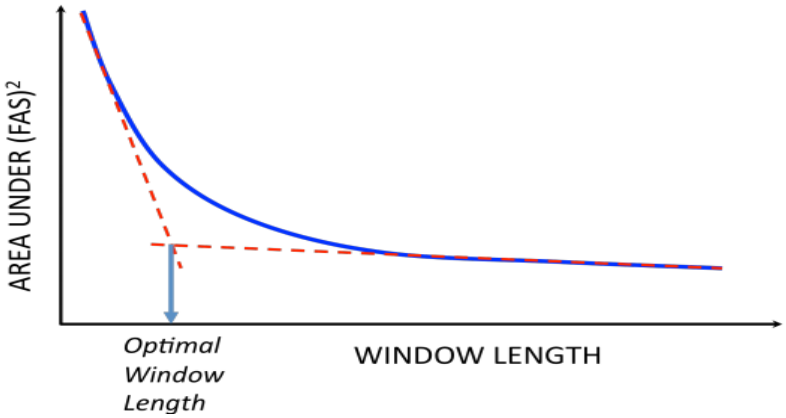

Figure 5.2. Estimation of optimal smoothing window

The numerator and denominator Fourier spectra are smoothed independently by their corresponding optimal-length smoothing windows when calculating transfer functions for the structure by taking spectral ratio. The smoothing window for both the numerator and denominator records must be same in a common practice; however, there are no scientific justifications for doing this (Safak, 2006).

5.2. Ambient Vibration Data

Ambient vibration data set that are collected on 27/03/2015 at 10:30 am and at 11:30 am and on 13/09/2015 at 10:30 am as well as on 16/03/2016 at 10:50 am are extracted. Figures 5.3, 5.4, 5.5, and 5.6 show acceleration time-history plots of raw data sets obtained on those dates and times.

In addition, the number of data points was split into 6000 point windows, which is a much more feasible amount of data to work with due to the fact that signal to noise ratio is high. Figure 5.7 shows only the calculated average data in the EW direction of the data set 270320151030.

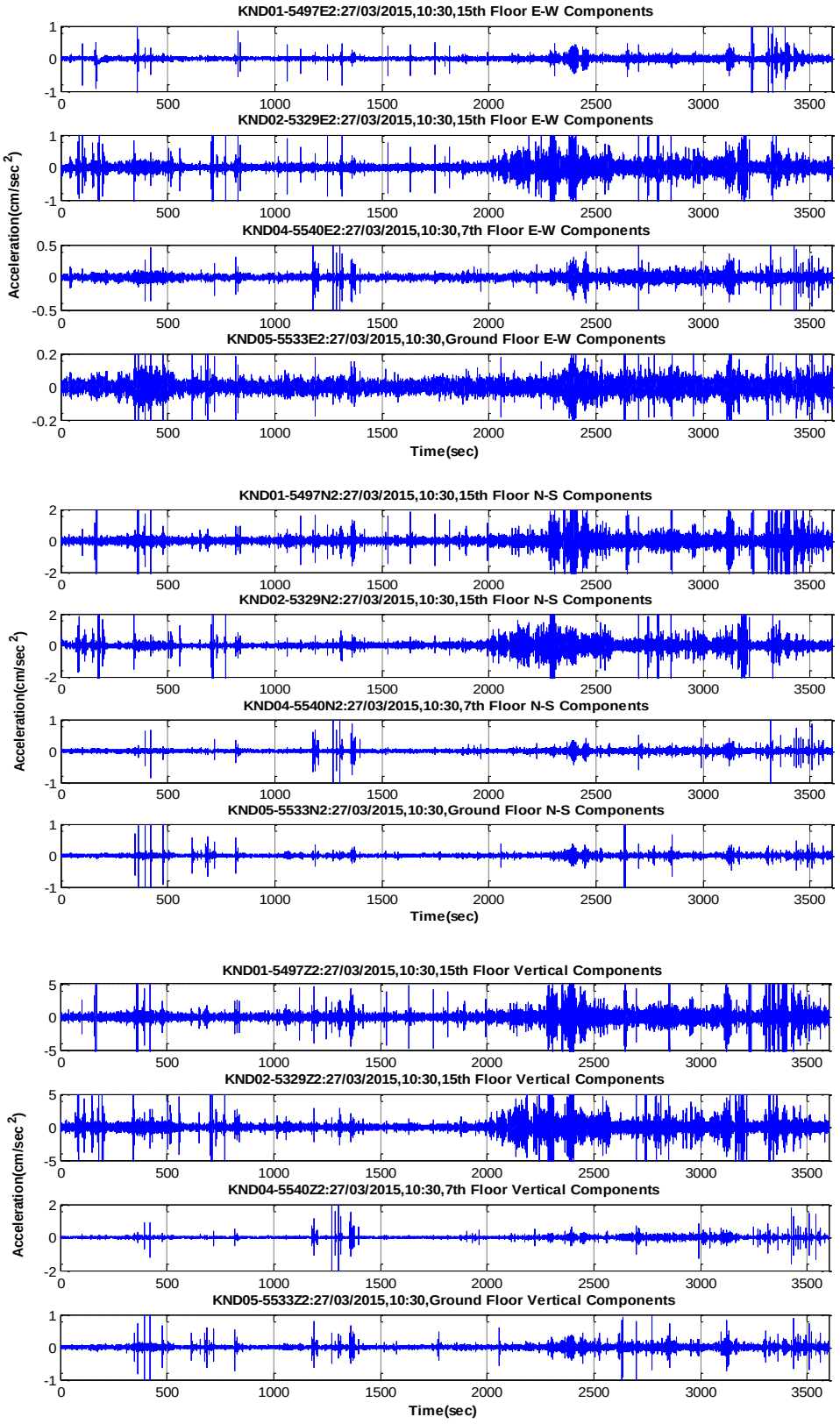

Figure 5.3. Original acceleration-time history plots for 27 March 2015 (270320151030) data sets: EW (top), NS (middle) and UD (bottom) components.

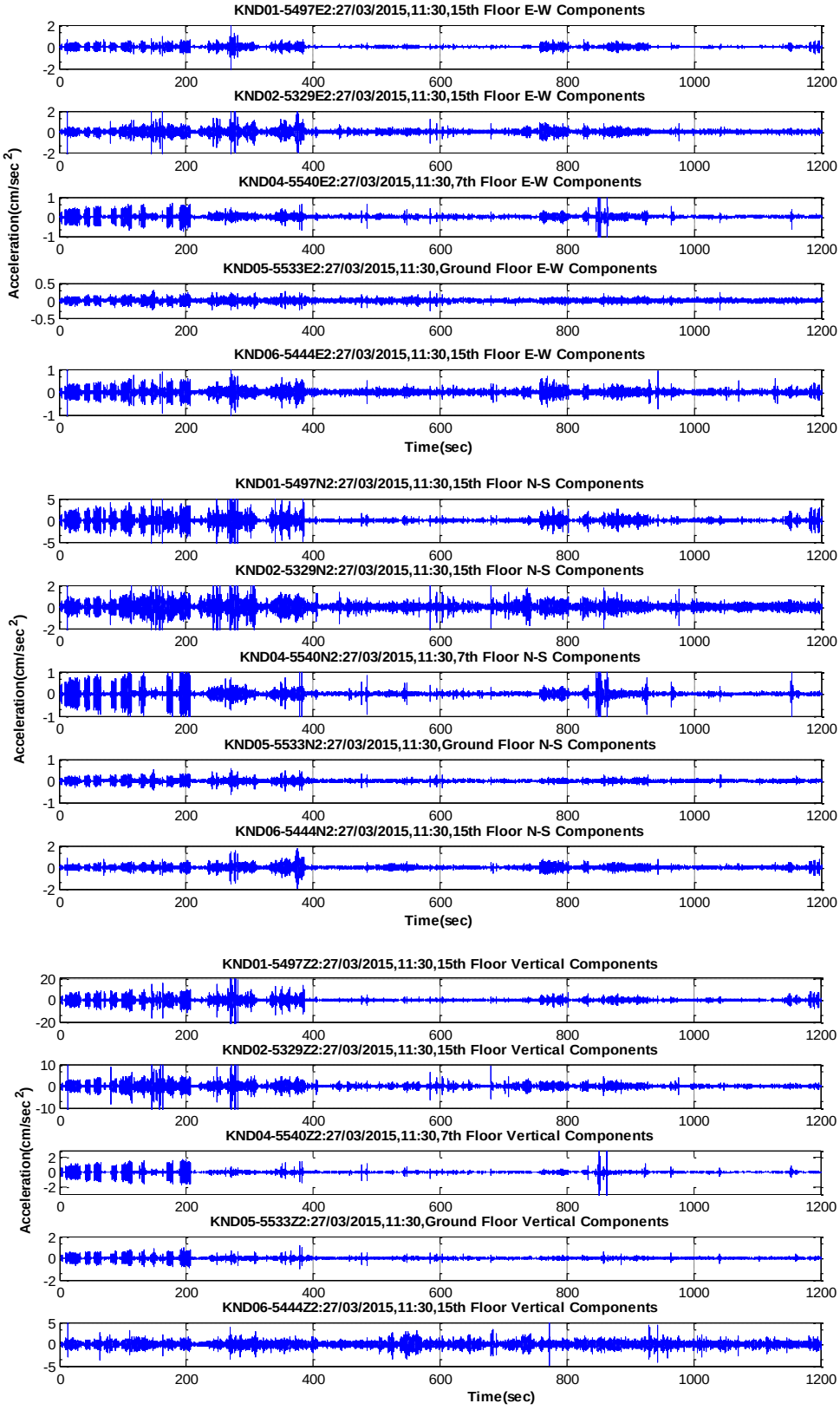

Figure 5.4. Original acceleration-time history plots for 27 March 2015 (270320151130) data sets: EW (top), NS (middle), UD (bottom)

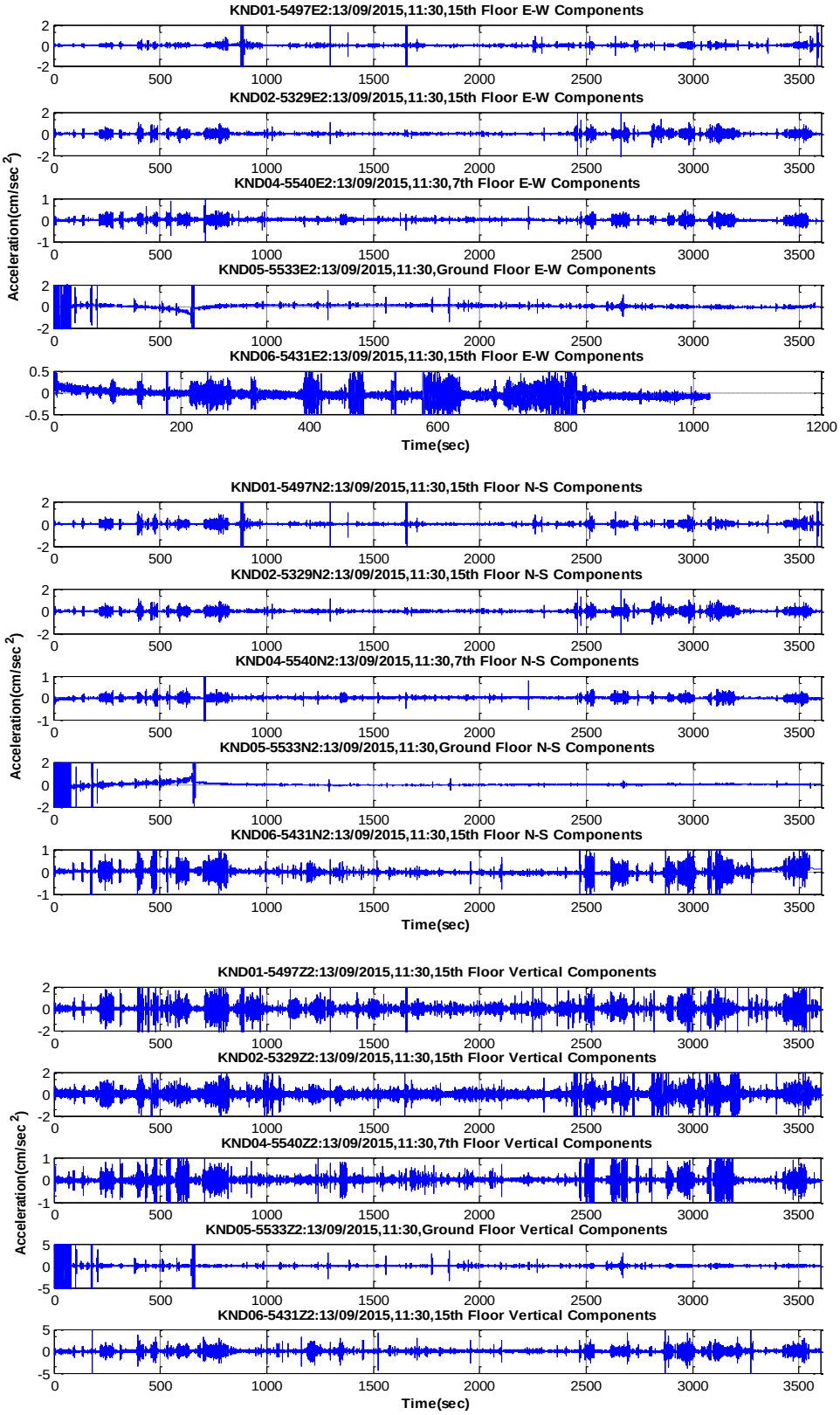

Figure 5.5. Original acceleration-time history plots for 13 September 2015 (130920151130) data sets: EW (top), NS (middle), UD (bottom)

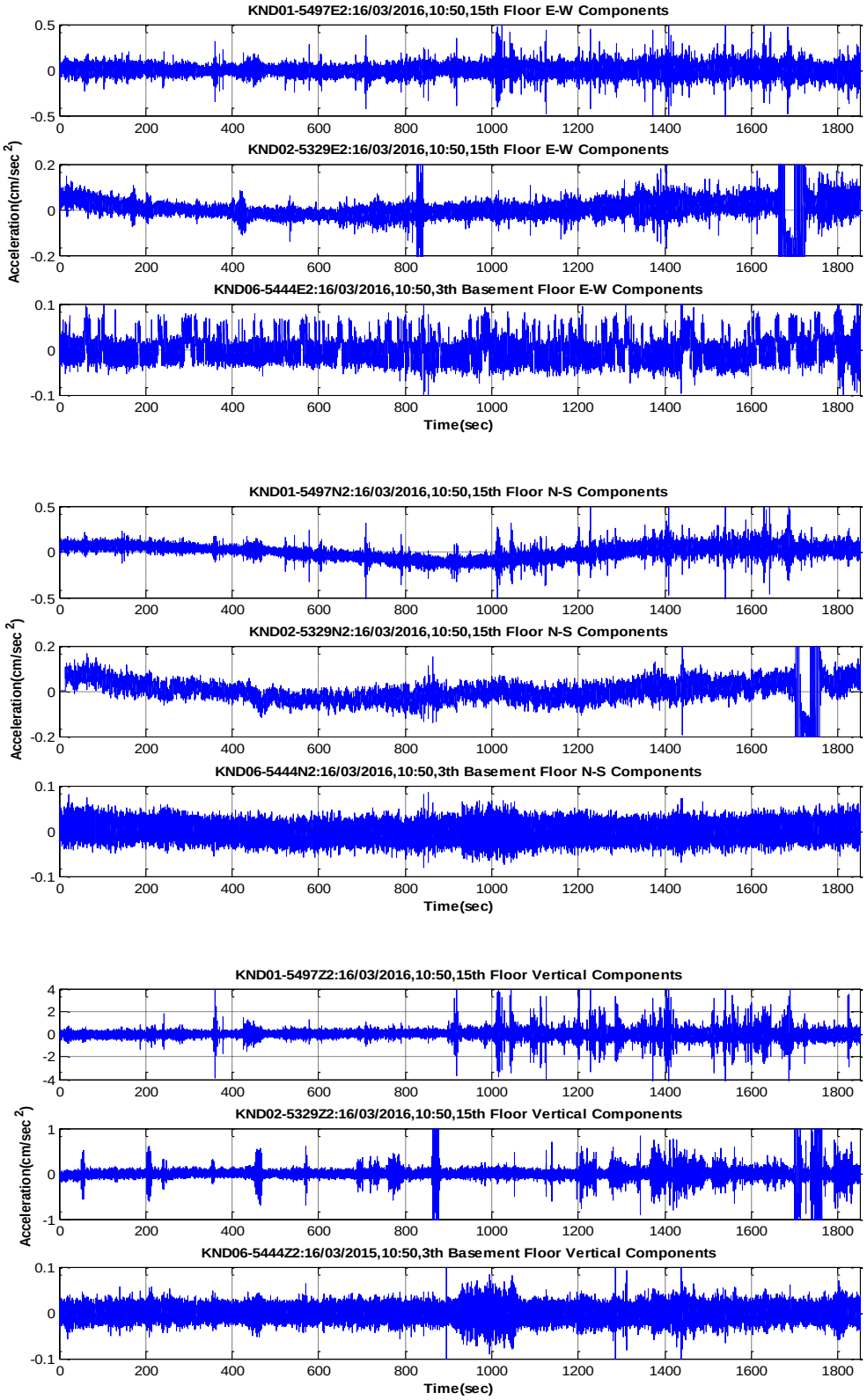

Figure 5.6. Original acceleration-time history plots for 16 March 2016 (160320161050) data sets: EW (top), NS (middle), UD (bottom)

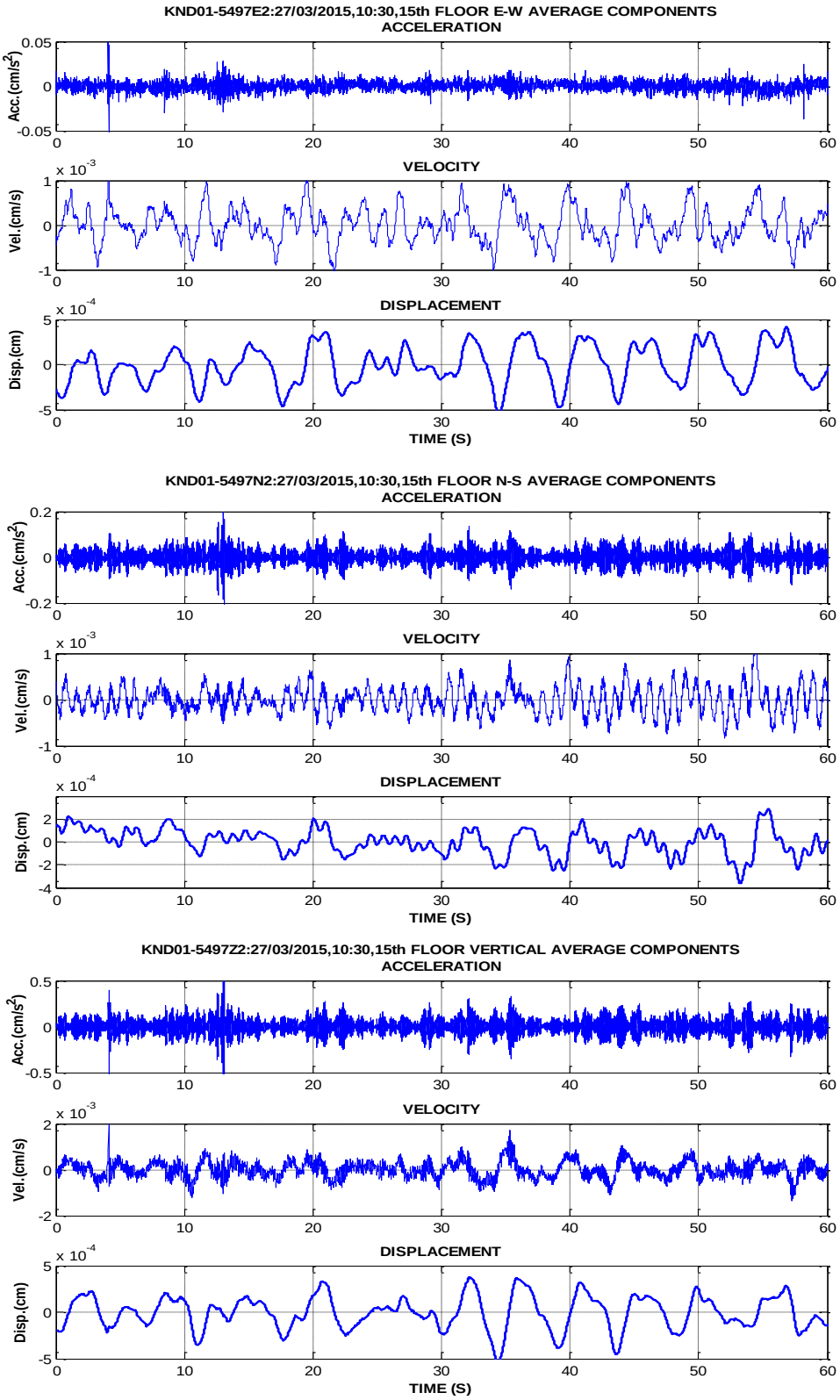

Figure 5.7. Time-history plots of average acceleration and calculated velocity and displacement for data set KND01-5497:27/03/2015, 10:30. EW (top), NS (middle), UD (bottom)

Before calculating of Fourier Amplitude Spectra (FAS), acceleration records are divided into one-minute segments. Then these data have been filtered to remove noise from signal. A band-pass filter with a 0.20 Hz low corner frequency and 10 Hz high corner frequency was used. The frequency range was specifically chosen to show the critical natural frequencies of structure vibration. Because of that the signal has a higher noise effect in higher frequencies, it is difficult to distinguish between structural and noise modes at frequencies higher than 10 Hz. Consequently, the highest possible frequencies resolution up to 10 Hz is calculated, and frequencies higher than 10 Hz are subtracted from the modal estimation. Thus, distortions and shifts of the reference baseline can be corrected for especially data set 16032016 (Case 3) and their results are obtained consistently in physical velocities and displacements. The recorded accelerations are then double integrated to obtain modal displacements at corresponding floors.

The Fourier amplitude spectra of each segment are calculated following de-trending to remove the linear trend from input data. Each window is overlapped with 50%. This spectrum has been smoothed according to optimum smoothing window length before calculating the ratio. The smoothing helps to decrease the effect of noise. The type of smoothing window is selected Hamming window. The optimal smoothing window length is selected as 11. All velocities, displacements and Fourier amplitude spectrum were calculated for all locations. The Smoothed FAS (SFAS) are given in figures between 5.8 and 5.15. The Fourier amplitude spectra are computed for the two horizontal components and the vertical components based on a moving window of about 60 second.

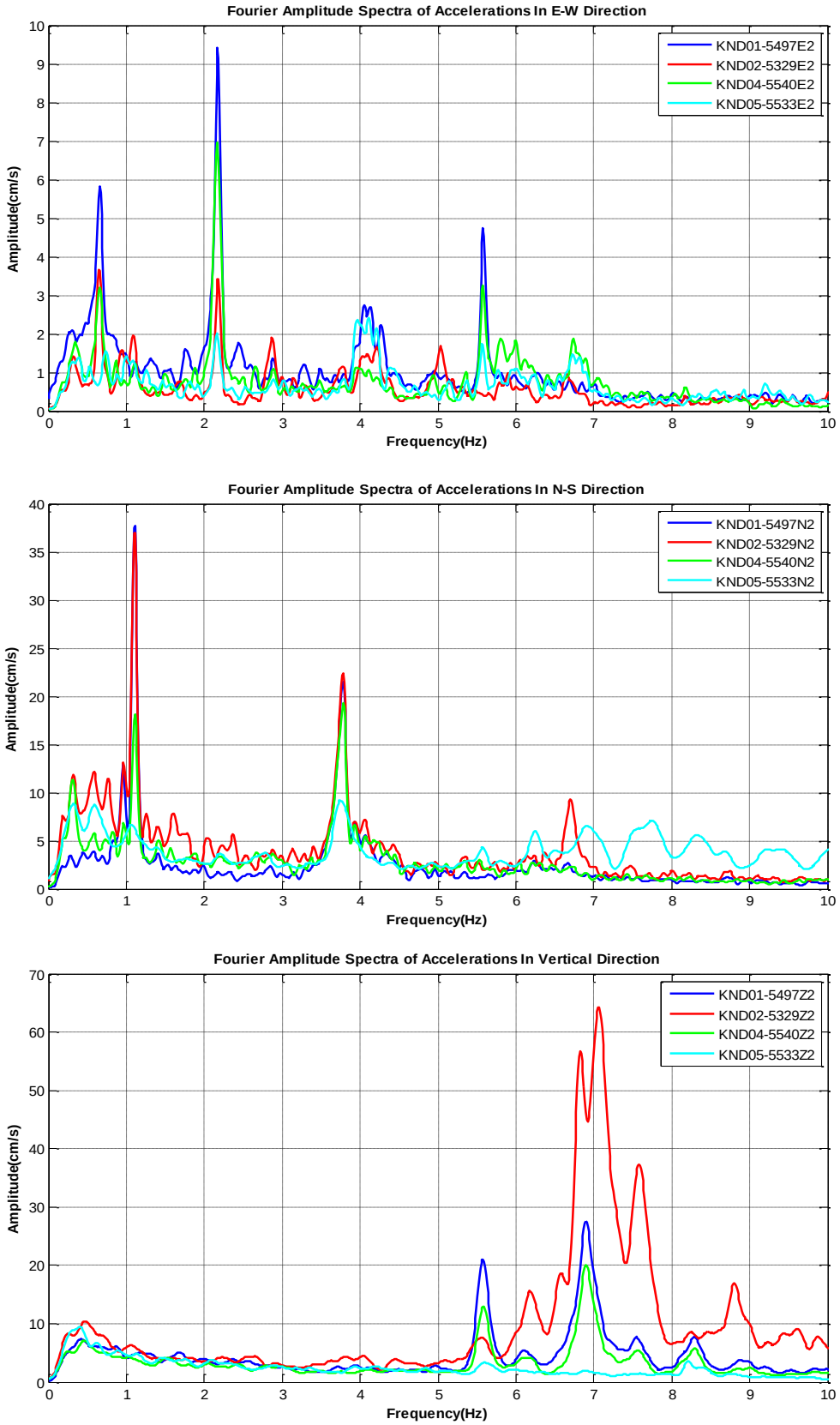

Figure 5.8. Smoothed Fourier Amplitude Spectra of records at 10.30 a.m. on 27 March 2015 (Case 1). (a) EW component (b) NS component (c) UD component

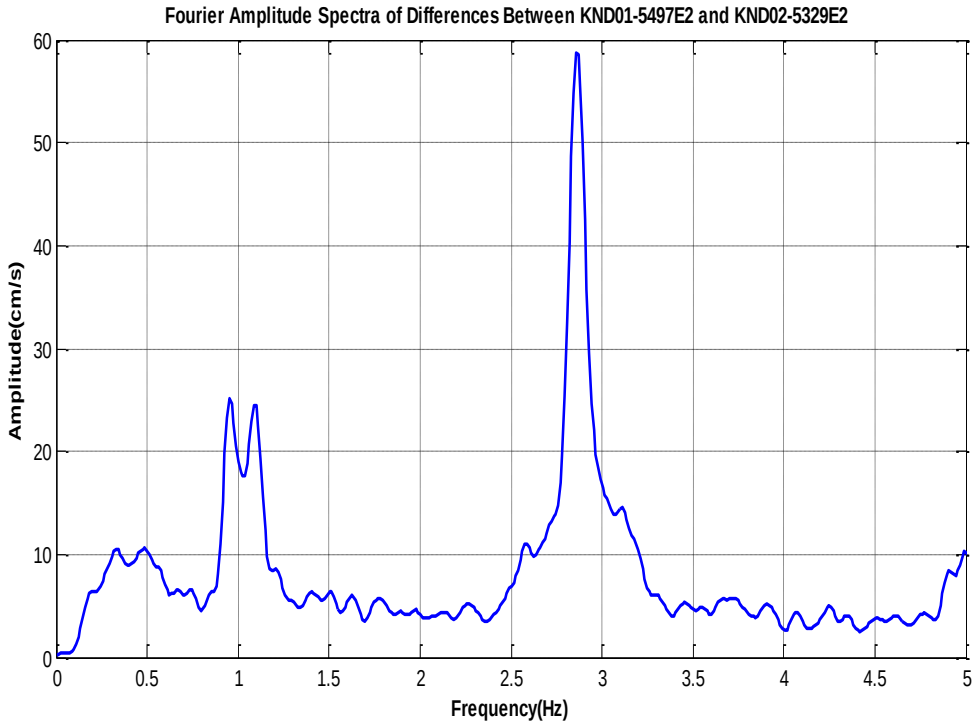

Figure 5.9. Smoothed Fourier Amplitude Spectra of records at 10.30 a.m. on 27 March 2015 (Case 1). Torsional frequencies (f_1=0.94 Hz and f_2=2.90 Hz) are identified from Smoothed Fourier Amplitude Spectra of differences (EW) between two parallel accelerations.

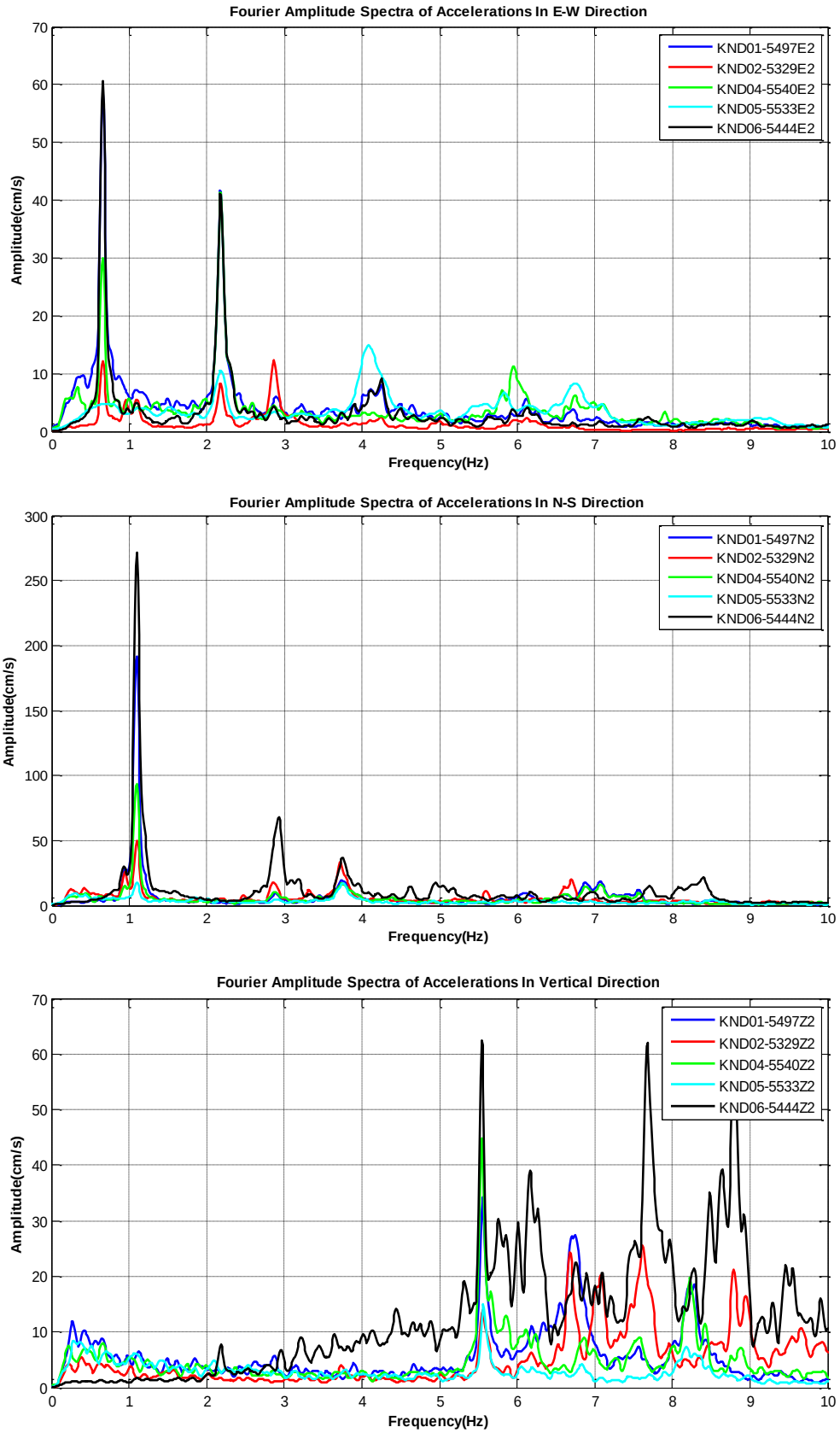

Figure 5.10. Smoothed Fourier Amplitude Spectra of records at 11.30 a.m. on 27 March 2015 (Case 1). (a) EW component (b) NS component (c) UD component

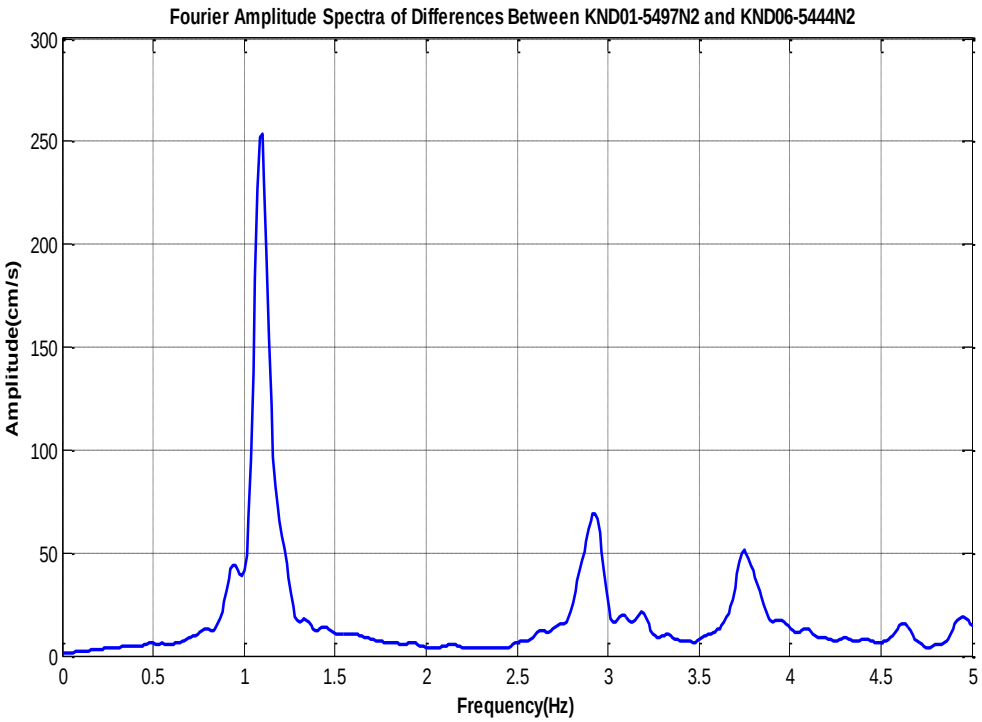

Figure 5.11. Smoothed Fourier Amplitude Spectra of records at 11.30 a.m. on 27 March 2015 (Case 1). Torsional frequencies (f_1=0.94 Hz and f_2=2.90 Hz) are identified from Smoothed Fourier Amplitude Spectra of differences (NS) between two parallel accelerations.

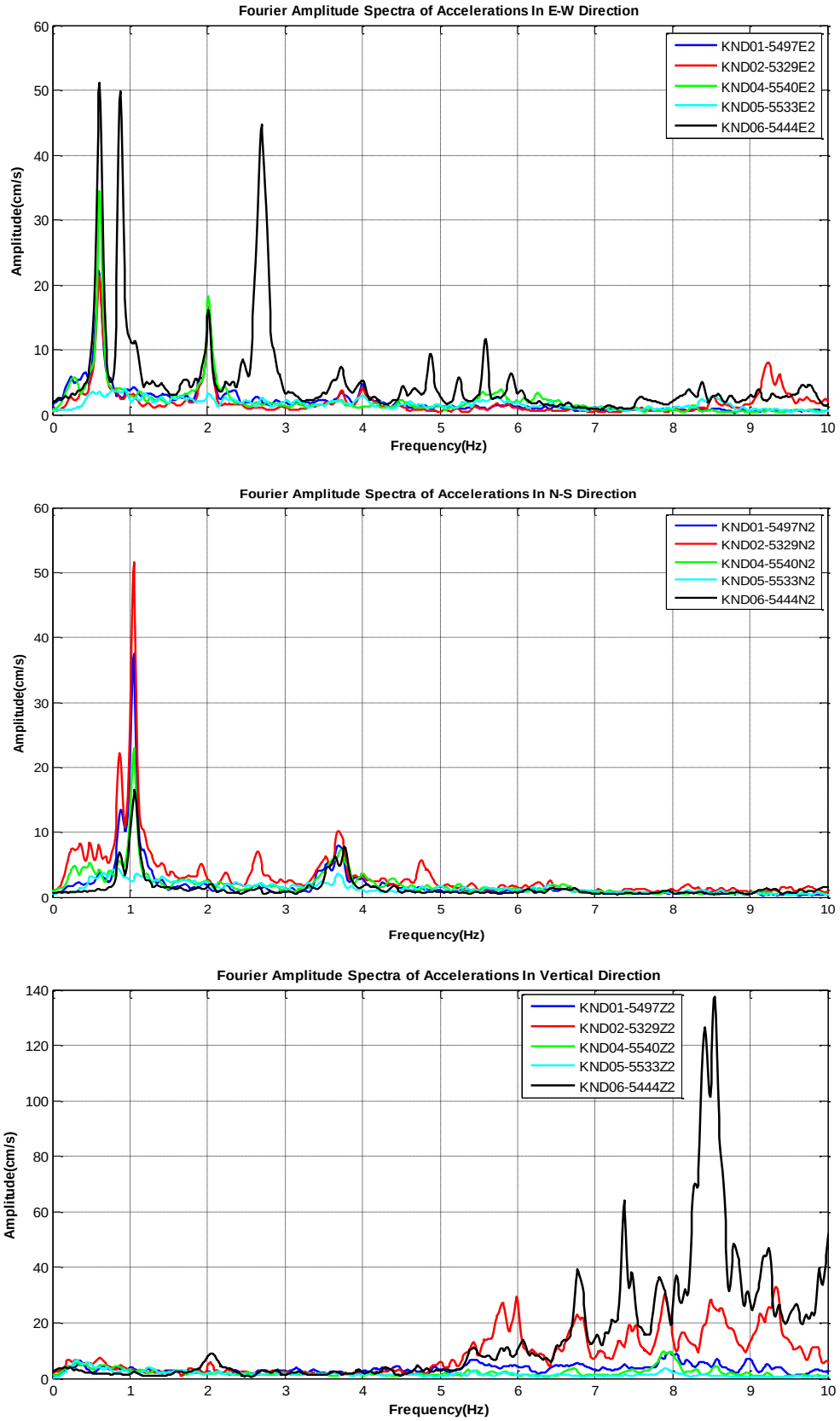

Figure 5.12. Smoothed Fourier Amplitude Spectra of records at 11.30 a.m. on 13 September 2015 (Case 2). (a) EW component (b) NS component (c) UD component

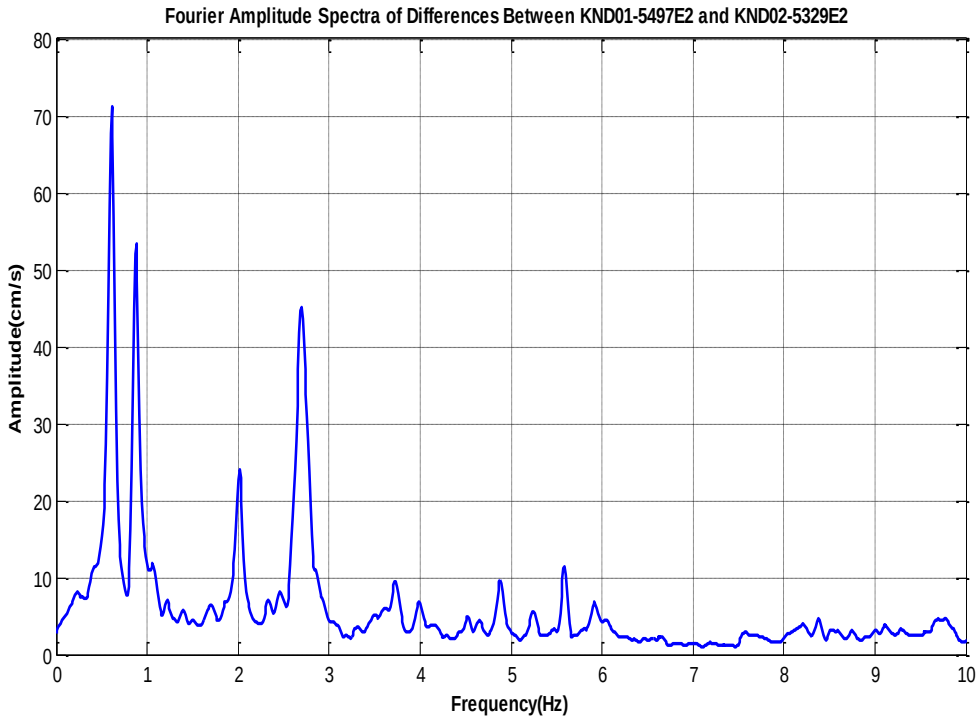

Figure 5.13. Smoothed Fourier Amplitude Spectra of records at 11.30 a.m. on 13 September 2015 (Case 2). Torsional frequencies (f_1=0.87 Hz and f_2=2.70 Hz) are identified from Smoothed Fourier Amplitude Spectra of differences (EW) between two parallel accelerations.

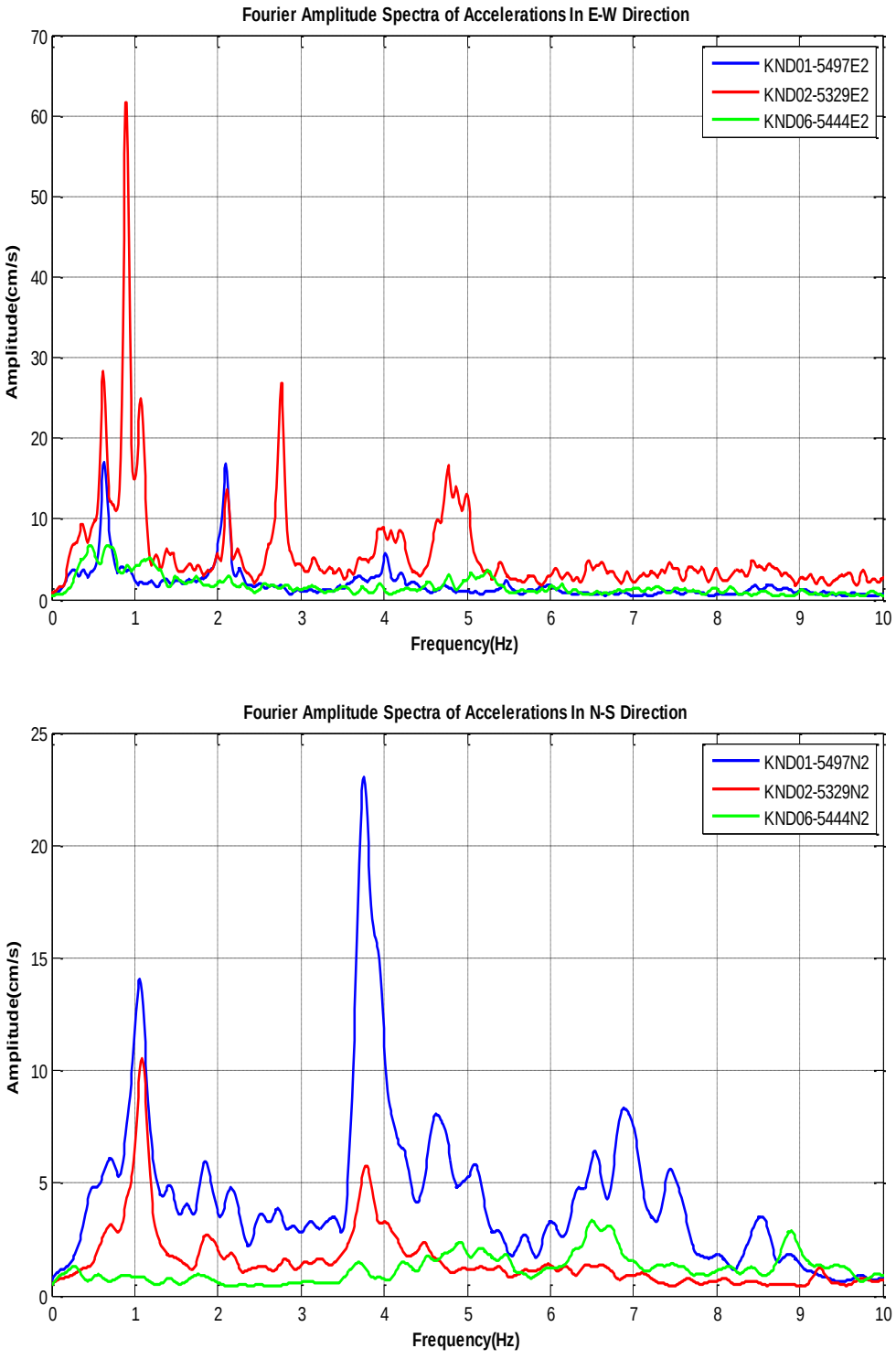

Figure 5.14. Smoothed Fourier Amplitude Spectra of records at 10.50 a.m. on 16 March 2016 (Case 3). (a) EW records (b) NS Direction records.

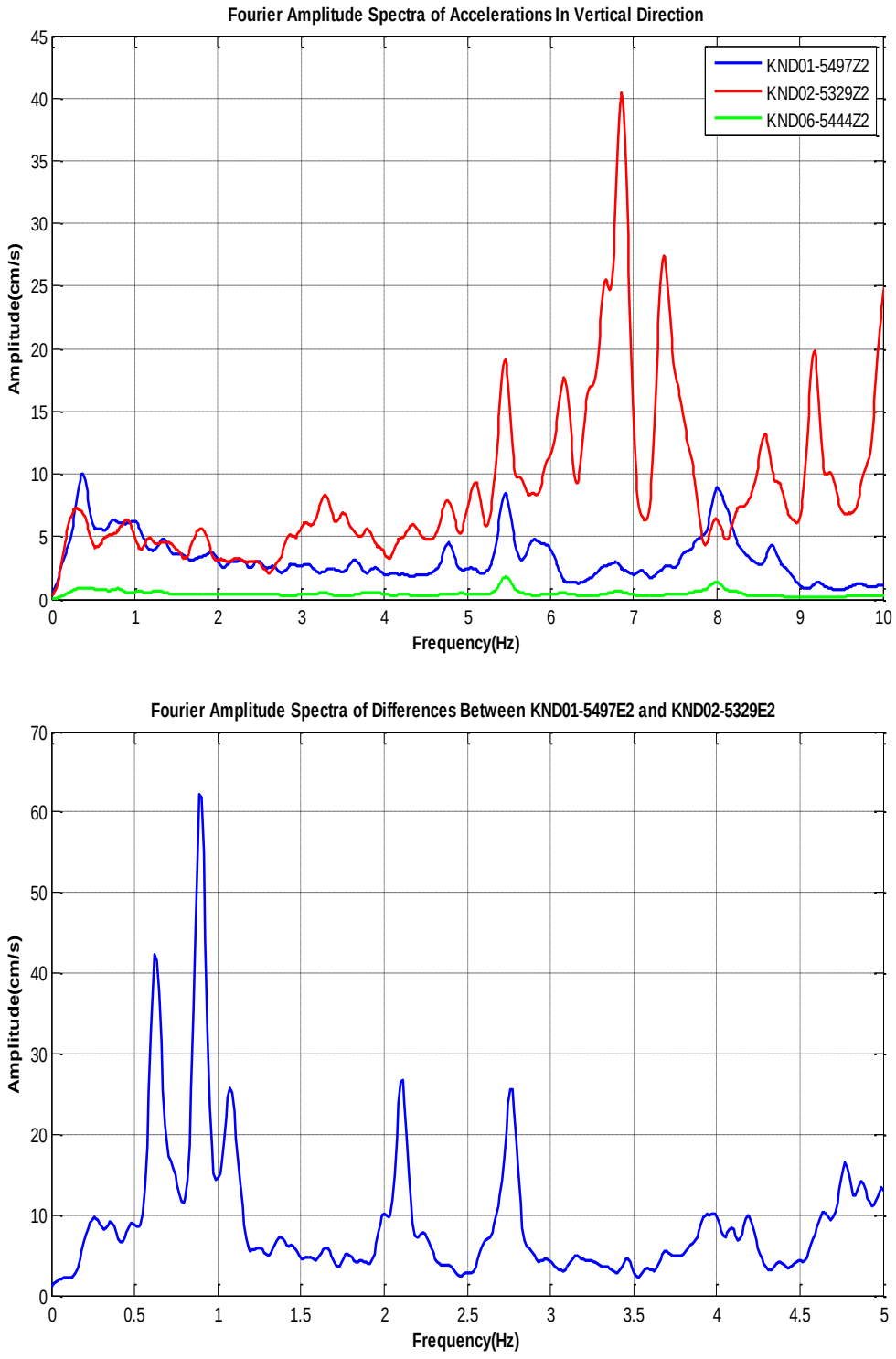

Figure 5.15. Smoothed Fourier Amplitude Spectra of records at 10.50 a.m. on 16 March 2016 (Case 3). (a) UD records (b) Torsional frequencies (f_1=0.89 Hz and f_2=2.77 Hz) are identified from Smoothed Fourier Amplitude Spectra of differences (EW) between two parallel accelerations.

5.3. Modal Frequencies

The identification of the modal frequencies is to inspect FAS of the records. FAS reach peak values at frequencies related to modal frequencies due to resonance effects. If the structural forces acting on the structure are a certain frequency, this frequency in the FAS of record may also appear as one of the maximum ones. Besides, for cases where we have the records of the response (i.e., the output) and the excitation (i.e., the input), the input-to-output transfer function is calculated, which is the output/input ratio of the FAS (Şafak and Çaktı, 2014). This ratio is called transfer function. In general, the excitation has a wide frequency band for cases where we do not have the excitation record (e.g., wind-induced vibrations), and so there is no need to calculate transfer function. However, in this study, transfer functions will calculate and plot in Section 5.5.2. In this part, Smoothed Fourier Amplitude Spectra were calculated and plotted for all stations to identify the peaks in the SFAS of the response corresponds to modal frequencies. Torsional frequencies are identified from Smoothed Fourier Amplitude Spectra of differences between two parallel accelerations.

In Figures 5.8 and 5.10, the first sharp peak occurs at 1.11 Hz in the NS components and at 0.66 Hz in the EW components for 270320151030 and 270320151130 data sets. These amplitudes are the fundamental frequency of vibration for the building and increase with increasing height of the floors. The second bending modes at frequencies at 2.16 Hz and 3.78 Hz show up in the EW and NS directions with rising amplitude from lower to upper floors, respectively. The first two torsional modes are identified at frequencies of 0.94 Hz and 2.90 Hz in Figures 5.9 and 5.11. It is important that the peaks in the vertical component at 7.60 Hz, 8.20 Hz, and 8.80 Hz can be recognized as tension, since there are no important energies at these frequencies range on the two horizontal parts; however, the amplitude is increasing with the floor level on the vertical direction. A summary of the frequencies for Case 1 is given in Table 5.1.

Table 5.1. The natural frequencies obtained SFAS from the data sets 270320151030 and 270320151130.

Mode	Mode Descriptions	Frequency (Hz) from Fourier Amplitude Analysis
1	1st translational mode (EW)	0.66
2	1st torsional mode	0.94
3	1st translational mode (NS)	1.11
4	2nd translational mode (EW)	2.16
5	2nd torsional mode	2.90
6	2nd translational mode (NS)	3.78

In Figures 5.12 shows the first translational modes in the EW and NS directions at frequencies 0.61 Hz and 1.05 Hz for 130920151130 data sets, respectively. These amplitudes are the fundamental frequency of vibration for the building and increase with increasing height of the floors. In the second frequency range, the second bending modes at frequencies at 2.01 Hz and 3.66 Hz demonstrate in the EW and NS components, respectively. The EW component increases amplitude with the story reaching a peak at the 7th level and decrease a little bit at the 15th floor. The amplitude of latter component increases with the story reaching a peak at the 15th level and the amplitudes of 7th and 15th floors are almost same. The first two torsional modes are identified at frequencies of 0.87 Hz and 2.70 Hz in Figure 5.13. The peak in the vertical component at 6.80 Hz, 7.50 Hz, and 8.60 Hz can be recognized as tension, since there are no important energies at these frequencies range on the two horizontal parts; however, the amplitude is increasing with the floor level on the vertical direction. A summary of the frequencies for Case 2 are given in Table 5.2.

Figure 5.14 demonstrates the Smoothed Fourier amplitude where the maximum points are the natural frequencies of the structure for data set 160320151050. It is obtained that the frequencies of the first and second bending modes are 0.62 Hz and 2.11 Hz, respectively in the EW direction as well as 1.05 Hz and 3.77 Hz, respectively in the NS

direction as the result of ambient vibration tests. The first two torsional modes are identified at frequencies of 0.89 Hz and 2.77 Hz in Figure 5.15. A summary of the frequencies for Case 3 are given in Table 5.3.

Table 5.2. The natural frequencies obtained SFAS from the data set 130920151130.

Mode	Mode Descriptions	Frequency (Hz) from Fourier Amplitude Analysis
1	1st translational mode (EW)	0.61
2	1st torsional mode	0.87
3	1st translational mode (NS)	1.05
4	2nd translational mode (EW)	2.01
5	2nd torsional mode	2.70
6	2nd translational mode (NS)	3.66

Table 5.3. The natural frequencies obtained SFAS from the data set 160320161050.

Mode	Mode Descriptions	Frequency (Hz) from Fourier Amplitude Analysis
1	1st translational mode (EW)	0.62
2	1st torsional mode	0.89
3	1st translational mode (NS)	1.05
4	2nd translational mode (EW)	2.11
5	2nd torsional mode	2.77
6	2nd translational mode (NS)	3.77

For three different construction stages, Smoothed Fourier Amplitude Spectra in the NS direction plot also provide evidence of modal coupling (i.e. vibration modes which have both translational and rotational motion). The first and second torsional modes are a good example of this behavior.

The changes in the building's the first fundamental frequencies from obtained the ambient vibration data sets follow a clear trend, except for Case 3. The differences of the variation in the first two natural frequencies between Case 1 and Case 2 are approximately lower than 7.5% and 7%, respectively. In Case 2, the natural frequencies decrease naturally due to increasing the mass and no contribution to stiffness by the façade system. In Case 3, all glass curtain walls assembly and other whole operations of the monitoring building were completed. Due to the fact that the total mass is higher than Case 2, the natural frequencies obtained ambient vibration tests were observed on increase about 1.6% for first fundamental frequencies in the EW direction and about 5% for second fundamental frequencies. The first fundamental frequency in the NS direction is same. That is why the building stiffness is higher than Case 2 since the gaps of the slabs were closed with steel construction and it gives the structure a little stiffness. The correlations of Smoothed FAS (SFAS) plot for three data sets are provided in Figures 5.16 and 5.17 and the natural frequencies are listed in Table 5.4. They verify that the obtained frequencies are consistent for all three cases.

Table 5.4. Comparison of the natural frequencies obtained using SFAS from the ambient vibration data sets for three different construction stages.

Mode	**Mode Shape**	**Ambient Vibration Test#1**	**Ambient Vibration Test#2**	**Ambient Vibration Test#3**
		Frequency(Hz)	**Frequency(Hz)**	**Frequency(Hz)**
1	1st translational EW	0.66	0.61	0.62
2	1st translational NS	1.11	1.05	1.05
3	2nd translational EW	2.16	2.01	2.11
4	2nd translational NS	3.78	3.66	3.77
5	1st torsional	0.94	0.87	0.89
6	2nd torsional	2.90	2.70	2.77

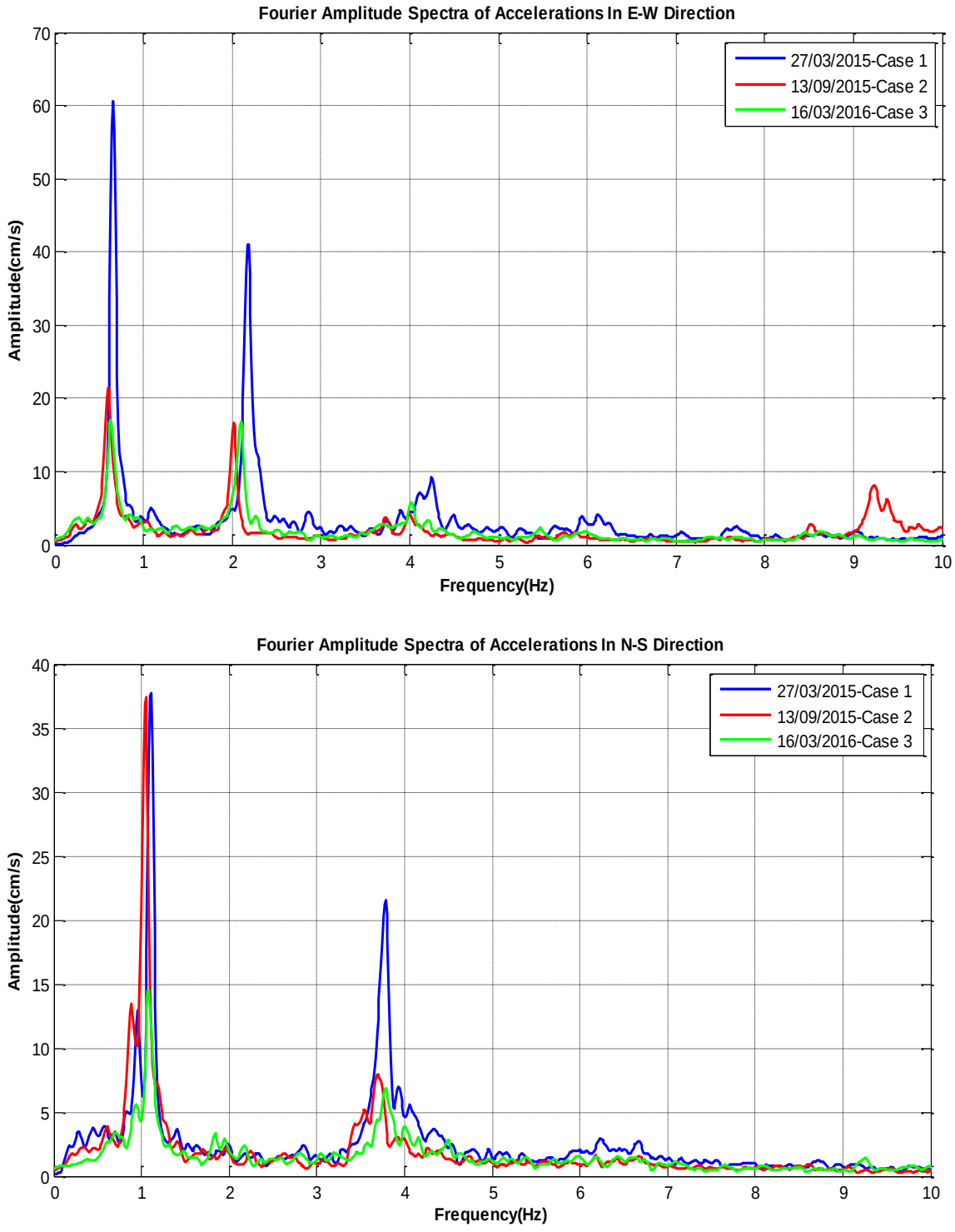

Figure 5.16. Correlation of Spectral Analysis (SFAS) of Ambient Vibration Data at different construction stages. (a) East-West Direction records (b) North-South Direction records

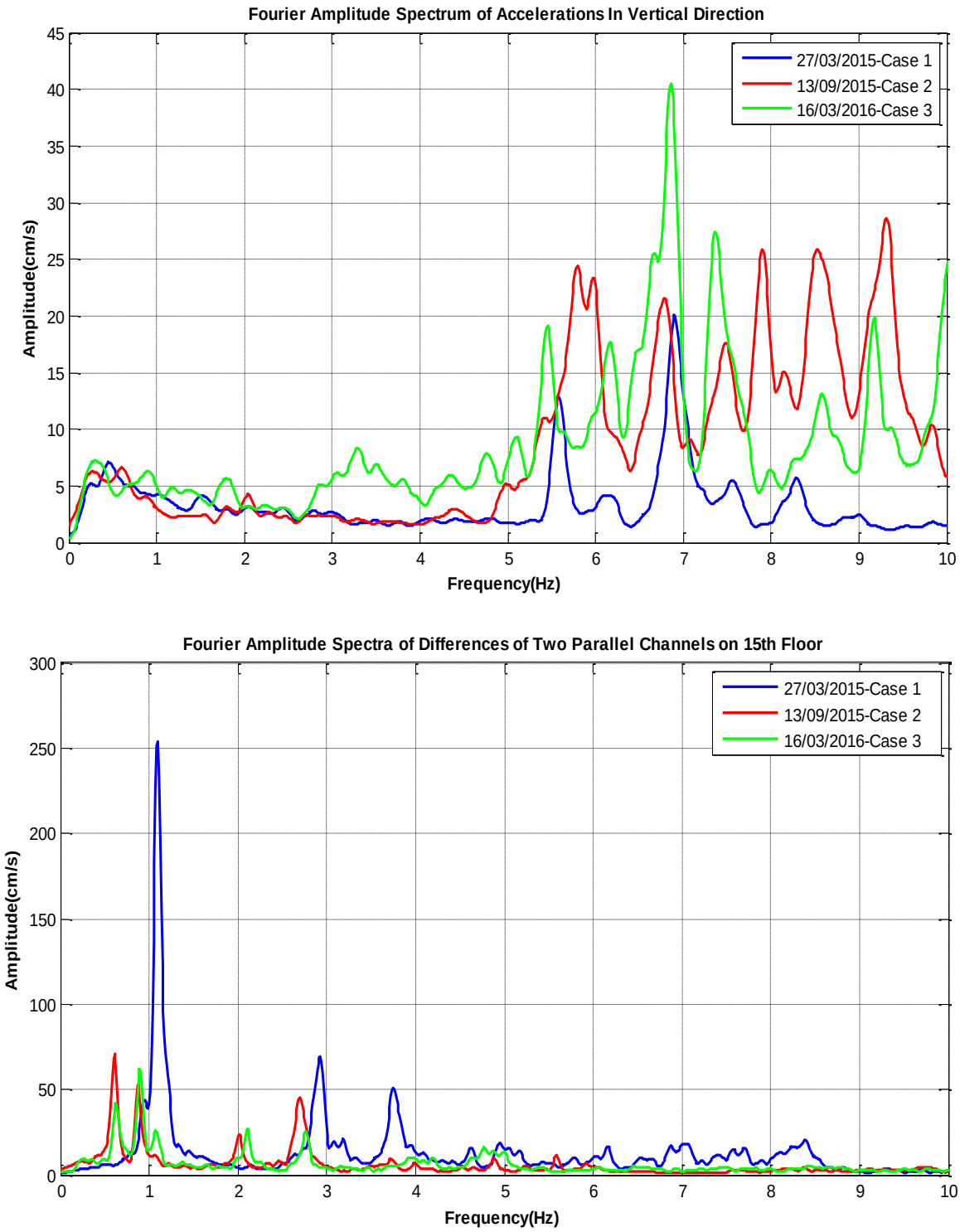

Figure 5.17. Correlation of Spectral Analysis (SFAS) of Ambient Vibration Data at different construction stages. (a) Vertical Direction records (b) Torsional frequencies for three construction stages are identified from the difference between two parallel accelerations.

5.4. Spectral Analysis

In spectral analysis, S_{xx} and S_{yy} are square matrices, which are the cross power spectral density of the data obtained two different sensors. These indices are the power spectral density of the accelerations in two horizontal directions, respectively, and S_{xy} is the cross-spectrum density of two horizontal directions. Detailed spectral analyses of the 270320151030, 270320151130,130920151130, and 160320161050 data sets are presented. Power spectral density graphs, cross-spectrum (S_{xy}), phase angle and coherency for 270320151030, 270320151130, and 130920151130 data sets are plotted and calculated. Thus, repeatability in identification of translational modal frequencies is provided to exhibit. Also, these data of Figures from 5.18 to 5.23 show at first two modes in near-perfect coherence and consistent phase angles corresponding to the first and second modal frequencies for the translational modes in the EW and NS directions. The analysis confirms that the frequencies 0.65 Hz and 2.17 for the EW direction correspond to translation as well as the frequencies 1.10 Hz and 3.79 Hz for the NS direction correspond to translation for 270320151030 and 270320151130 data sets, and the frequencies 0.61 Hz and 2.03 Hz for the EW direction correspond to translation as well as the frequencies 1.05 Hz, and 3.70 Hz for the NS direction correspond to translation for the data set 130920151130, since the phase is consistent and the coherence is nearly one at the these locations.

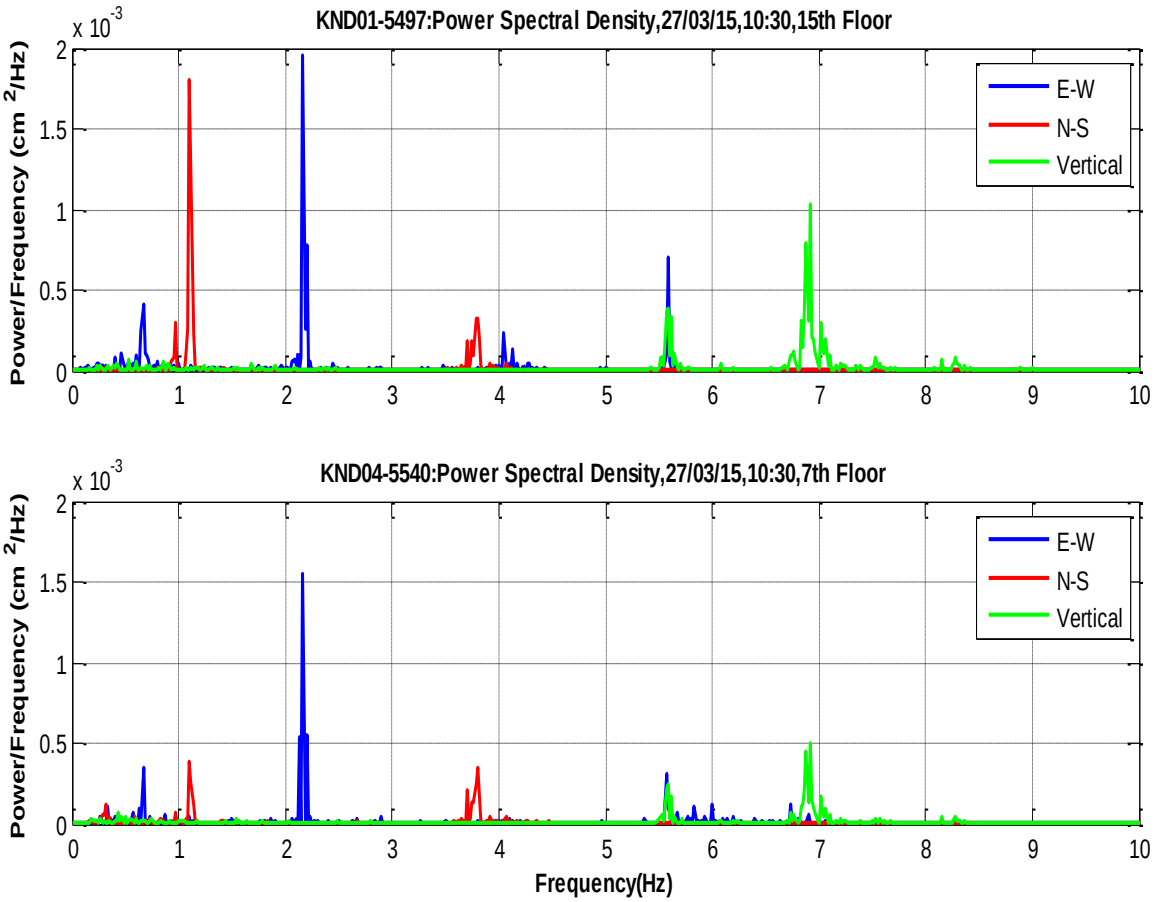

Figure 5.18. PSD of records at 10:30 a.m. on 27 March 2015 using data from level 15 and 7 for East-West, North-South, and Vertical Direction. The blue, red, and green lines demonstrate the East-West, North-South, and Vertical Direction, respectively.

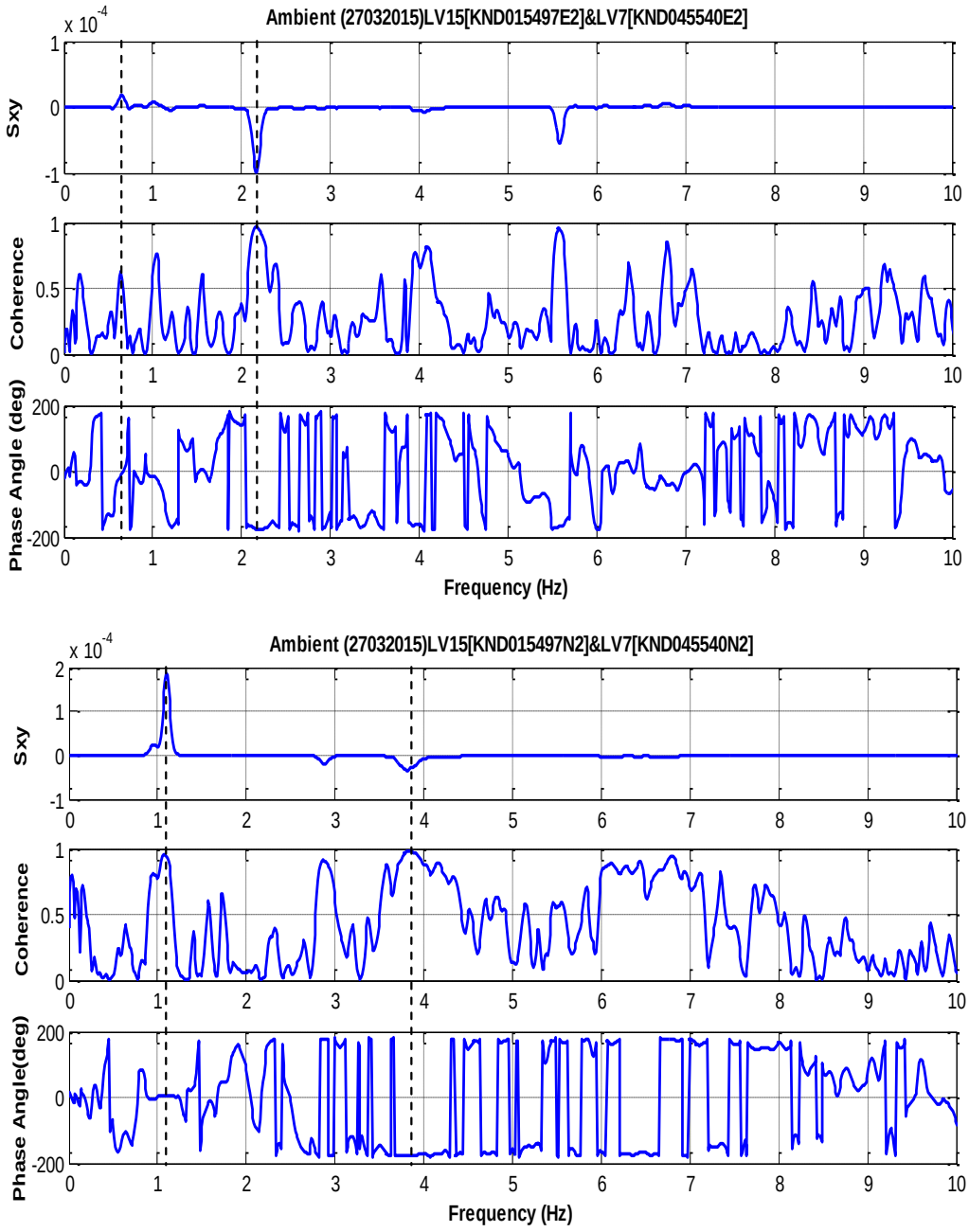

Figure 5.19. Using data set 270320151030 from floors 15 and 7, S_{xy}, phase angle and coherency plots for (a) EW (b) NS (c) Vertical direction.

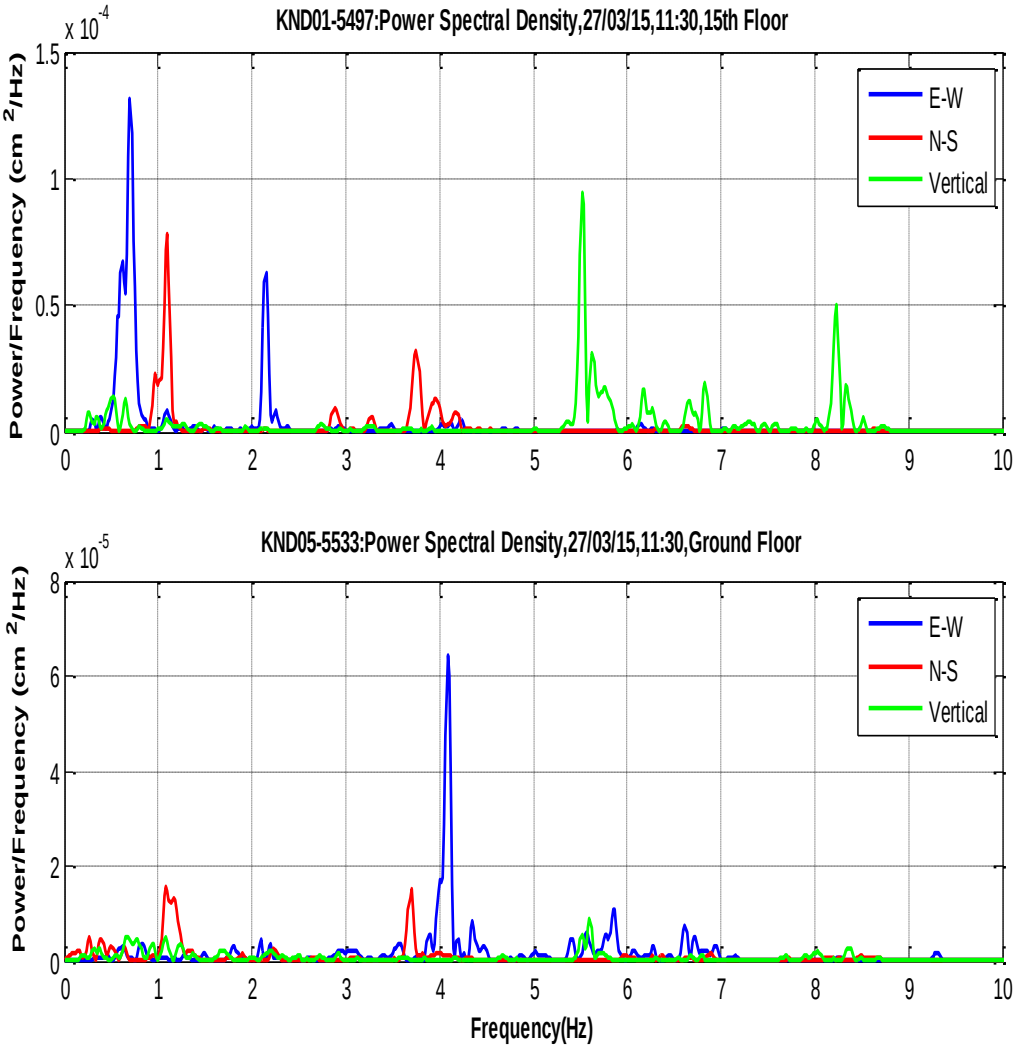

Figure 5.20. PSD of records at 11:30 a.m. on 27 March 2015 using data from level 15 and 7 for East-West, North-South, and Vertical Direction. The blue, red, and green lines demonstrate the EW, NS, and UD Directions, respectively.

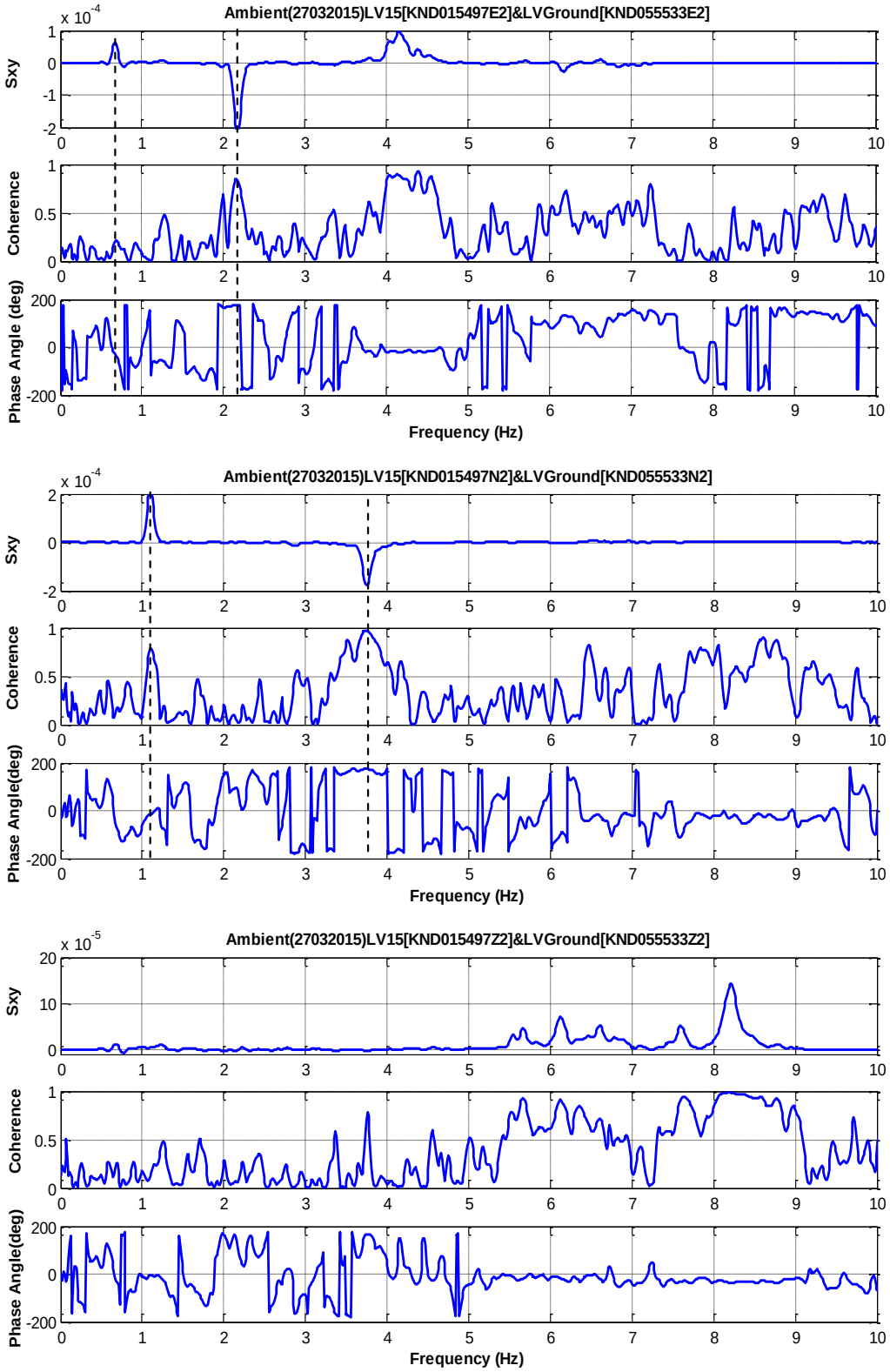

Figure 5.21. Using data set 270320151130 from levels 15 and Ground, S_{xy}, phase angle and coherency plots for (a) EW (b) NS (c) Vertical direction.

Table 5.5. The Natural Frequencies Obtained Using Spectral Analysis from the data sets 270320151030 and 270320151130.

Mode	Mode Descriptions	Frequency (Hz) from Spectral Analysis
1	1st translational mode (EW)	0.65
2	1st translational mode (NS)	1.10
3	2nd translational mode (EW)	2.17
4	2nd translational mode (NS)	3.79

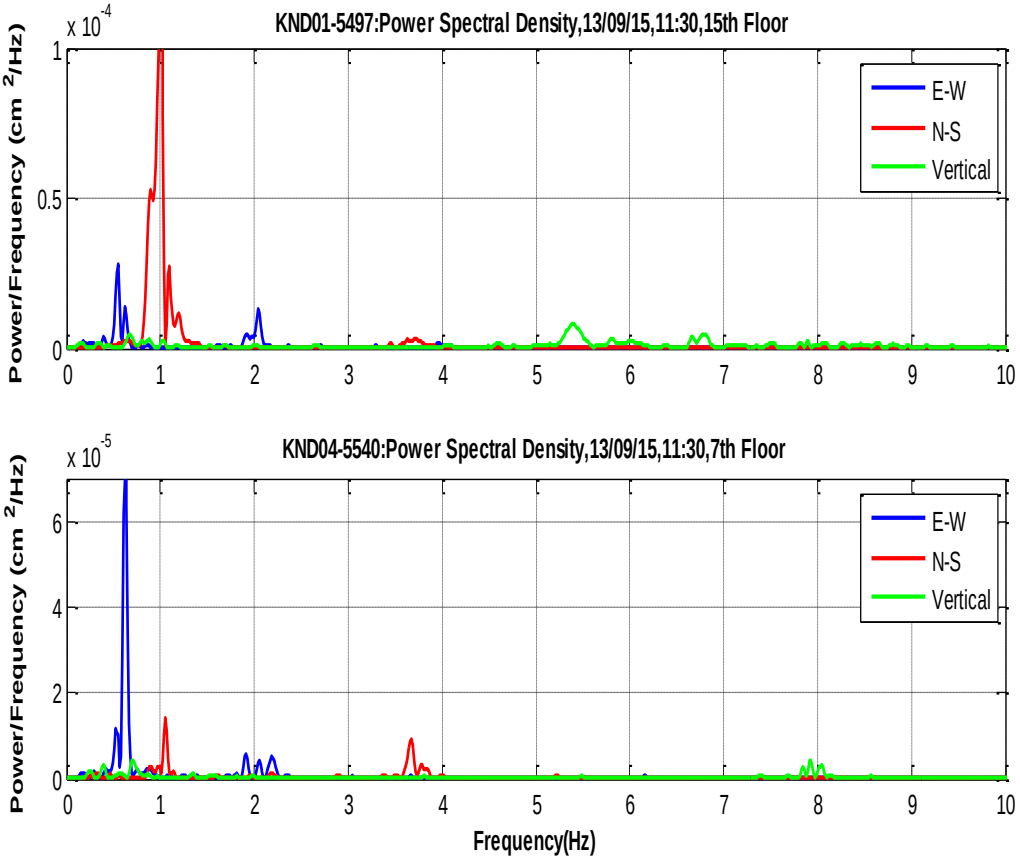

Figure 5.22. PSD of recorded at 11:30 a.m. on 13 September 2015 using data from level 15 and 7 for East-West, North-South, and Vertical Direction. The blue, red, and green lines demonstrate the East-West, North-South, and Vertical Direction, respectively.

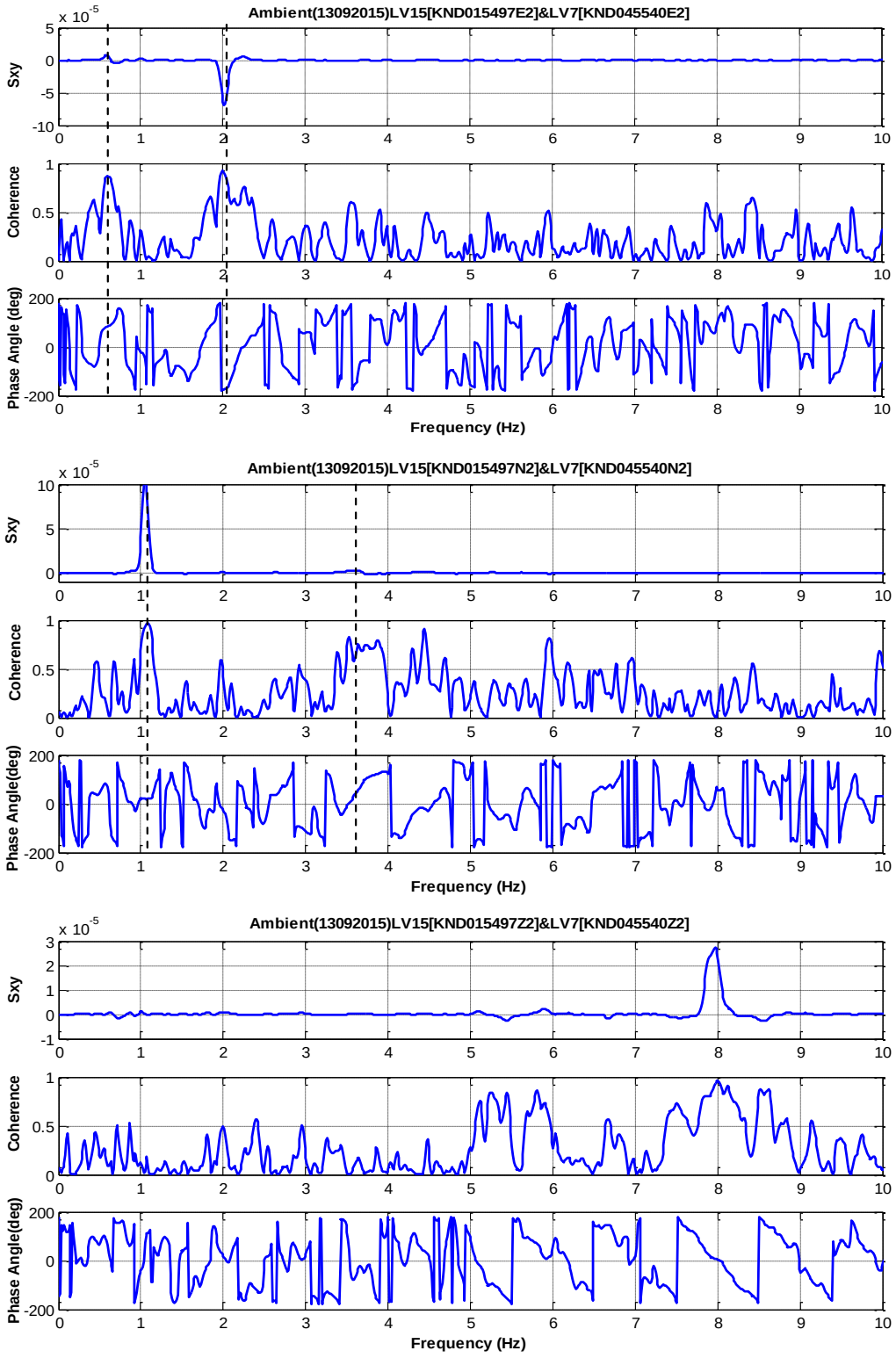

Figure 5.23. Using data set 130920151130 from levels 15 and 7, S_{xy}, phase angle and coherency plots for (a) EW (b) NS (c) Vertical direction

Table 5.6. The natural frequencies obtained using Spectral Analysis from the data set 130920151130.

Mode	Mode Descriptions	Frequency (Hz) from Spectral Analysis
1	1st translational mode (EW)	0.61
2	1st translational mode (NS)	1.05
3	2nd translational mode (EW)	2.03
4	2nd translational mode (NS)	3.70

5.5. System Identification

A correct well-known finite element model is needed to symbolize the dynamics of the structure so as to suppose the response of a structure. The process of building a modal model of a physical system using experimental data is identified system identification. System identification of ambient vibration structures using output-only identification techniques has become a key issue in structural health monitoring and assessment of structures and this analysis was calculated obtained the ambient data test and compare them with those determined by spectral analyses. It is aim to identify the relevant properties of monitoring building from measurements of the output(s) of the given system. The measured outputs are the story accelerations. The outputs are recorded by the sensor network. The natural frequencies, mode shapes and modal damping ratios are modal parameters of the ambient vibration structures.

There are several mathematical models on the output-only identification techniques such as parametric methods in the time-domain and non-parametric in the frequency-domain. Each identification method in either the time domain or the frequency one has its own advantage and limitation. Non-parametric models such as transfer functions and coherence functions are called non-parametric methods since they do not involve direct estimation of physical or mathematical model parameters (Akira, 2003). Among the nonparametric methods in the frequency domain, FDD has been very widely used recently for output-only system identification through the ambient vibration measurements due to

its reliability, straightforward and effectiveness. The modal parameters are estimated via Singular Value Decomposition of the cross-spectrum matrix. These values contain frequency and damping information and singular vectors contain mode shape information. The main advantage of this method is relatively useful to implement and use since this method is not in need of any inputs and it is useful of detecting close modes.

5.5.1. Ambient Vibration Recordings Processing Using Frequency Domain Decomposition

The determination of dynamic properties such as the natural frequencies and corresponding mode shapes is done through modal analysis. Operational modal analysis procedures need ambient vibration in order to calculate the corresponding Power Spectral Density (PSD) functions and so that the consistent approximations of the modal factors extract as possible. In this study, the Frequency Domain Decomposition is carried out for whole data of all channels in the 23 storey reinforcement building.

The main step of this technique is the Spectral Density matrices were calculated for all the series of datasets. The dimension of the matrix is n x n and n is the number of transducers. In this study, the size of the matrices of three data sets is 12 x 12 for Case 1 and Case 2 and 9 x 9 for Case 3. Each element of those matrices is a Spectral Density function. The diagonal elements of the matrix are the real valued Spectral Densities between a response and Auto Power Spectral Density.

The measured data are processed using a MATLAB code developed for FDD analysis so as to determine the system modal parameters. These modal parameters are then compared with those obtained via finite element model. Modal peak in the frequency domain can be placed by a peak-picking technique on the plot of the singular values starting from the Singular Value Decomposition of Equation 3.17 (Pioldi *et al.*, 2014).

Figure 5.24, 5.25, and 5.26 demonstrate the cross power spectral density matrix where the peaks are the natural frequencies of structure monitored. In following Figures 5.24, 5.25, and 5.26, First Singular Value/Frequency graphs related to each adopted ambient vibrations were presented, with aim to check their characteristics, those are their

frequency contents and associated with singular value for each frequency. The limit of the frequency x-axes is associated with the Nyquist frequency of the signal, though the limit of the y-axis is the singular values of the data sets. The Nyquist frequency is to half of the recording frequency adopted by the structure monitored system. Nyquist frequency of the signal was re-sampled at a lower sampling rate and frequency axes in figures were showed until 10 Hz. The singular values of the data sets represent the power of the signals, in terms of spectra ($[(cm/s^2)^2/Hz]$).

As mentioned earlier, the singular vectors in Equation 3.18 correspond to an estimation of the mode shapes, and the corresponding singular values are the Spectral Densities of the singular degree freedom system stated in Equation 3.16. 12 singular values, and 12 singular vectors for each frequency were obtained for the most significant 6 singular values are shown.

As a result, the spectral eigenvalues and eigenvectors characterize modal factors of the structures. By peak-picking, applied to the first singular values, 6 significant modes were obtained in the frequency between 0.0 Hz to 10.0 Hz. Estimated peak frequencies will compared with analytical finite element model (FEM) results to identify natural frequencies associated with order of mode shapes. The modes are numbered on the plot. Modal frequencies identified are listed in Table 5.7, Table 5.8 and Table 5.9.

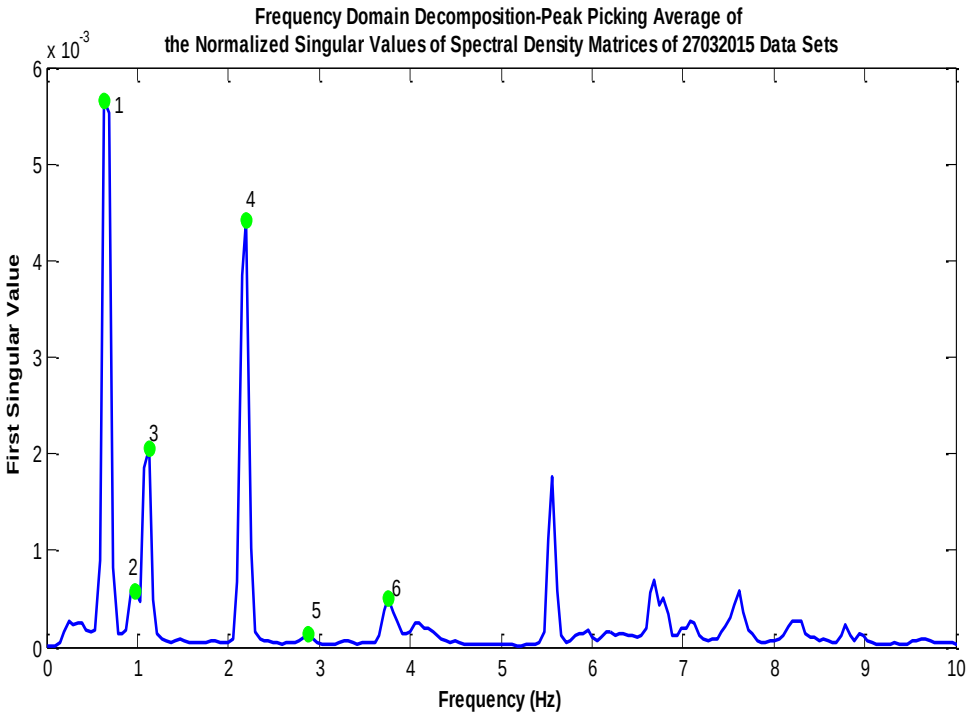

Figure 5.24. First Singular values of the spectral density matrices of data sets 27032015 and selected frequencies of interest

Table 5.7. The natural frequencies obtained FDD technique from the data sets 27032015 at 10:30 and 11:30

Mode	Mode Descriptions	Frequency (Hz) from FDD Technique
1	1st translational mode (EW)	0.66
2	1st torsional mode	0.92
3	1st translational mode (NS)	1.11
4	2nd torsional mode	2.89
5	2nd translational mode (EW)	2.17
6	2nd translational mode (NS)	3.78

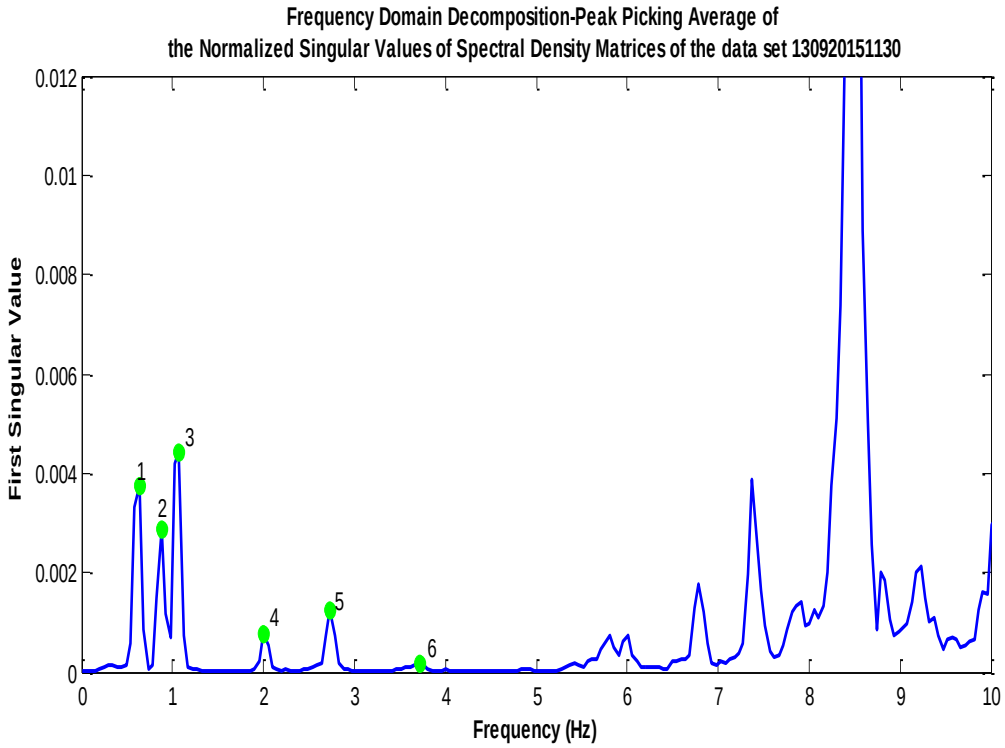

Figure 5.25. First Singular values of the spectral density matrices of the data set 130920151130 and selected frequencies of interest.

Table 5.8. The natural frequencies obtained FDD technique from the data set 130920151130.

Mode	**Mode Descriptions**	**Frequency (Hz) from FDD Technique**
1	1st translational mode (EW)	0.61
2	1st torsional mode	0.87
3	1st translational mode (NS)	1.07
4	2nd torsional mode	2.72
5	2nd translational mode (EW)	2.00
6	2nd translational mode (NS)	3.71

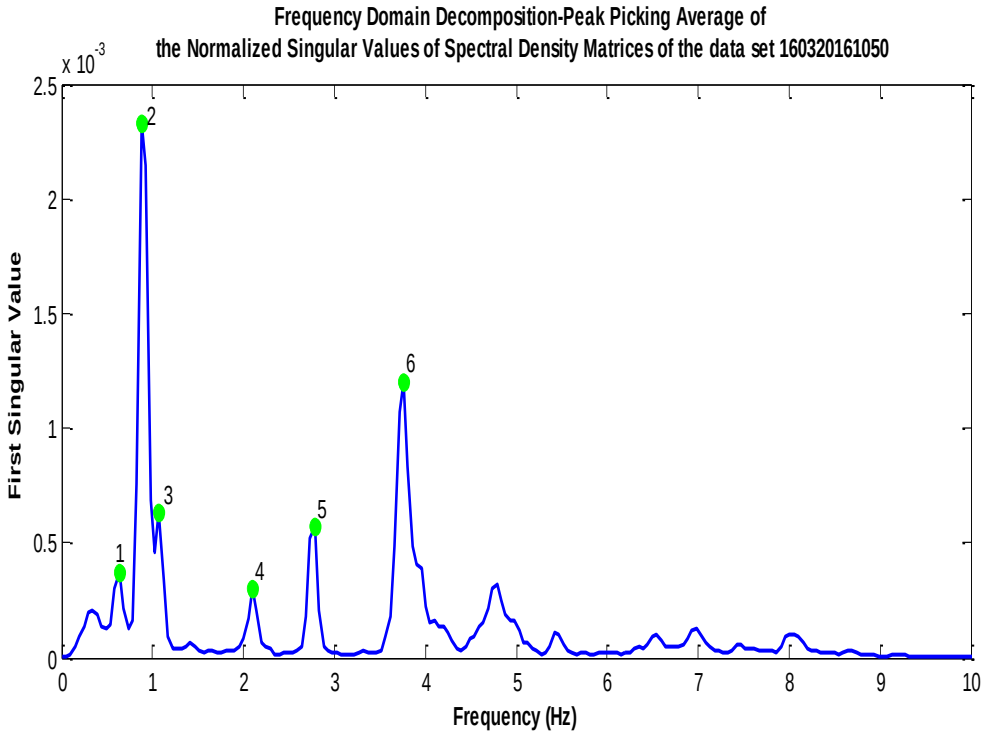

Figure 5.26. First Singular values of the spectral density matrices of the data set 160320161050 and selected frequencies of interest

Table 5.9. The natural frequencies obtained FDD technique from the data set 160320161050.

Mode	Mode Descriptions	Frequency (Hz) from FDD Technique
1	1st translational mode (EW)	0.62
2	1st torsional mode	0.88
3	1st translational mode (NS)	1.07
4	2nd torsional mode	2.76
5	2nd translational mode (EW)	2.10
6	2nd translational mode (NS)	3.76

5.5.2. Transfer Function Model

Transfer function estimate is a model in the frequency domain that is a Fourier transform of a transient response model (Akira, 2003). Due to the fact that the noise function is included in the Fourier transform of the output signal, this transfer function models may not be a sufficient and accurate enough. As a result, spectral ratios of the system in all directions were obtained. The first basement level acceleration records for data sets 27032015 and 13092015 and the third basement level acceleration records for data set 16032016 were identified as input sequences because of that monitoring structure has rigid structural wall at this level while the 15th level accelerations were identified as output sequences. The transfer function model defines the association between the input and output of the system as shown in the following equation, where $G_{yy}(\omega)$ is output and $G_{xx}(\omega)$ is input:

$$H(\omega) = \frac{Gyy(\omega)}{Gxx(\omega)} \tag{5.1}$$

5.5.2.1. Spectral Analysis of Ambient Vibration Data. The main purpose of system identification is to determine the dynamic properties of a structure using experimental data. The spectral analysis is a more accurate method of estimation, as it is able to decrease the effects of noise since the output and noise functions are uncorrelated. If the transfer functions for the structure are calculated by taking spectral ratios, it is important that the numerator and denominator Fourier spectra are smoothed independently by their corresponding optimal length smoothing windows (Şafak *et al.*, 1997). The coherence function indicates the correlation coefficient between the input and output sequences. Figures from 5.19 to 5.24 in section 5.4 showed the power spectral density and coherence function between base floor and roof floor plots. When obtaining spectral ratio, data processing in Sections 5.1 was applied. In the case of this study, the sampling frequency is changed from 100 Hz to 20 Hz, thus changing the sampling period to 0.05 seconds. The calculated FAS are then smoothed by using running Hamming smoothing windows with optimum lengths. The optimum lengths of smoothing windows are determined as 11. The optimal window is obtained where the decay of this curve slows down significantly. The sampling interval of the records is 100 Hz. All signals from building are decimated by five, and standard 4th order of band-pass Butterworth filter with corner frequencies of 0.20 Hz

and the frequency of the decimated data is 10 Hz. Therefore, by filtering the data, the number of data points is reduced from 6000 to 1200, which is a much more feasible amount of data to work with. The Spectral Ratio of EW and NS direction were shown from Figure 5.27 through Figure 5.32 and modal frequencies were given in Tables 5.10, 5.11, and 5.12.

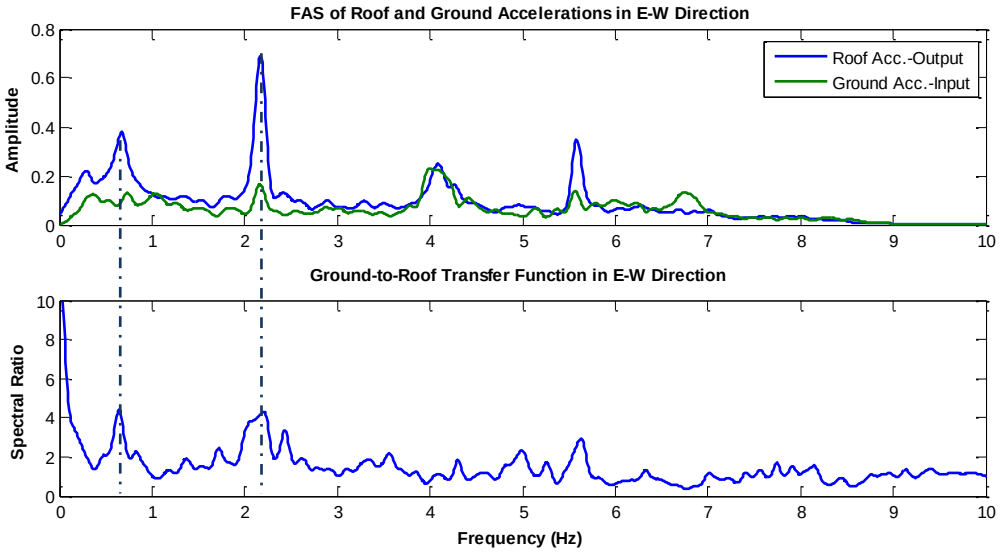

Figure 5.27. Transfer function of a 23-storey tall building of EW direction obtained data sets 27032015.

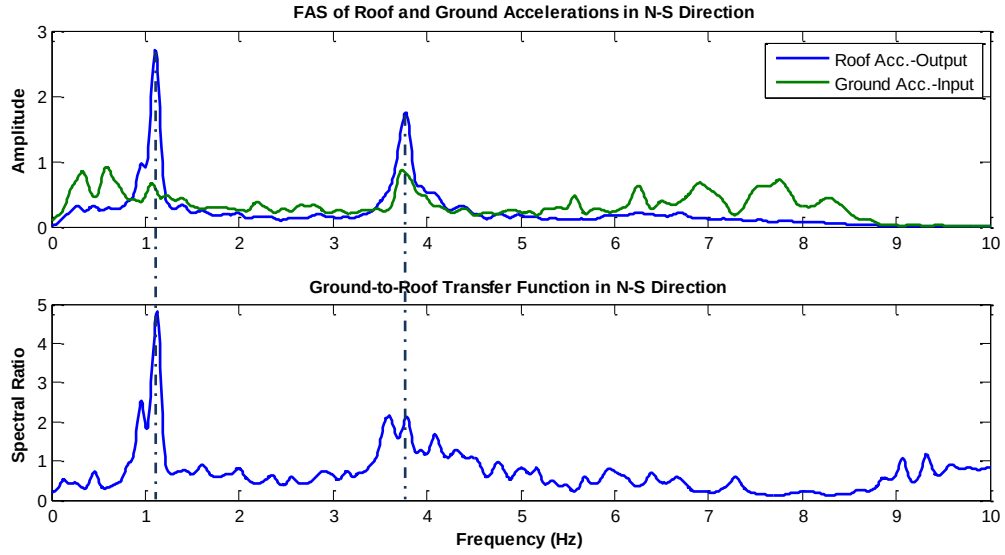

Figure 5.28. Transfer function of a 23-storey tall building of NS direction obtained data sets 27032015.

Table 5.10. The natural frequencies obtained Spectral Ratio from the data sets 27032015.

Mode	Mode Descriptions	Frequency (Hz) from Spectral Ratio
1	1st translational mode (EW)	0.65
2	1st translational mode (NS)	1.12
3	2nd translational mode (EW)	2.17
4	2nd translational mode (NS)	3.77

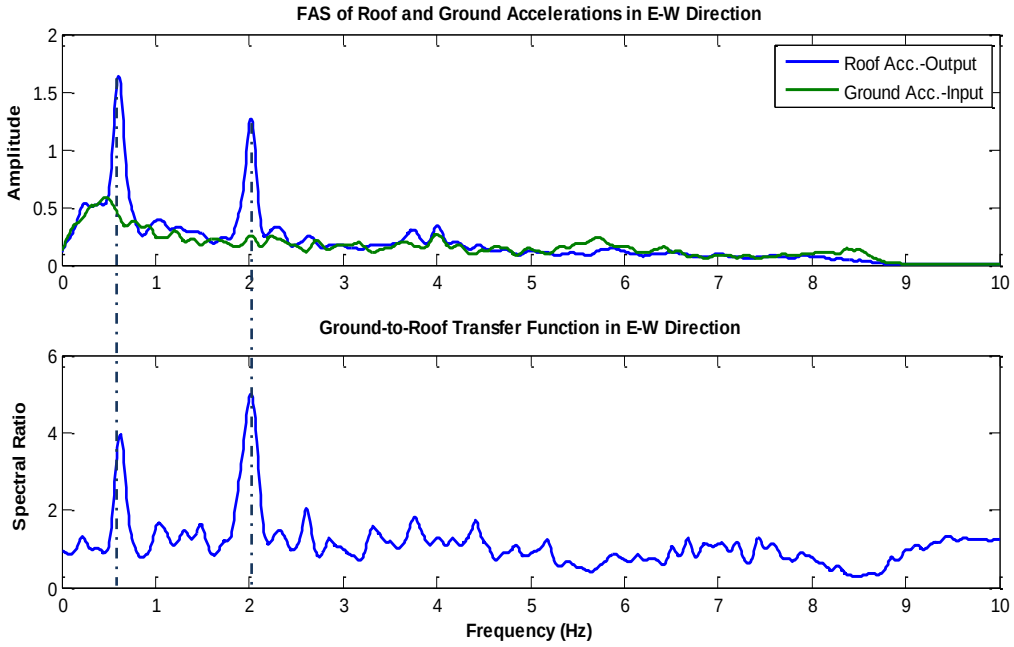

Figure 5.29. Transfer function of a 23-storey tall building of EW direction obtained data sets 130920151130.

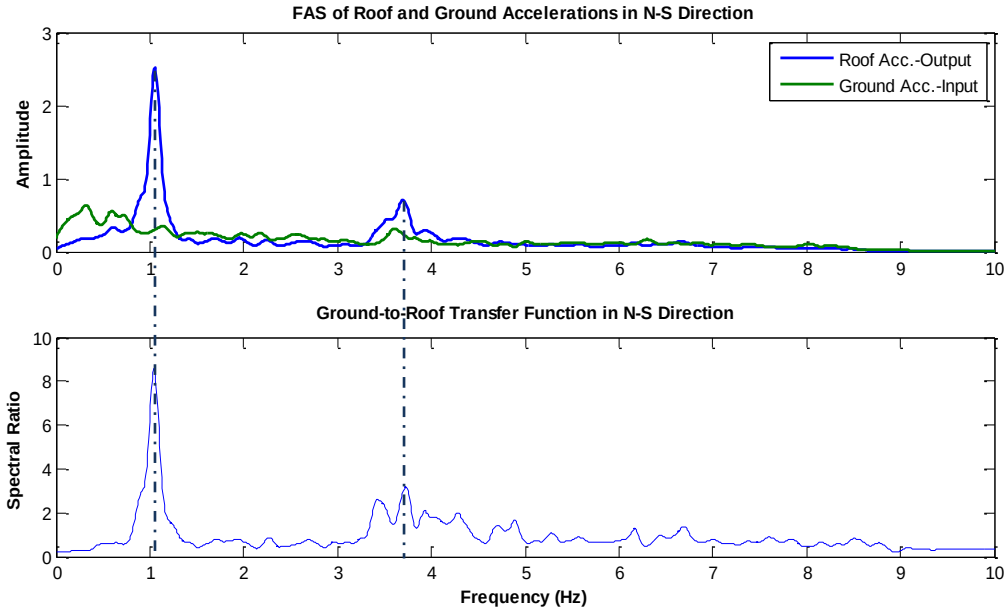

Figure 5.30. Transfer function of a 23-storey tall building of NS direction obtained data sets 130920151130.

Table 5.11. The natural frequencies obtained Spectral Ratio from the data set 130920151130.

Mode	Mode Descriptions	Frequency (Hz) from Spectral Ratio
1	1st translational mode (EW)	0.61
2	1st translational mode (NS)	1.05
3	2nd translational mode (EW)	2.03
4	2nd translational mode (NS)	3.75

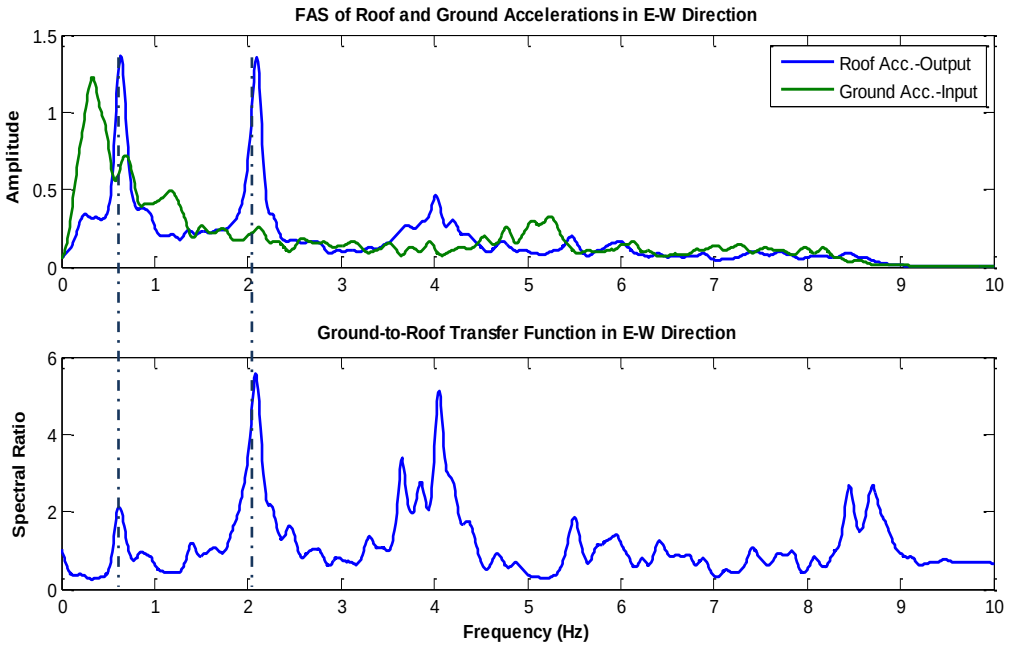

Figure 5.31. Transfer function of a 23-storey tall building of EW direction obtained data sets 160320161050

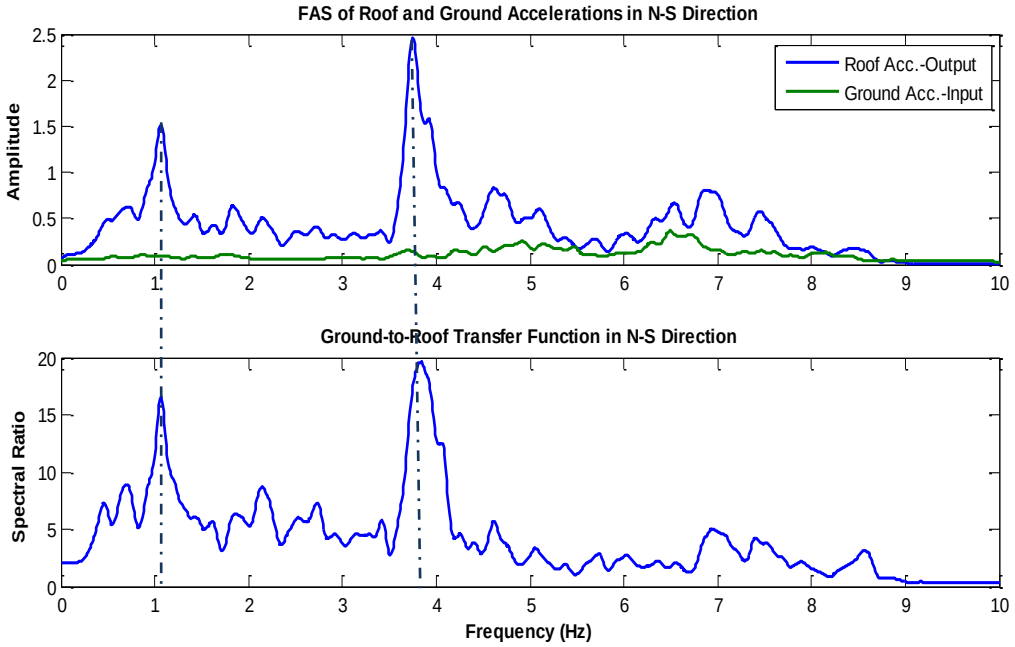

Figure 5.32. Transfer function of a 23-storey tall building of NS direction obtained data sets 160320161050.

Table 5.12. The natural frequencies obtained Spectral Ratio from data set 160320161050.

Mode	Mode Descriptions	Frequency (Hz) from Spectral Ratio
1	1st translational mode (EW)	0.62
2	1st translational mode (NS)	1.05
3	2nd translational mode (EW)	2.10
4	2nd translational mode (NS)	3.77

5.5.3. Identification of Mode Shapes from Ambient Vibration Tests

In this part it is aimed to obtain deformation shape of the structure from ambient vibrations. The modes shapes will be compared to the identified frequency using the ambient vibration tests and finite element models. Mode shapes can be identified by inspecting the modal displacement time histories provided that all records are time-synchronized. The building's motion at a sufficiently large number of floors above ground level are measured an accurate estimation of the mode shapes. In the monitoring building, there are only two instrumented floors above ground level. This is insufficient instrumentation to accurately estimate the mode shapes for all the significant modes since the height and the flexibility of the building is important to determine deformation shapes of the building. A simple approximation assumes that mode shapes between the instrumented floors are straight lines. Prior to determination of modal displacements, the accelerations around each modal frequency were applied narrow-band-pass filtering and then the filtered accelerations were double integrated to get modal displacements. The amplitude of each measuring point at that mode identified the direction by plotting modal displacement time histories together from top to bottom. Rotational vibrations in buildings are typically identified from the difference of two parallel horizontal accelerometers. In order to reduce the noise effects when taking the difference, we firstly band-pass filter the records around the torsional frequencies. Torsional frequencies are determined by investigating the modal displacement time histories of the two parallel sensors. The modes at which the displacements go in opposite direction indicate torsional modes. The torsional time histories by taking the difference of the signals were calculated after they are band-

pass filtered around torsional frequencies (Şafak *et. al.*, 2014). The lack of additional sensors on floors other than the 15th prevents comparing the torsional frequency with those from other floors.

A relationship of the deformation shapes obtained ambient vibration tests made. There was no significant difference between the mode shapes obtained for each construction stage (Case 1, Case 2, and Case 3) when compared with the other analysis methods.

Mode displacements were shown from Figure 5.33 through Figure 5.52. The mode shapes of the structure show to be regular. Due to the number of samples per cycle of the selected recorded acceleration signal, peak values of second mode displacement graphs are not smooth.

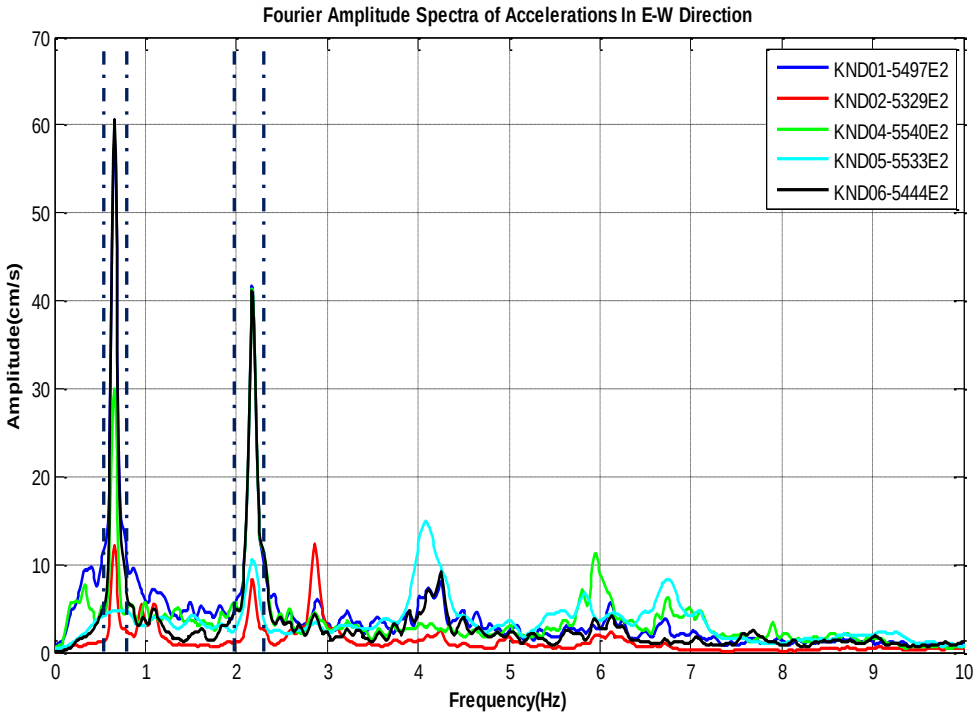

Figure 5.33. Modal frequency band selection from Smoothed Fourier Amplitude Spectrum in EW direction of the data sets 27032015.

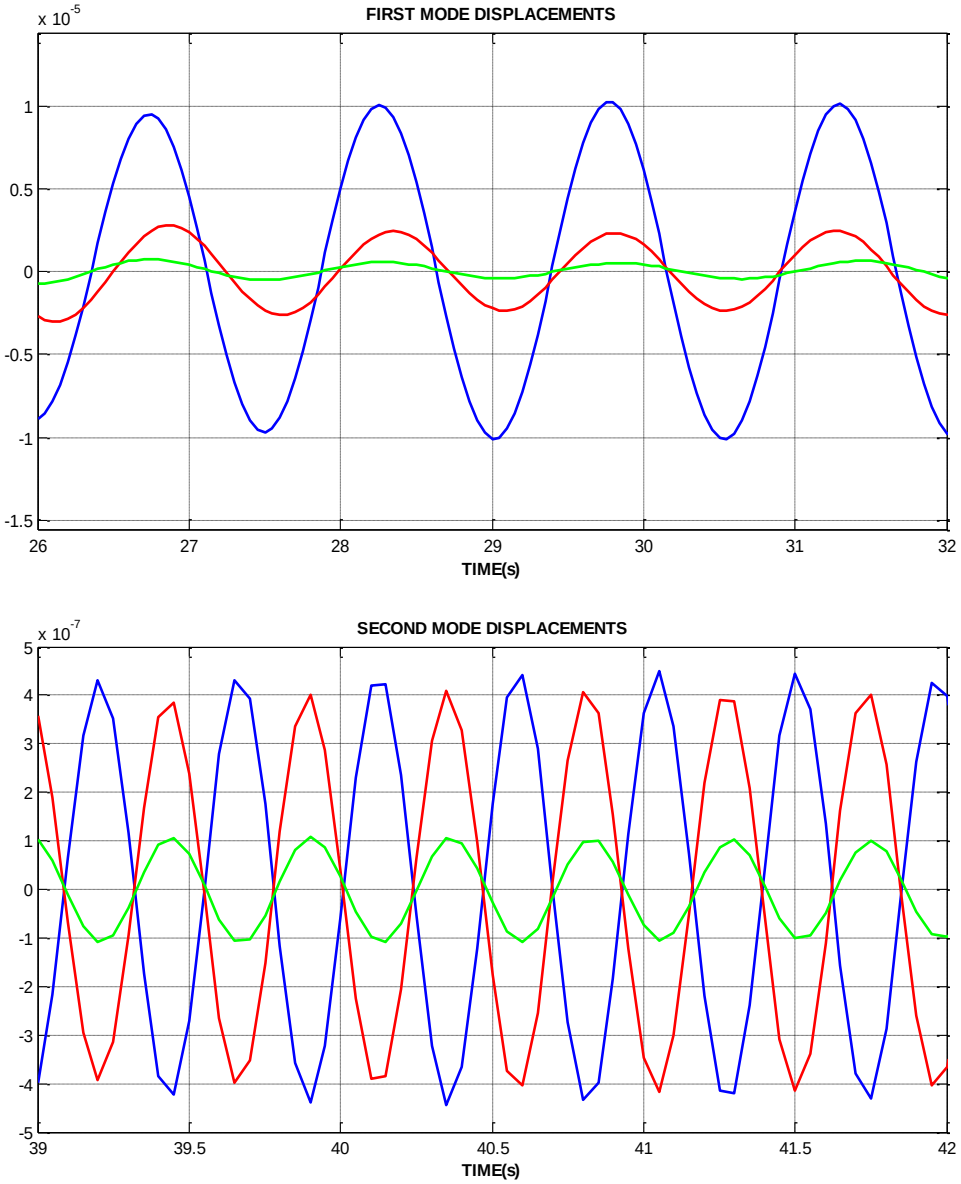

Figure 5.34. Mode displacements time histories recorded by three parallel sensors for EW direction at 0.66 Hz and 2.16 Hz, respectively. The blue, red, and green lines demonstrate 15th, 7th, and first basement floors respectively (a) First Mode Displacements (b) Second Mode Displacements

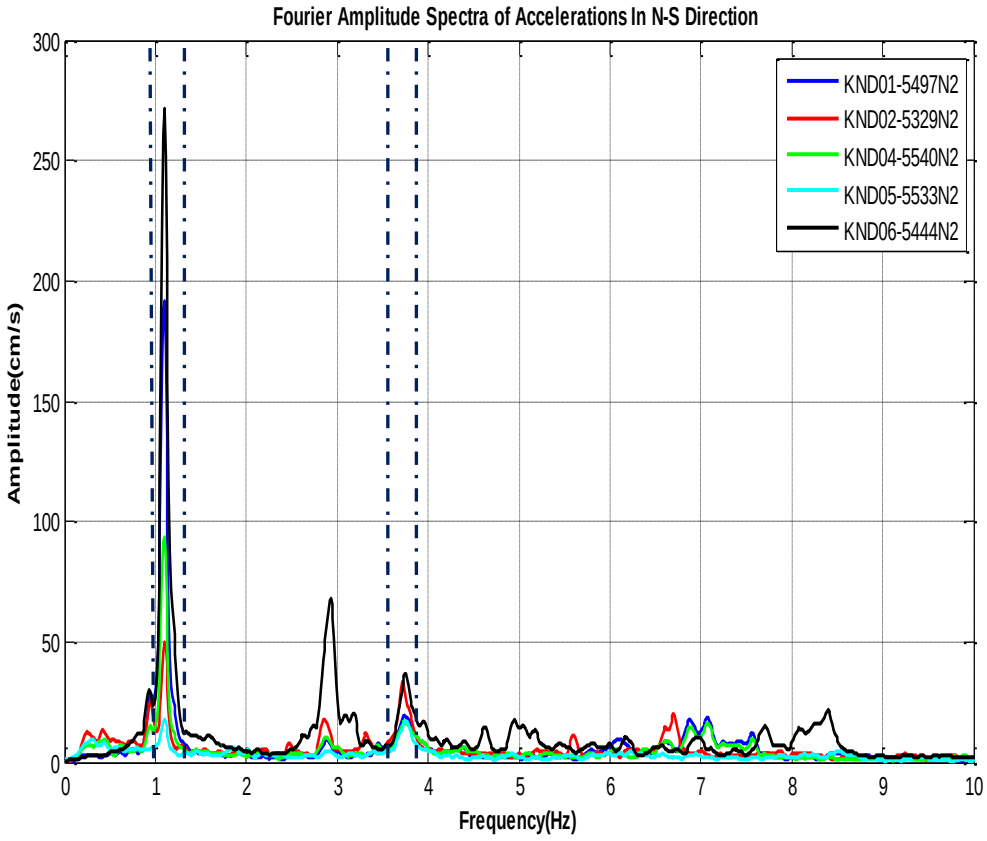

Figure 5.35. Modal frequency band selection from Smoothed Fourier Amplitude Spectrum in NS direction of the data sets 27032015

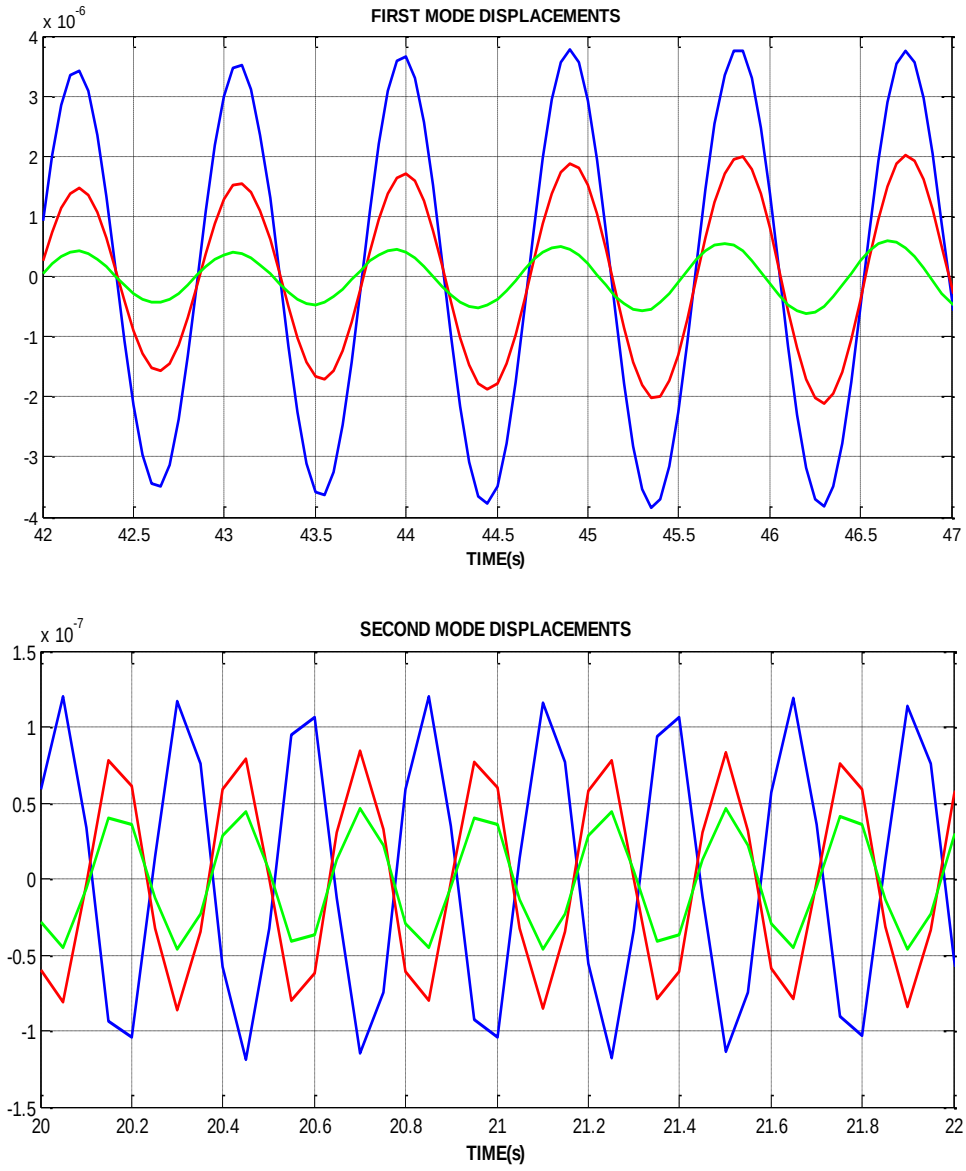

Figure 5.36. Mode displacements time histories recorded by three parallel sensors for NS direction at 1.11 Hz and 3.78 Hz, respectively. The blue, red, and green lines demonstrate 15th, 7th, and first basement floors respectively. (a) First Mode Displacements (b) Second Mode Displacements

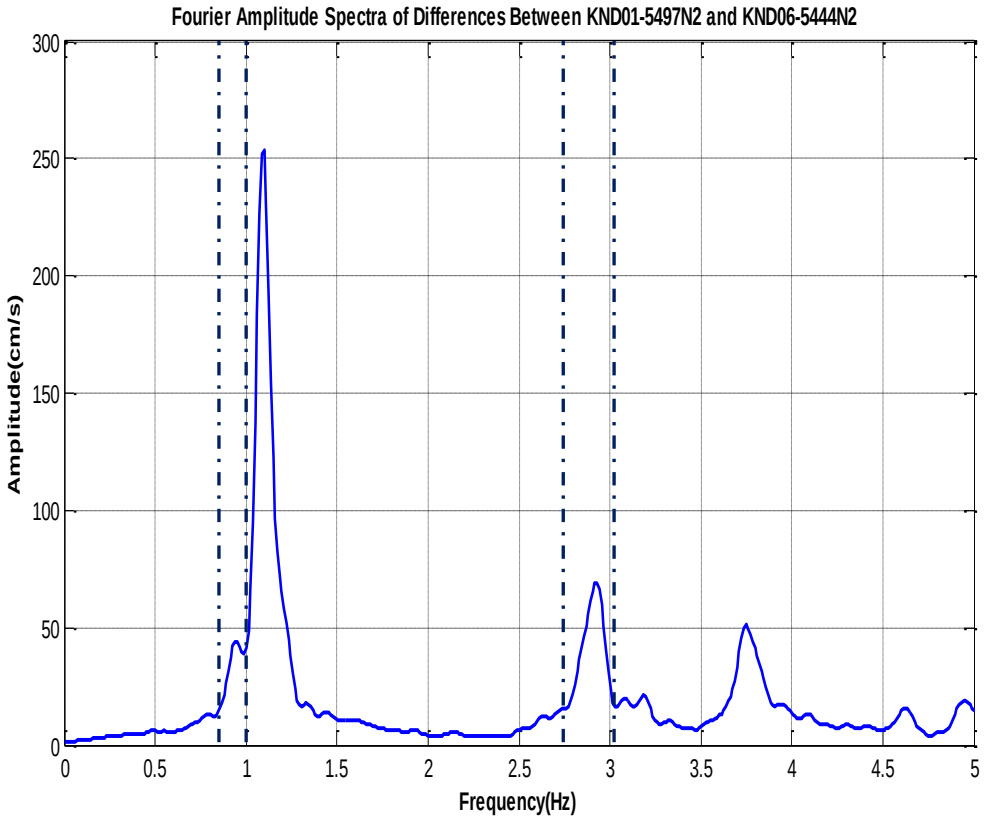

Figure 5.37. Modal frequency band selection from Smoothed Fourier Amplitude Spectrum in the difference NS directions between two parallel accelerations at roof of the data set 27032015. Amplitude spectrum of accelerations at the 15th floor displays the first two torsional frequencies.

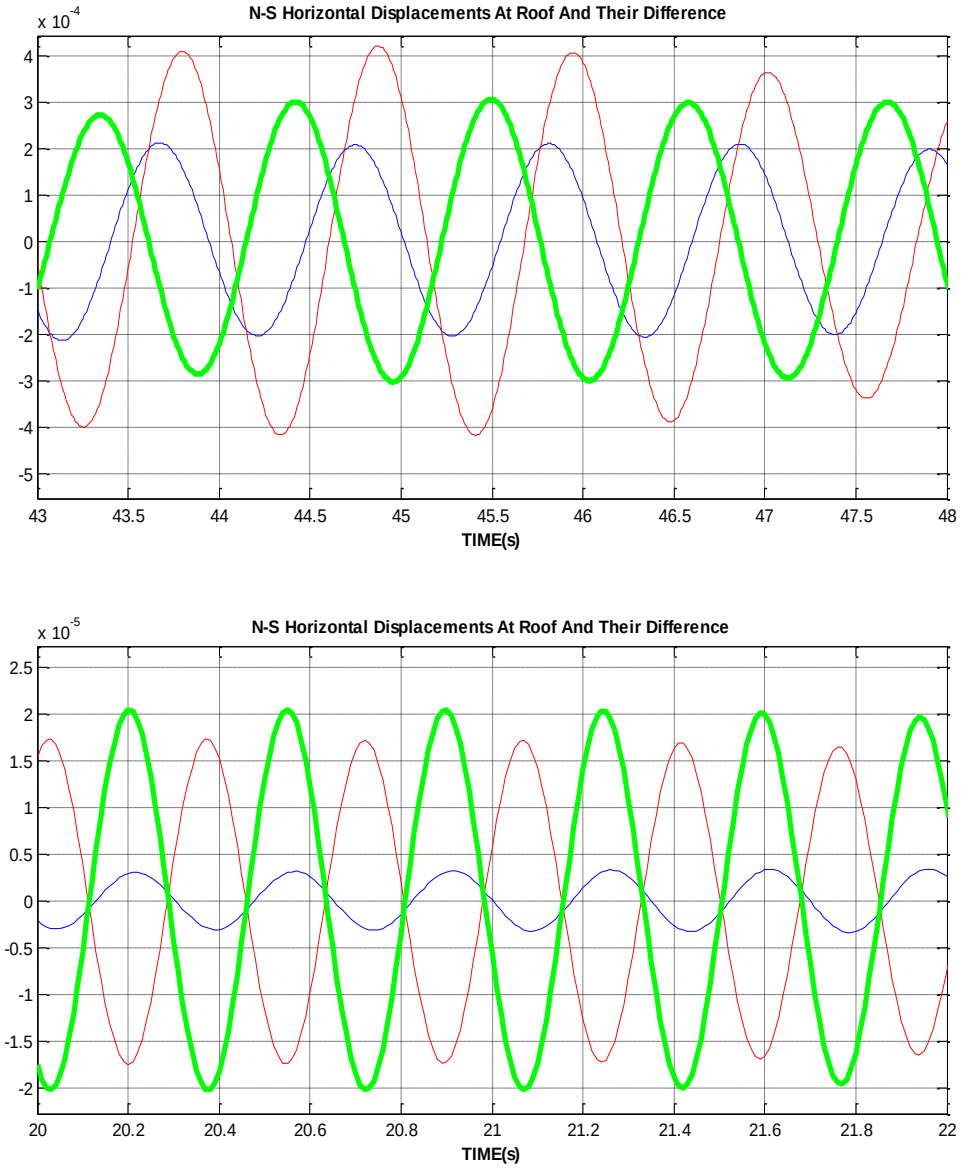

Figure 5.38. Mode displacements time histories recorded by two parallel sensors in NS direction at 0.94 Hz and 2.90 Hz, their differences representing torsional displacement at 15th floor. The blue, red, and green lines demonstrate KND01-5497N2, KND06-5444N2, and torsional displacement respectively. (a) First Mode Displacements (b) Second Mode Displacements

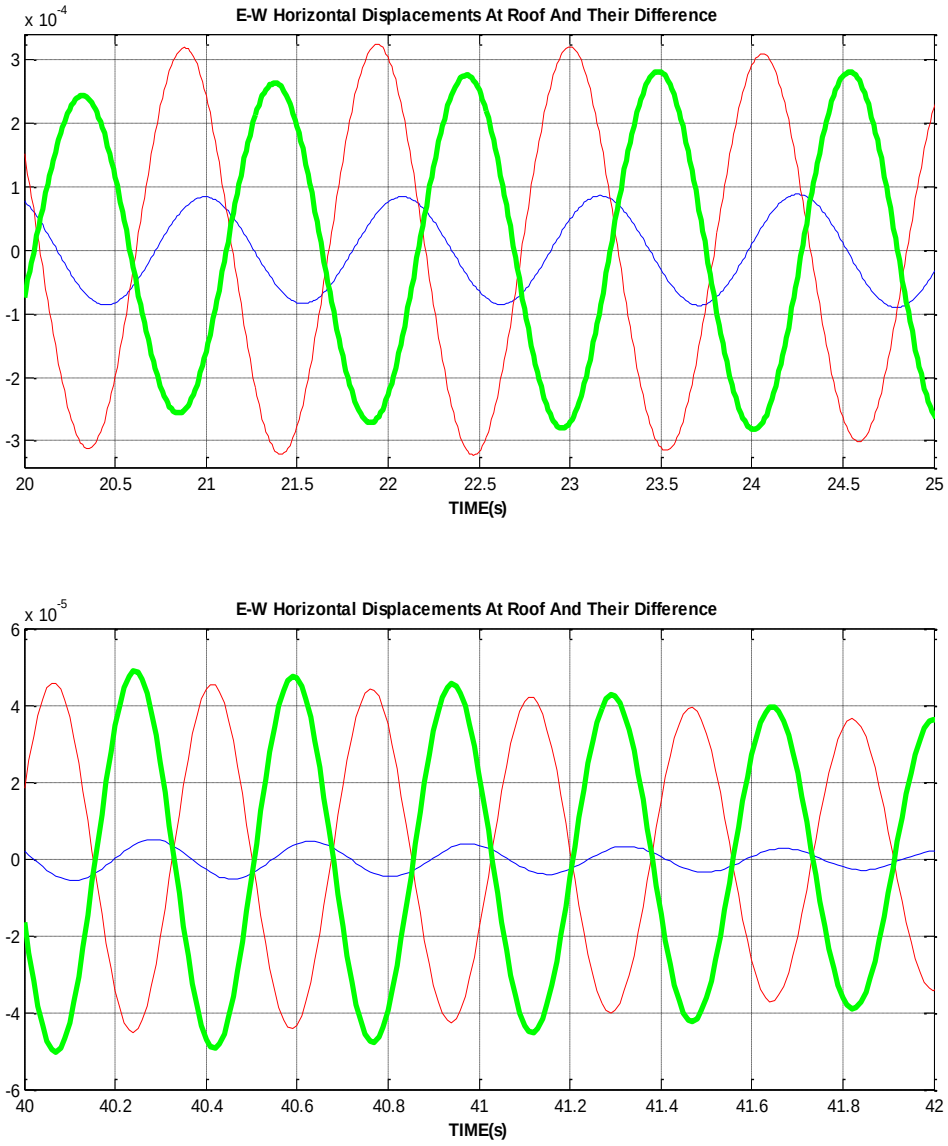

Figure 5.39. Mode displacements time histories recorded by two parallel sensors in EW direction at 0.94 Hz and 2.90 Hz, their differences representing torsional displacement at 15th floor. The blue, red, and green lines demonstrate KND01-5497E2, KND02-5329E2, and torsional displacement respectively. (a) First Mode Displacements (b) Second Mode Displacements

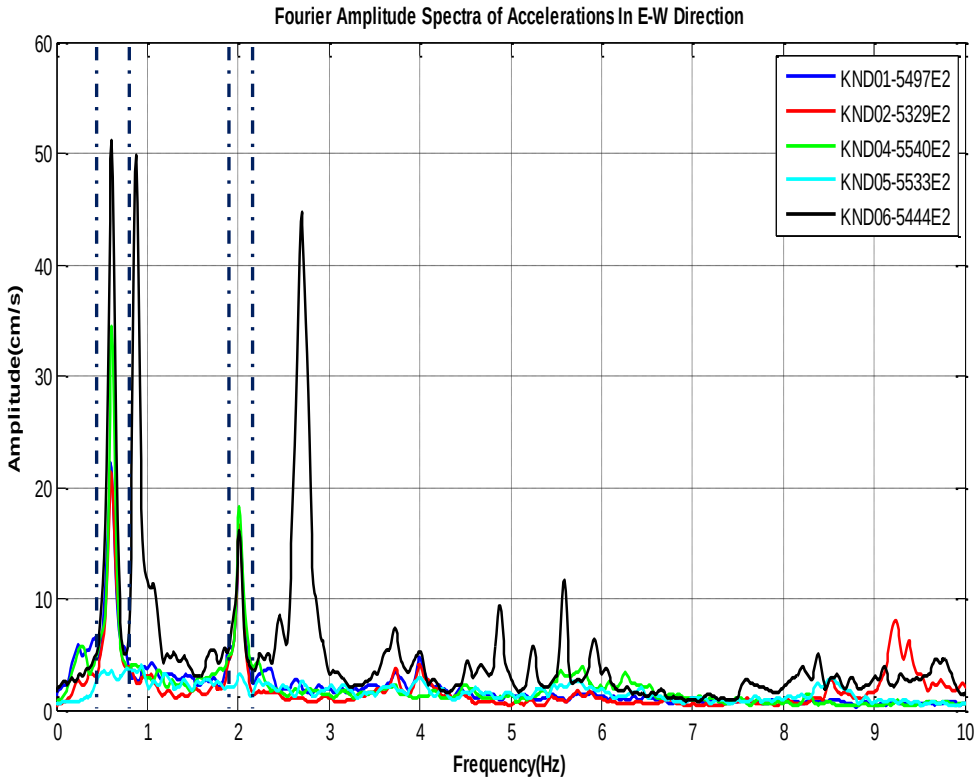

Figure 5.40. Modal frequency band selection from Smoothed Fourier Amplitude Spectrum in EW direction of the data set 13092015

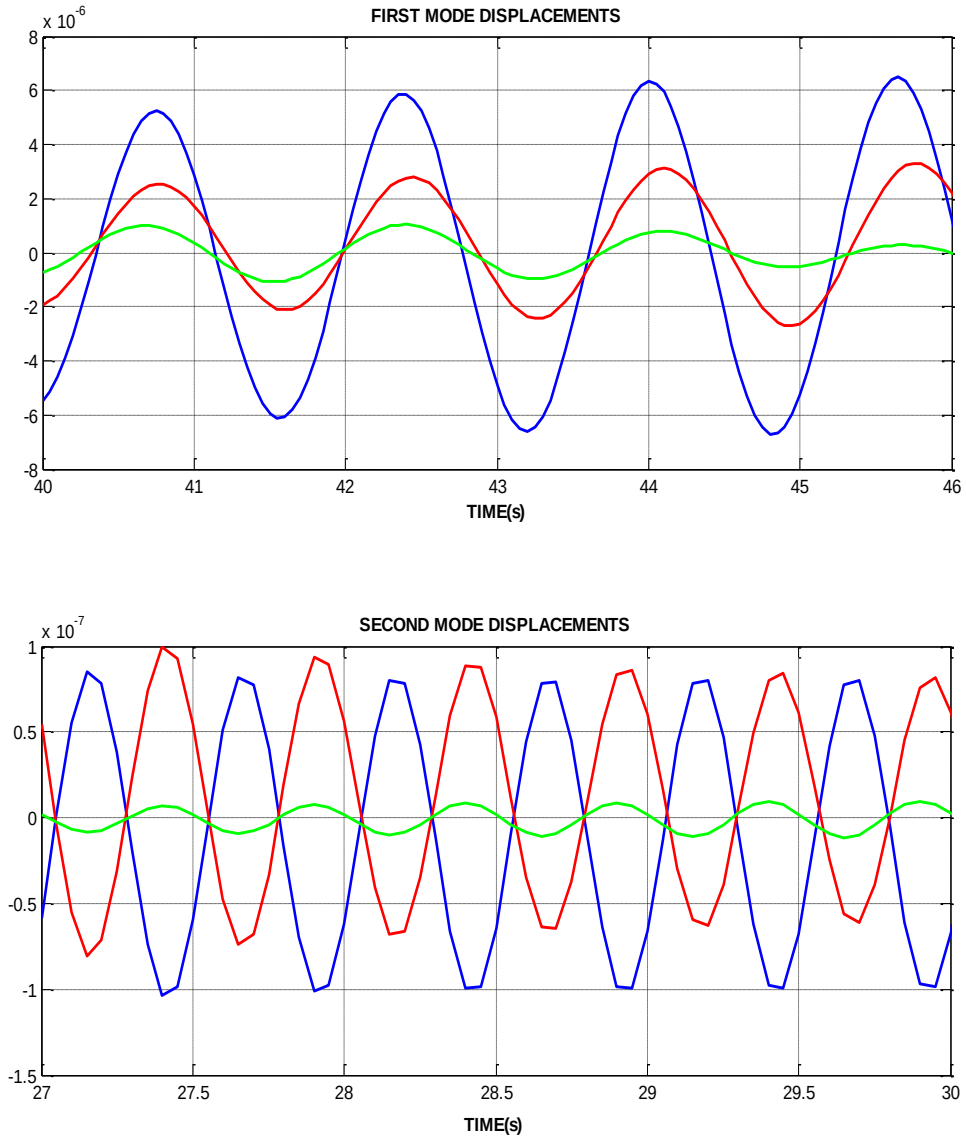

Figure 5.41. Mode displacements time histories recorded by three parallel sensors for EW direction at 0.61 Hz and 2.01 Hz, respectively. The blue, red, and green lines demonstrate 15th, 7th, and first basement floors respectively. (a) First Mode Displacements (b) Second Mode Displacements

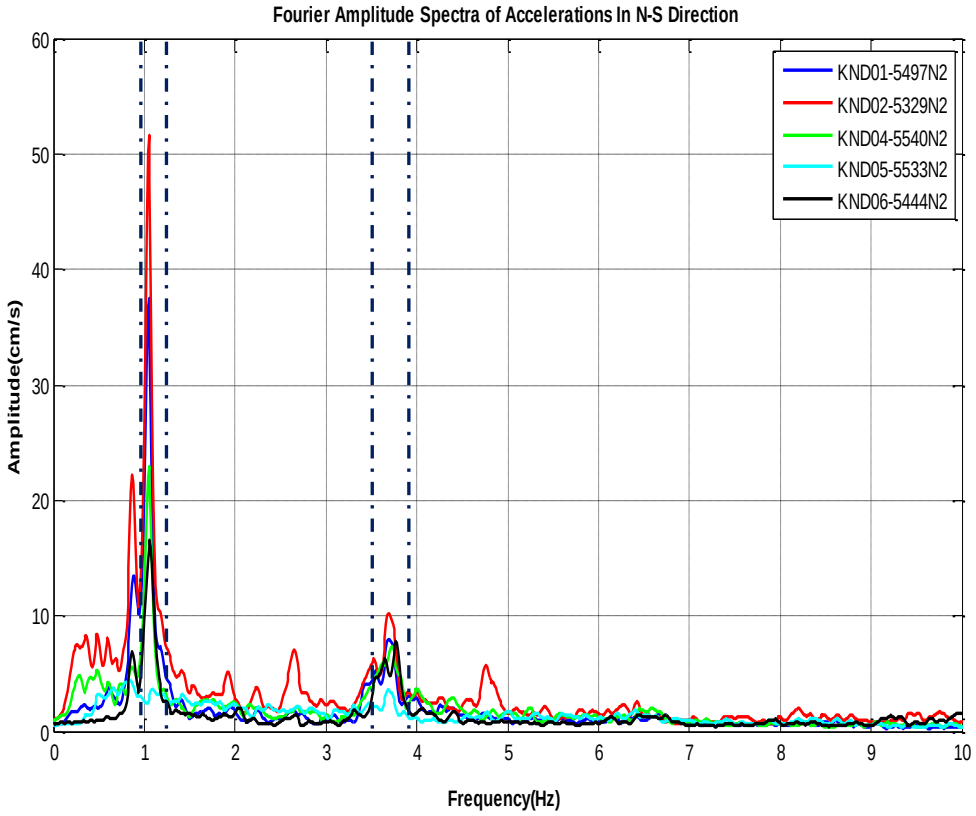

Figure 5.42. Modal frequency band selection from Smoothed Fourier Amplitude Spectrum in NS direction of the data set 13092015

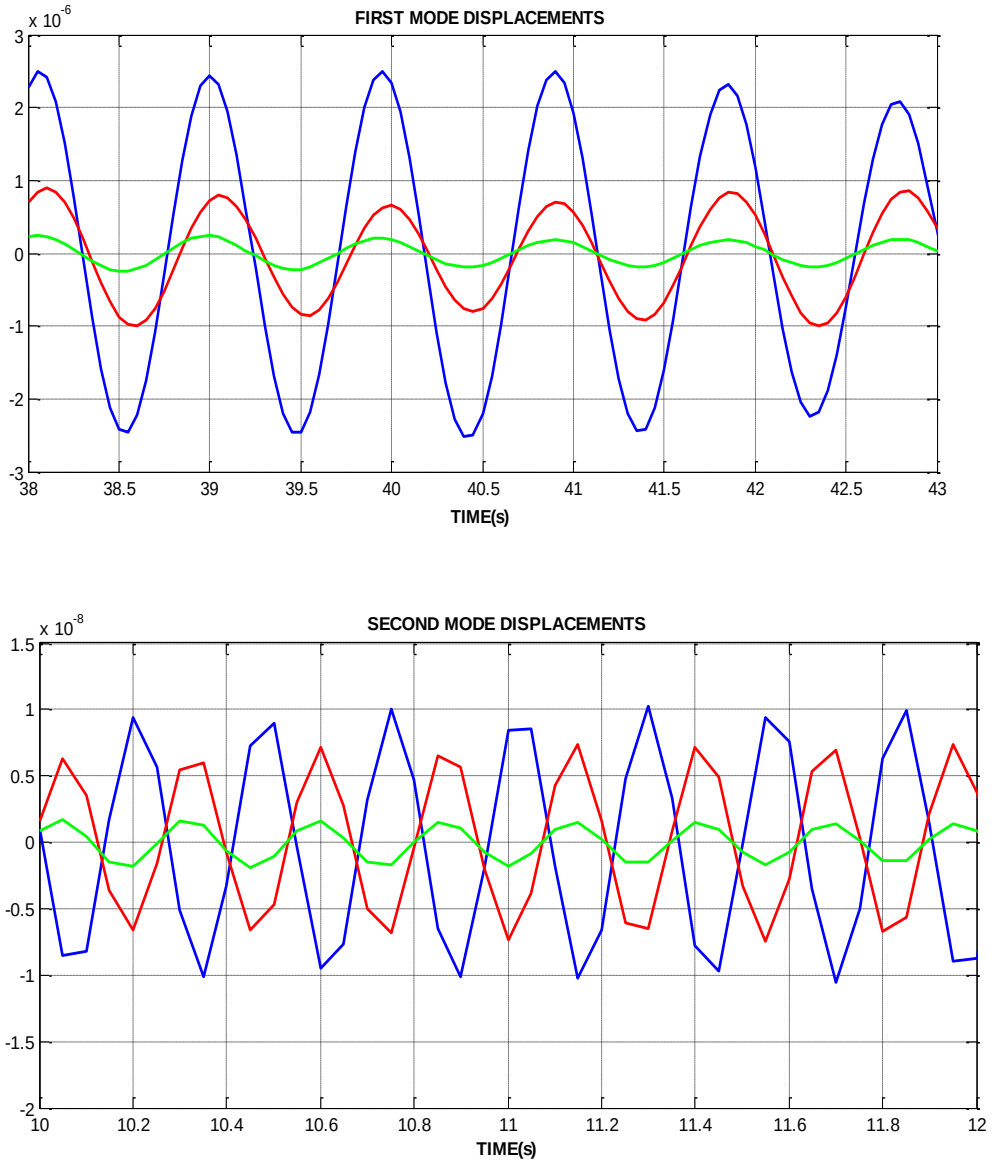

Figure 5.43. Mode displacements time histories recorded by three parallel sensors for NS direction at 1.05 Hz and 3.66 Hz, respectively. The blue, red, and green lines demonstrate 15^{th}, 7^{th}, and first basement floors respectively.

(a) First Mode Displacements (b) Second Mode Displacements

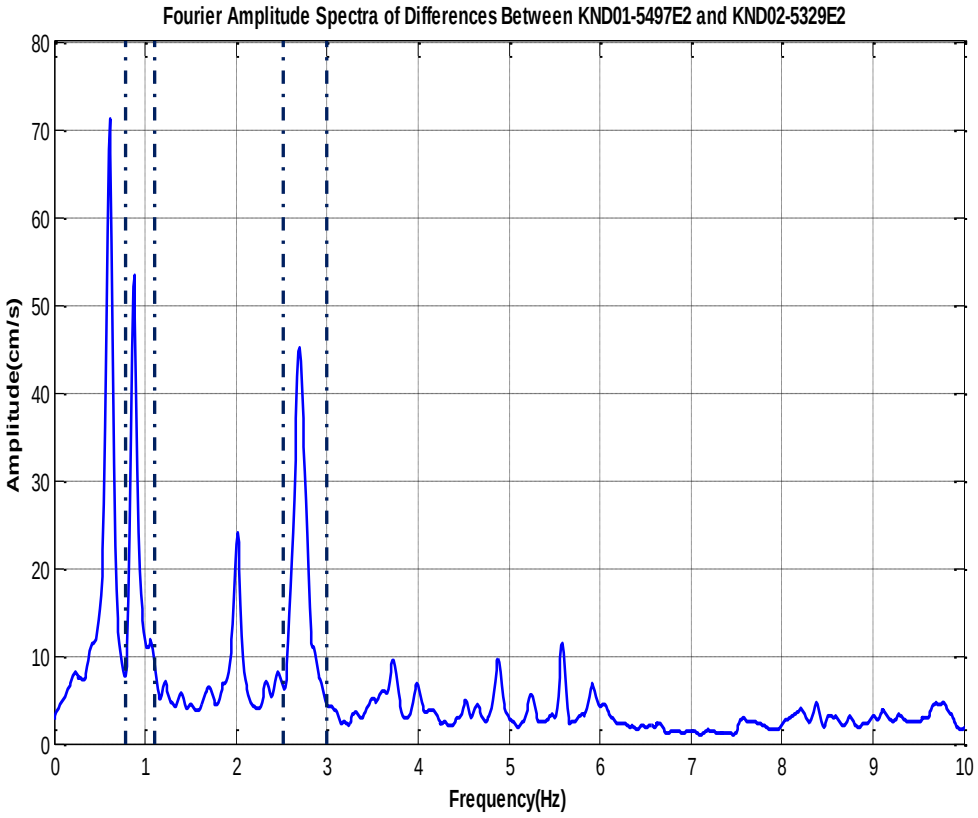

Figure 5.44. Modal frequency band selection from Smoothed Fourier Amplitude Spectrum in the difference NS directions between two parallel accelerations at roof of the data sets 13092015. Amplitude spectra of accelerations at the 15th floor displays the first two torsional frequencies. Torsional frequencies are also identified from the difference (E–W) between two parallel accelerations.

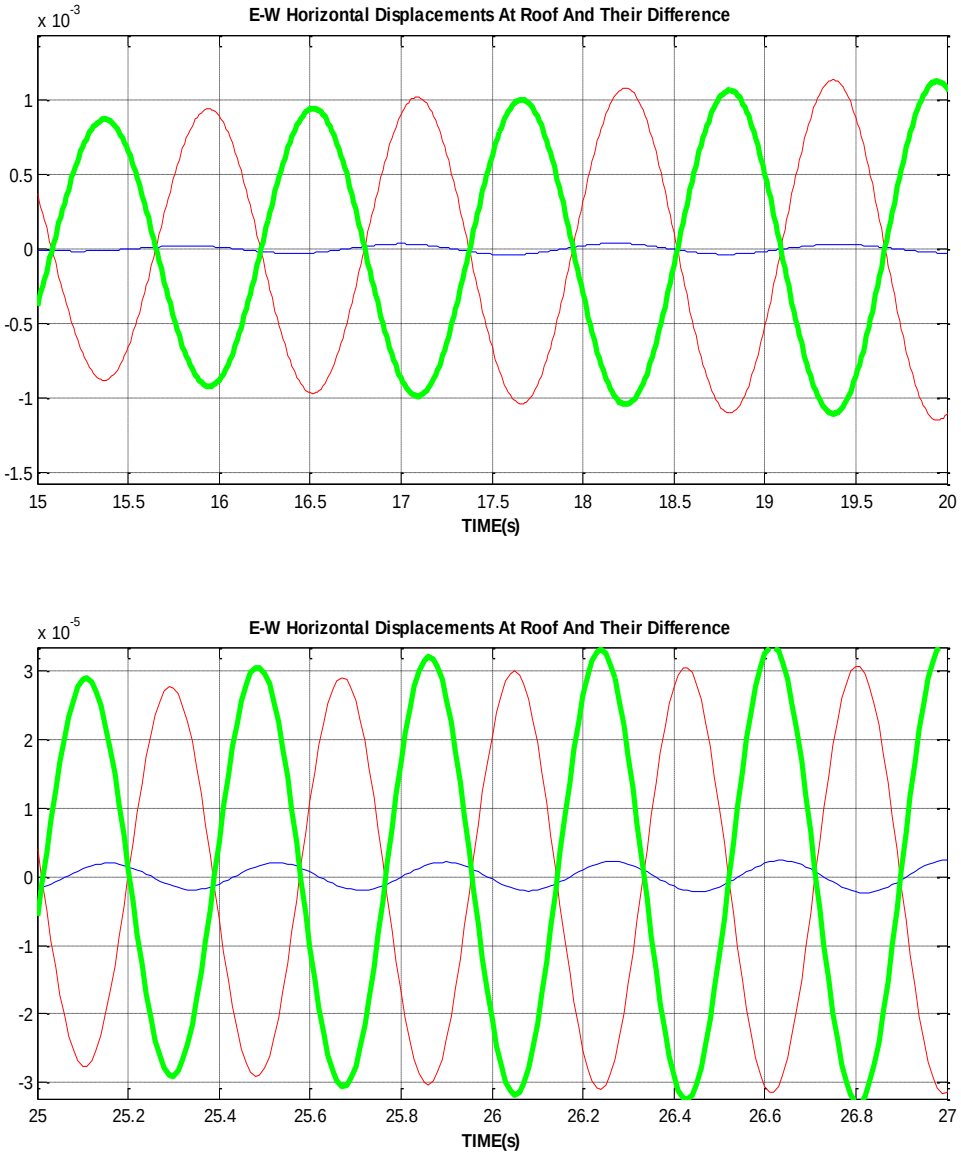

Figure 5.45. Mode displacements time histories recorded by two parallel sensors in EW direction at 0.87 Hz and 2.70 Hz, their differences representing torsional displacement at 15th floor. The blue, red, and green lines demonstrate KND01-5497E2, KND02-5329E2, and torsional displacement respectively. (a) First Mode Displacements (b) Second Mode Displacements

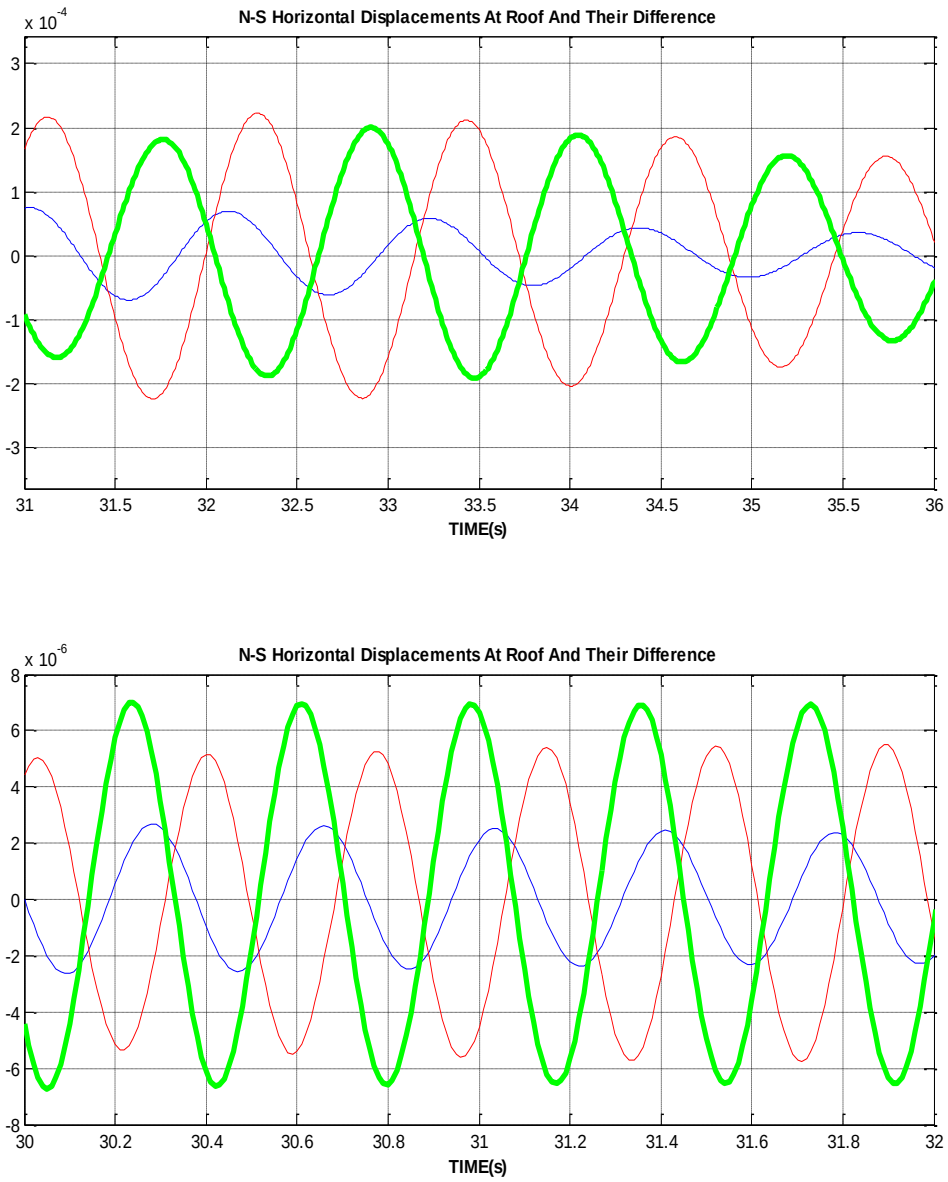

Figure 5.46. Mode displacements time histories recorded by two parallel sensors in NS direction at 0.87 Hz and 2.70 Hz, their differences representing torsional displacement at 15th floor. The blue, red, and green lines demonstrate KND01-5497N2, KND06-5444N2, and torsional displacement respectively. (a) First Mode Displacements (b) Second Mode Displacements

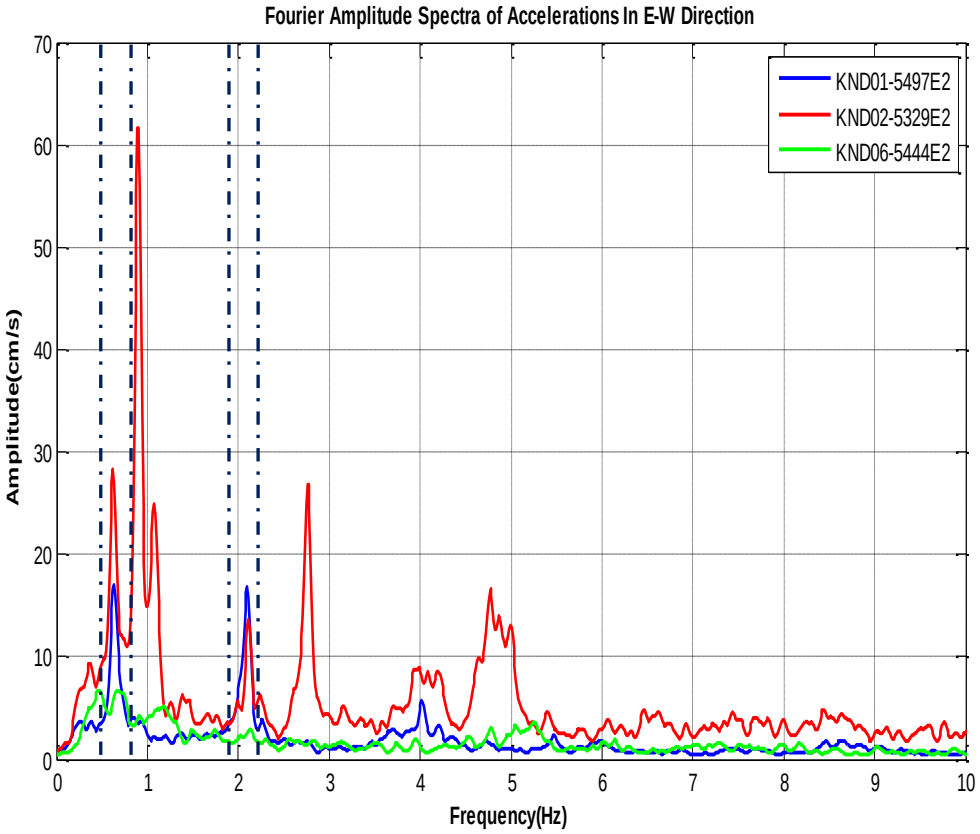

Figure 5.47. Modal frequency band selection from Smoothed Fourier Amplitude Spectrum in EW direction of the data set 16032016

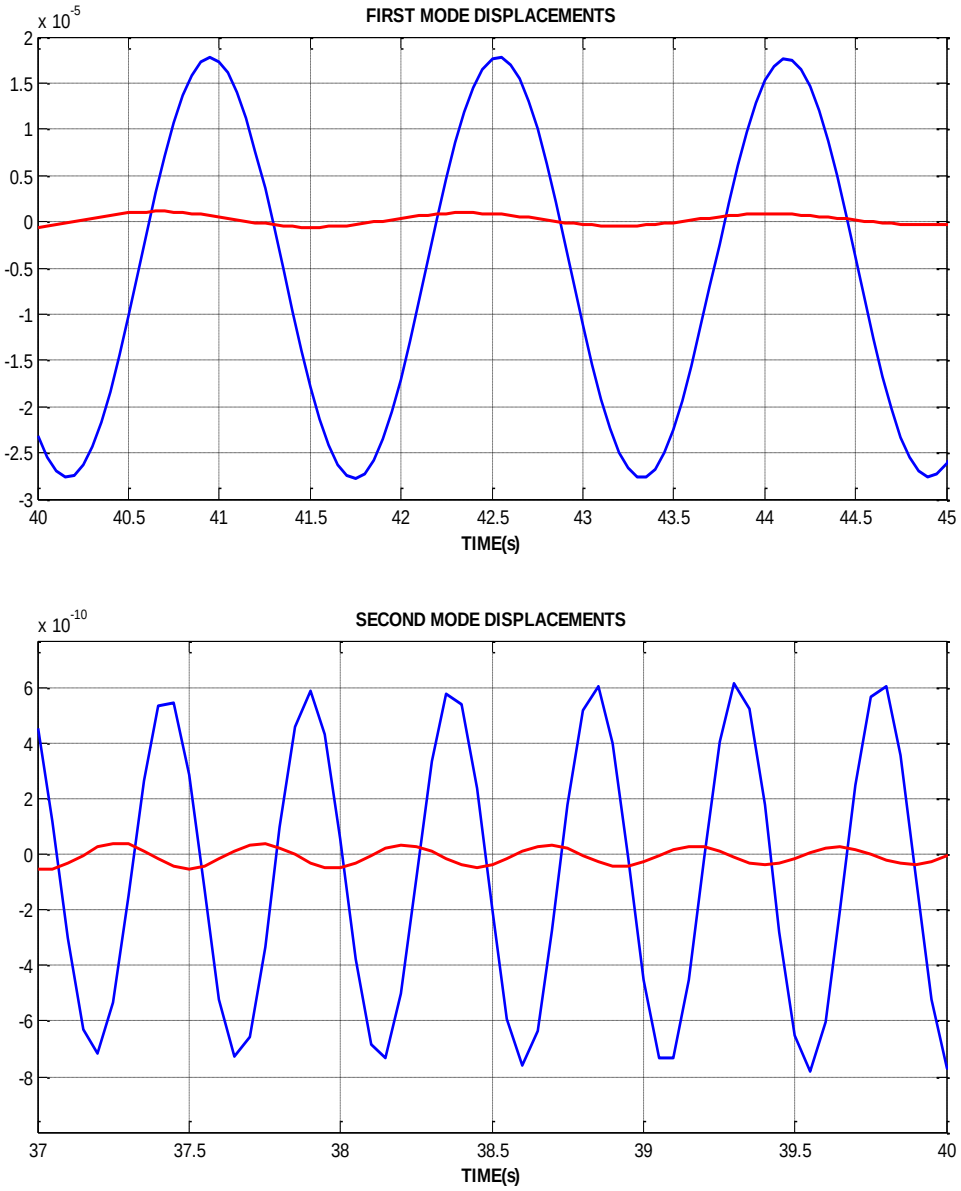

Figure 5.48. Mode displacements time histories recorded by three parallel sensors for EW direction at 0.62 Hz and 2.11 Hz, respectively. The blue, red, and green lines demonstrate 15th and third basement floors respectively. (a) First Mode Displacements (b) Second Mode Displacements

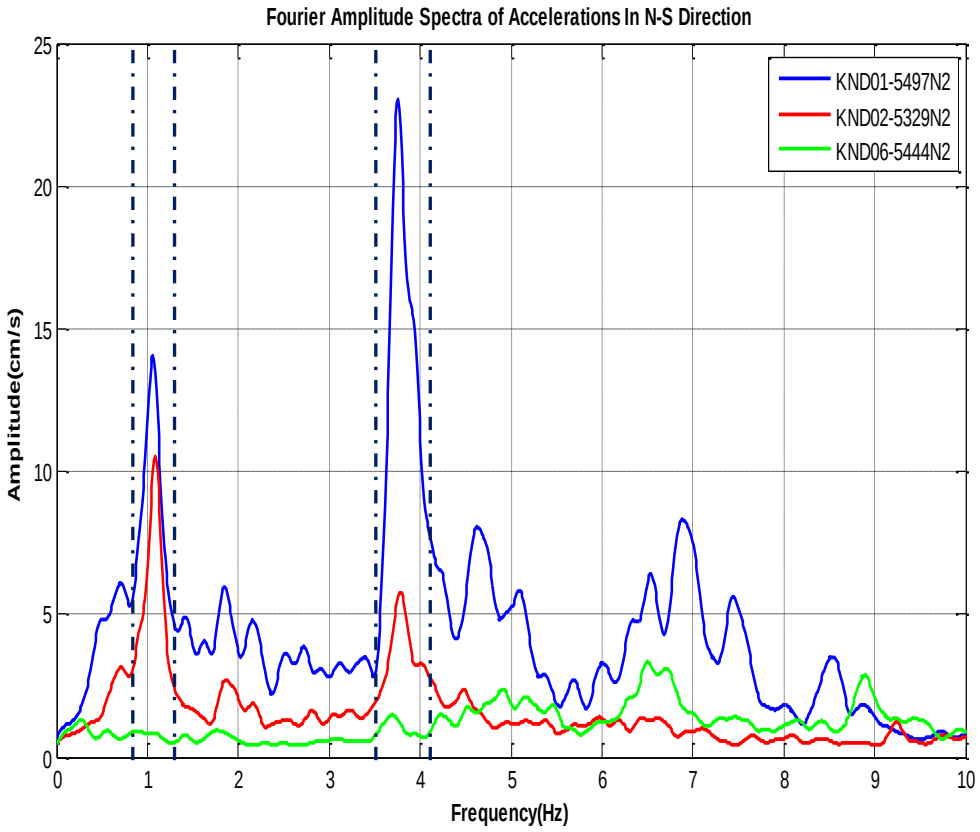

Figure 5.49. Modal frequency band selection from Smoothed Fourier Amplitude Spectrum in NS direction of the data set 16032016

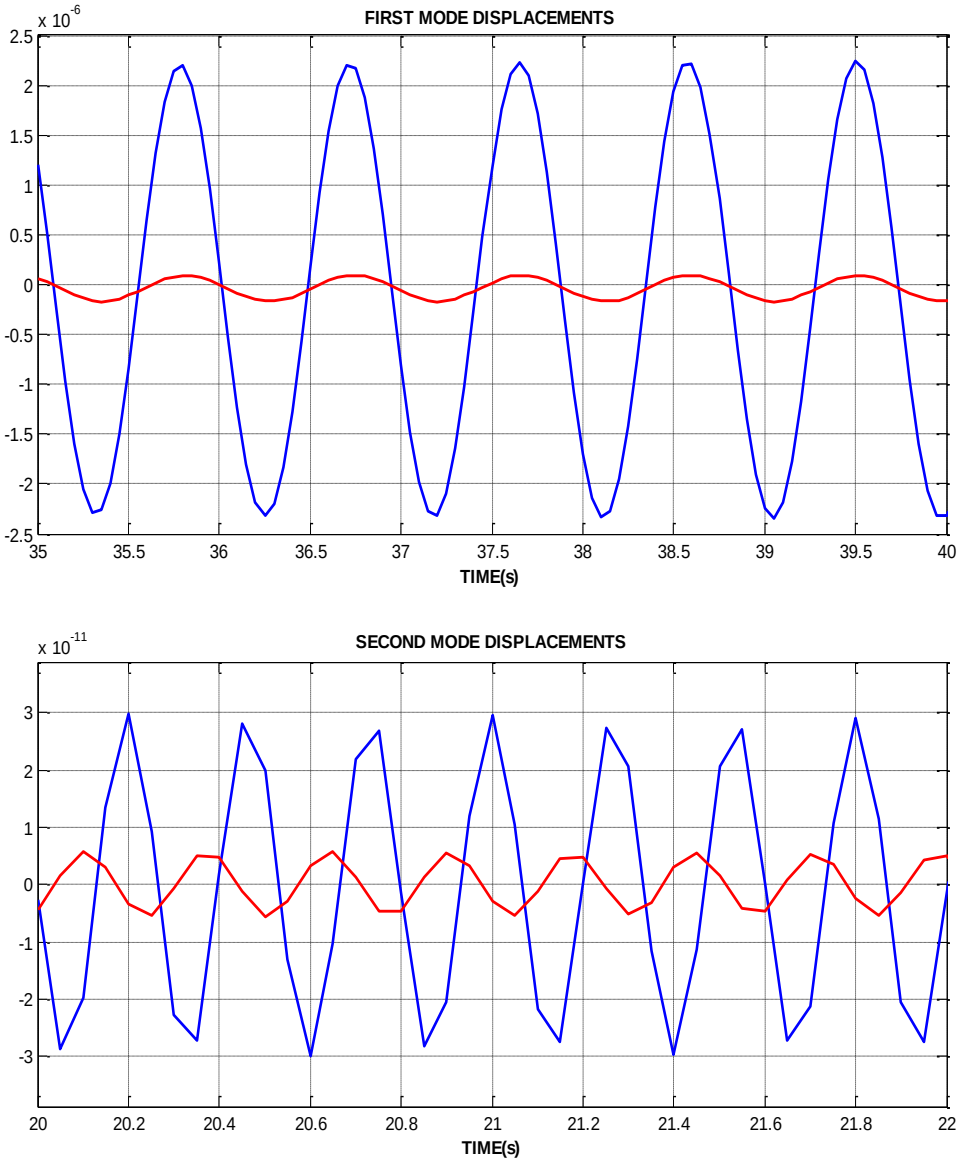

Figure 5.50. Mode displacements time histories recorded by three parallel sensors for NS direction at 1.11 Hz and 3.77 Hz, respectively. The blue, red, and green lines demonstrate 15th, 7th, and third basement floors respectively. (a) First Mode Displacements (b) Second Mode Displacements

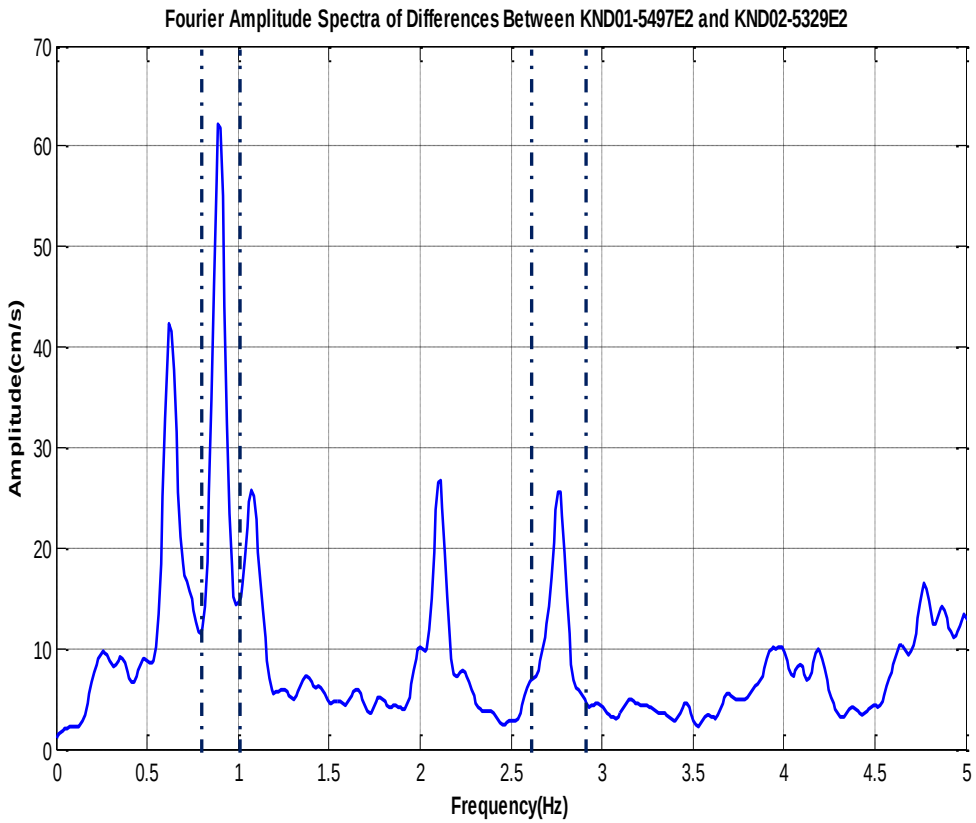

Figure 5.51. Modal frequency band selection from Smoothed Fourier Amplitude Spectrum in the difference NS directions between two parallel accelerations at roof of the data sets 16032016. Amplitude spectra of accelerations at the 15th floor display the first two torsional frequencies. Torsional frequencies are also identified from the difference (E–W) between two parallel accelerations.

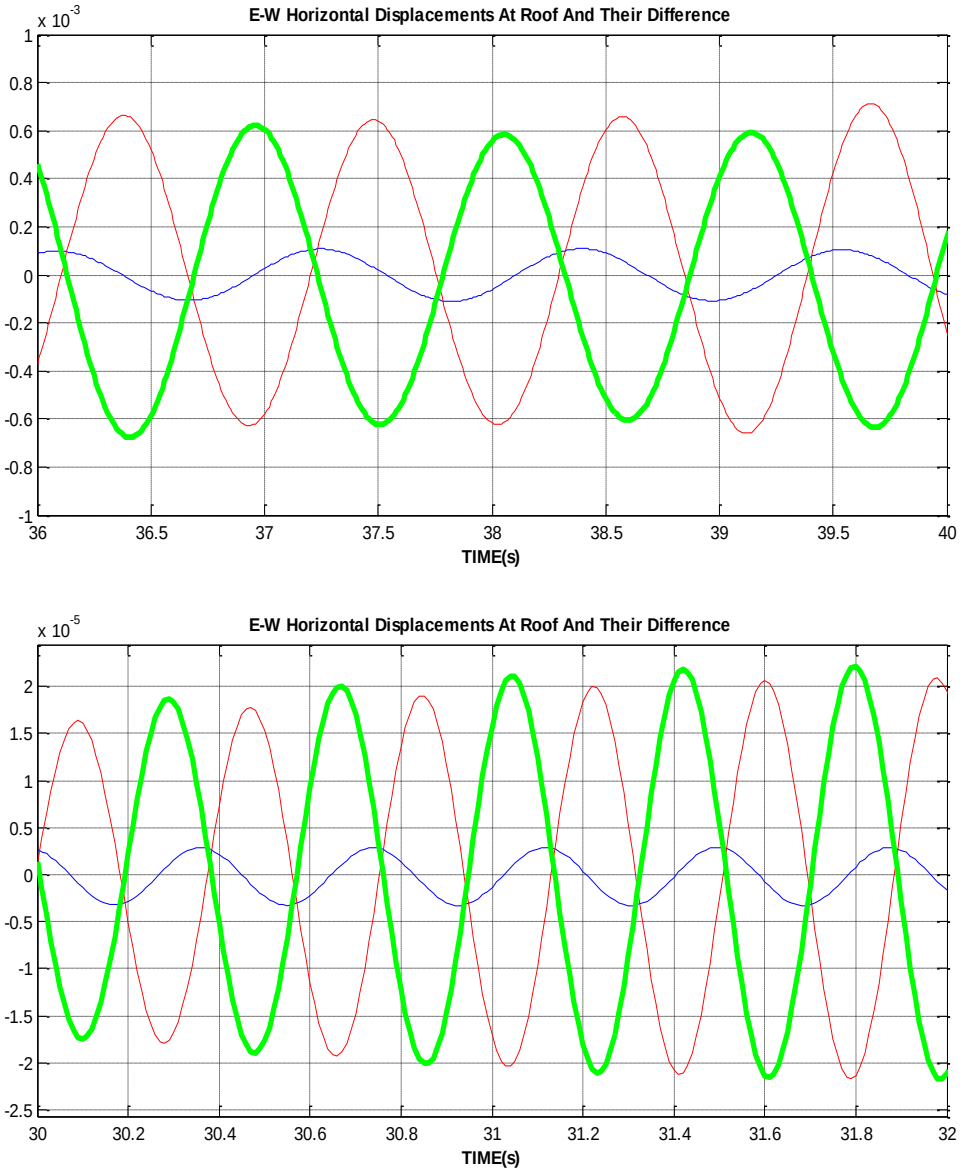

Figure 5.52. Mode displacements time histories recorded by two parallel sensors in EW direction at 0.89 Hz and 2.77 Hz, their differences representing torsional displacement at 15th floor. The blue, red, and green lines demonstrate KND01-5497E2, KND02-5329E2, and torsional displacement respectively. (a) First Mode Displacements (b) Second Mode Displacements

5.5.4. Identification of Modal Damping Ratios

It was impossible to know the exact damping ratio of a structure in the past unless a full-scale experiment was done. Nevertheless, in recent times it has been possible to achieve the damping rate of a building through structural health monitoring techniques. There are several simple techniques to determine modal damping ratios. The two most widely used techniques are the half- power bandwidth and the logarithmic decrement methods.

In this study half-power bandwidth is used. Fourier Amplitude Spectra of modal displacements were calculated and plotted for first two modes of all directions. SFAS of modal displacements were determined by narrow-band-pass filtering the records around the corresponding modal frequencies. Data processing that was presented in Section 5.1 was applied. Figure 5.53 illustrates the procedure for the particular case of the 1st EW mode for data set 27032015. Figure 5.53 demonstrates SFAS of modal displacements for first EW mode showing half-power bandwidth frequencies.

One of the most convenient of the method used is the half-power or band-width method. The damping ratio is determined from the frequencies at which the response amplitude f_{res} is reduced to the level $1/\sqrt{2}$ times and f_{max} is the peak value. It is then assumed that half the total power dissipation in this mode occurs in the frequency band between f_1 and f_2, where f_1 and f_2 are the frequencies corresponding to an amplitude of f_{max}. The details of the method is shown in standard texts (Chapter 3, Chopra A., 1995) that the damping ratio, ζ, for small ζ is approximately

$$\zeta = \frac{f_2 - f_1}{2f_{res}} \tag{5.2}$$

The modal damping ratios of the first translational and torsional modes are very low due to the fact that the amplitude of the vibrations during the ambient vibration is not large enough. The first modal damping percentages (<1.5%) are low. The table shows that damping in the system is mostly mass-proportional since the frequencies increase when modal damping ratios obtained half-power method decrease. Using the all data sets,

damping ratios of the first two modes obtained by half-power method for EW and NS directions identified and listed in Table 5.13 were calculated.

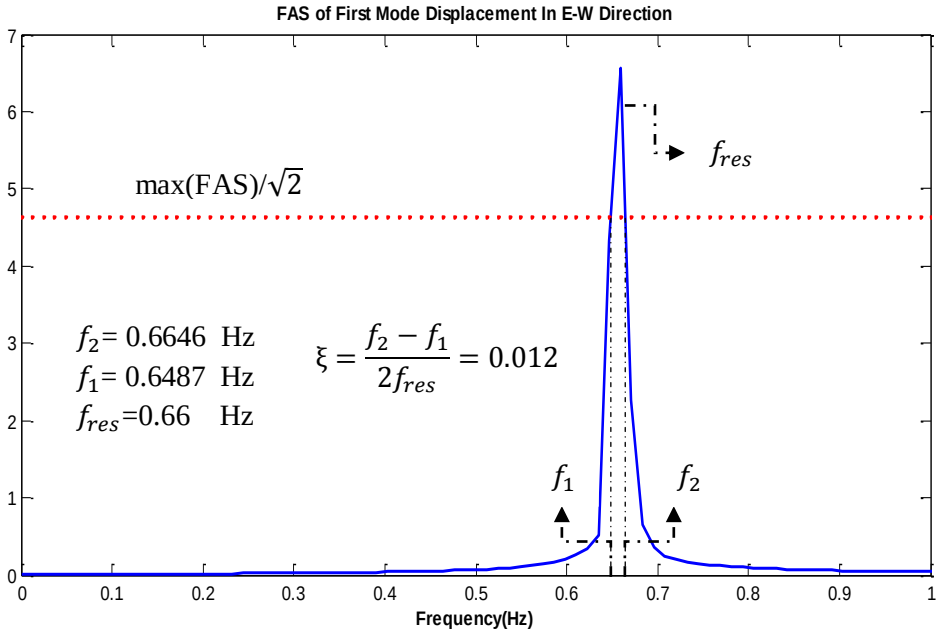

Figure 5.53. Spectrum for 1st EW mode showing half-power bandwidth frequencies

Table 5.13. Natural frequencies and modal damping ratios for all data sets obtained by half-power method.

Mode	Mode Shape	Amb. Vibration Test#1		Amb. Vibration Test#2		Amb. Vibration Test#3	
		Freq.(Hz)	Damp.(%)	Freq.(Hz)	Damp.(%)	Freq.(Hz)	Damp.(%)
1	1st translational EW	0.66	1.2	0.61	1.11	0.62	1.28
2	1st torsional	0.94	1.00	0.87	1.28	0.89	0.94
3	1st translational NS	1.10	0.86	1.05	0.62	1.05	0.76
4	2nd translational EW	2.16	0.39	2.01	0.37	2.11	0.40
5	2nd torsional	2.90	0.28	2.70	0.37	2.77	0.29
6	2nd translational NS	3.78	0.28	3.70	0.33	3.74	0.21

5.6. Analytical Study

The aim of this chapter is to generate mathematical models of the building and perform an analytical study. The dynamic properties such as natural frequencies and mode shapes obtained the ambient vibration tests and the analytical studies will be compared. The computer program SAP2000 version 16.0 was used for the analysis of two finite element models based on the design drawings.

Model #1, Model #2, and Model #3 were developed corresponding to the 3 cases. These models consist of concrete beams, columns, structural walls, and slabs. The shear walls are modeled with shell elements. Structural walls and slabs were also modeled by shell elements. Model #1 was included only self-mass of the structure. Model #2 was included non-structural elements that are leveling concrete, brick, and glass curtain wall in addition. Model #3 represented the completed building monitored. The curtain glass wall was added by distributed load. These masses were uniformly distributed over each floor. The foundation is modeled as a fixed base. This common assumption greatly simplifies the modeling procedure but ignores the potentially effect of soil-structure interaction. Finite Element Model in 3-D was shown in Figure 5.54. The building was designed according to the regulations of TS500 for gravity. The materials used are reinforced concrete type C40 (34000 MPa) and the modulus of elasticity is produced by the following formula:

$$Ec = 3250\sqrt{f_{ck}} + 14000\ (MPa) \tag{5.3}$$

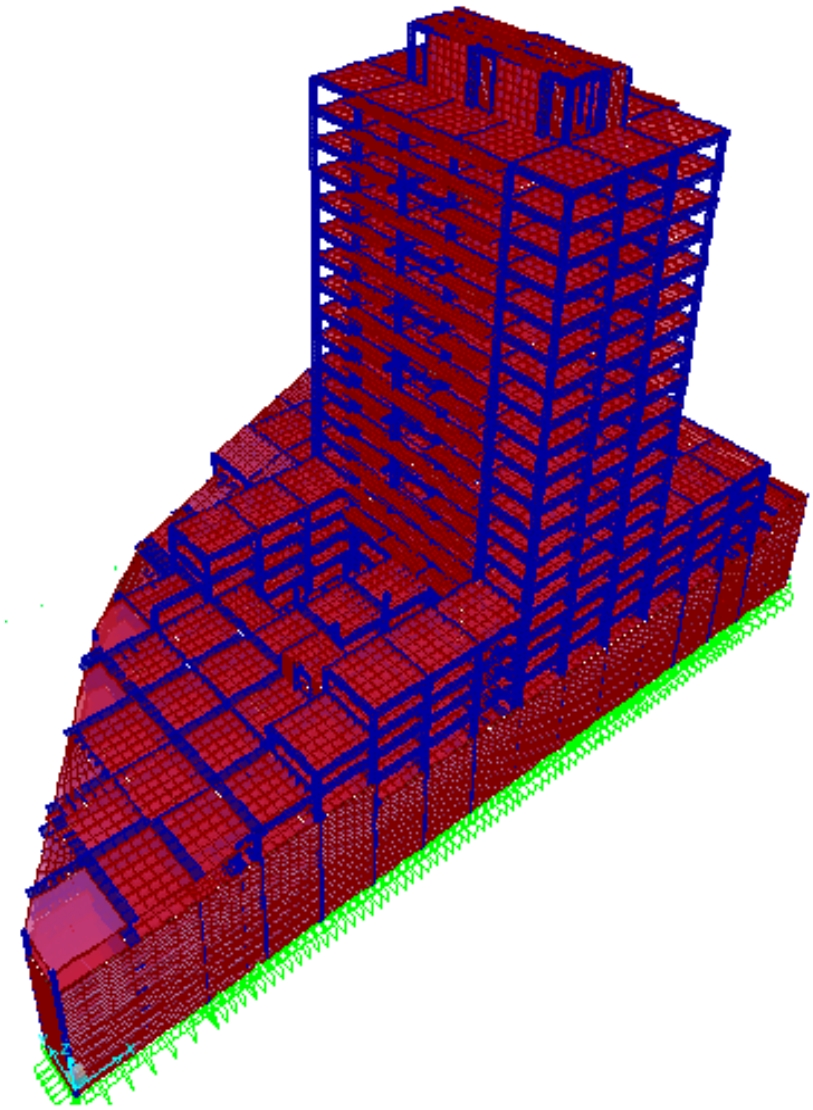

Figure 5.54. Sap2000 Full Finite Element 3D Model

Figures of the mode shapes obtained with the finite element 3D model are shown in Figures 5.55, 5.56 and 5.57. The classification of the first six natural frequencies (Hz) and the type of dominant motion (torsional or translational) of three finite element models respectively are represented in the Table 5.14, 5.15, and 5.16.

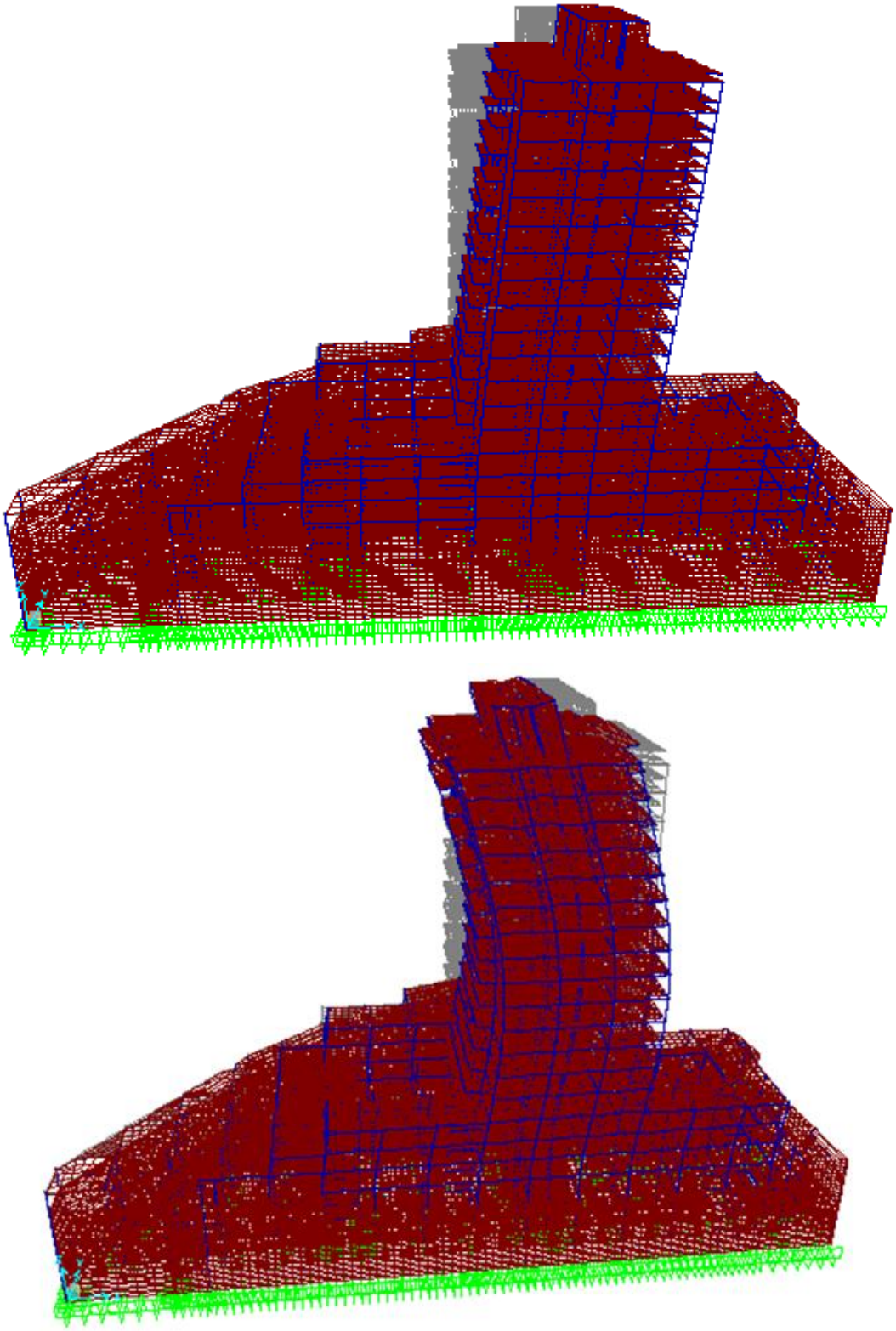

Figure 5.55. (a) Mode 1 - 1st E/W (b) Mode 2 - 2nd E/W

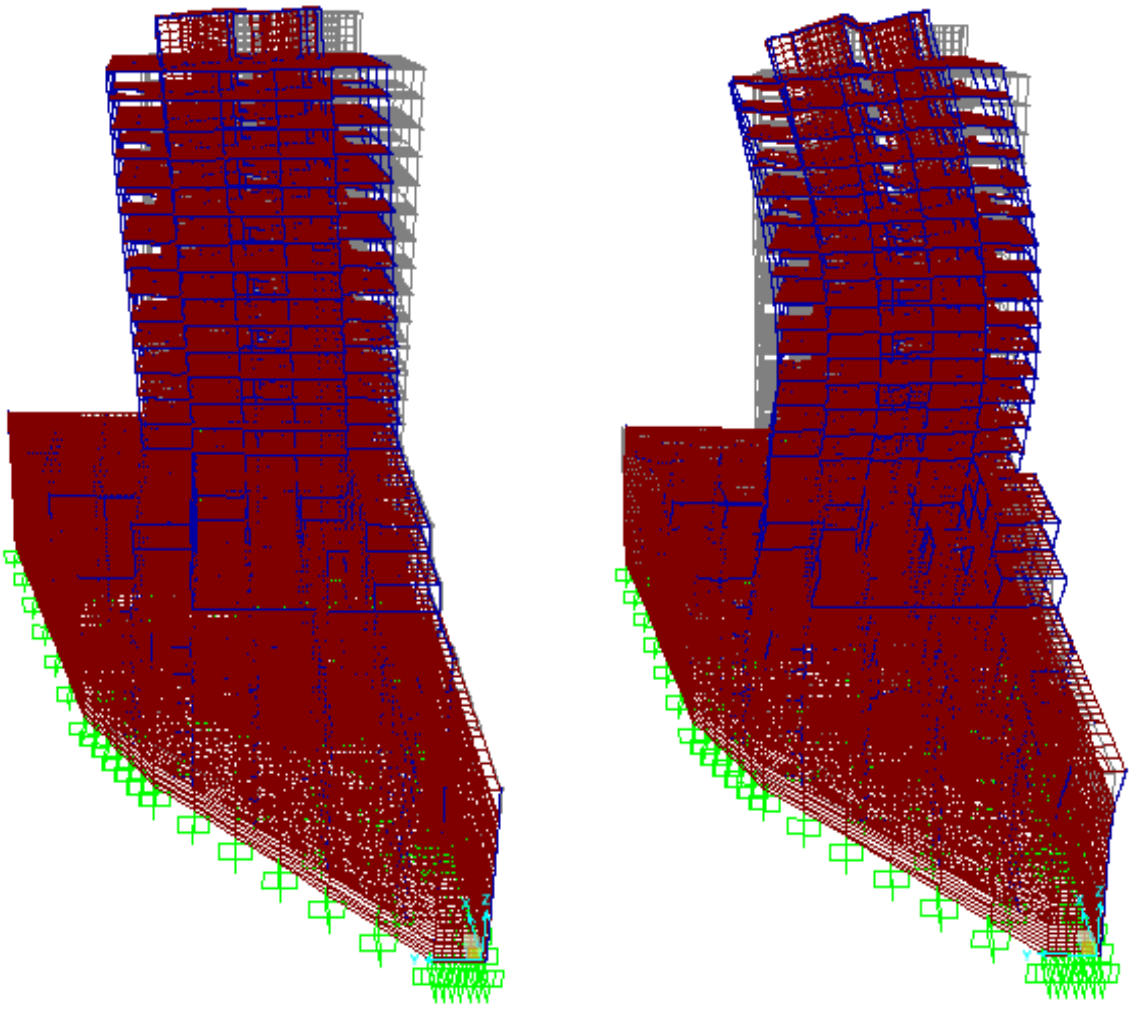

Figure 5.56. (a) Mode 1 - 1st N/S (b) Mode 2 - 2nd N/S

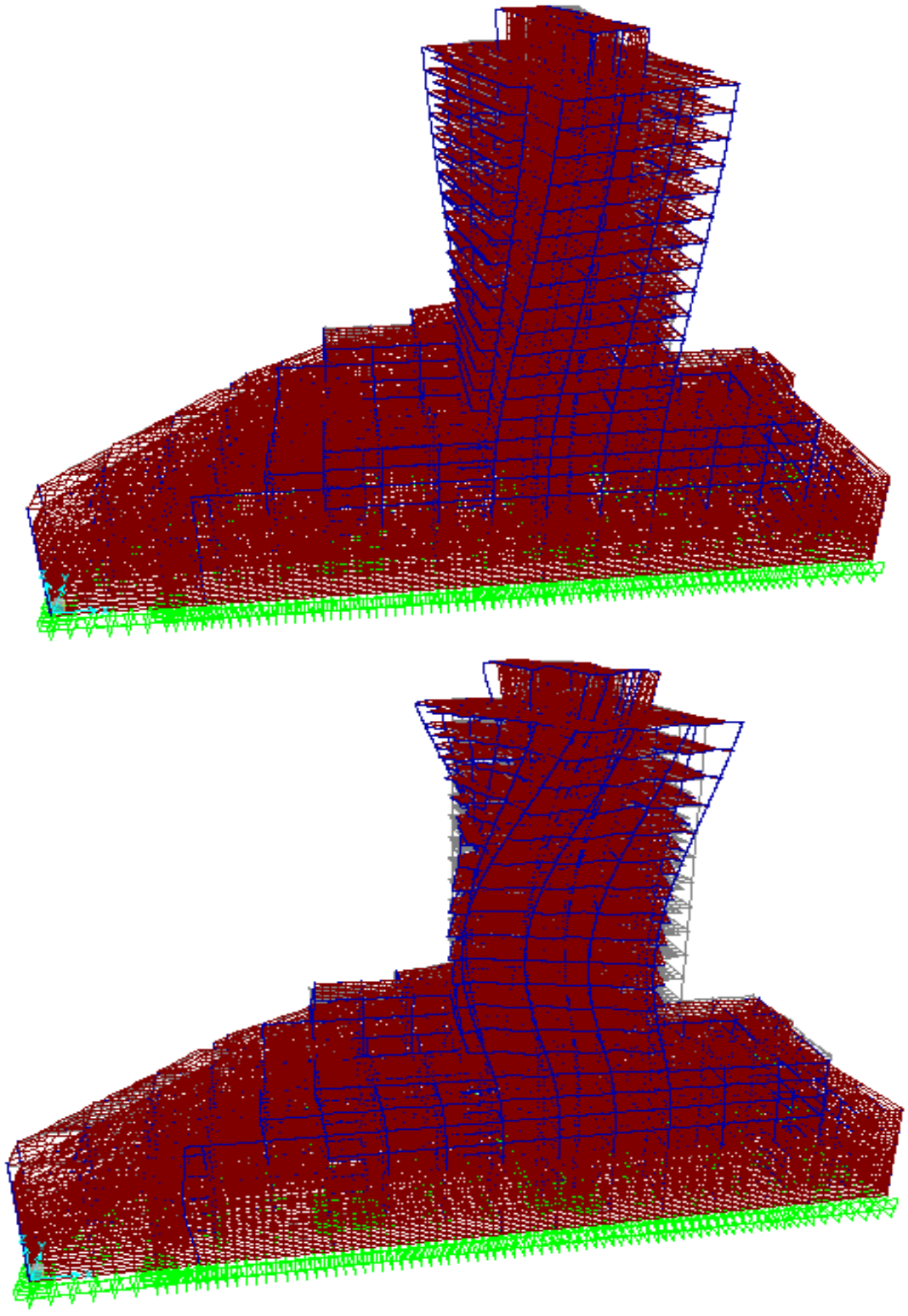

Figure 5.57. (a) Mode 1 - 1st Torsion (b) Mode 2 - 2nd Torsion

Table 5.14 Natural frequencies and dominant motions of Model #1.

Mode	Dominant Motion	Period (sec)	Frequency (Hz)	Circ. Freq. (rad/sec)	Eigenvalue
1	x-direction(EW)	1.64	0.61	3.83	14.7
2	1st torsional	1.13	0.89	5.59	31.2
3	y-direction(NS)	0.93	1.08	6.76	45.8
4	x-direction(EW)	0.46	2.17	13.65	186.4
5	2nd torsional	0.34	2.91	18.27	334.0
6	y-direction(NS)	0.232	4.31	27.09	733.8

Table 5.15 Natural frequencies and dominant motions of Model #2.

Mode	Dominant Motion	Period(sec)	Frequency(Hz)	Circ. Freq. (rad/sec)	Eigenvalue
1	x-direction(EW)	1.698	0.59	3.71	13.73
2	1st torsional	1.170	0.86	5.40	29.17
3	y-direction(NS)	0.962	1.04	6.53	42.63
4	x-direction(EW)	0.476	2.10	13.19	173.92
5	2nd torsional	0.356	2.82	17.71	313.63
6	y-direction(NS)	0.239	4.19	26.25	692.38

Table 5.16 Natural frequencies and dominant motions of Model #3.

Mode	Dominant Motion	Period (sec)	Frequency (Hz)	Circ.Freq. (rad/sec)	Eigenvalue
1	x-direction(EW)	1.698	0.59	3.71	13.73
2	1st torsional	1.176	0.85	5.34	28.49
3	y-direction(NS)	0.962	1.04	6.53	42.63
4	x-direction(EW)	0.478	2.09	13.13	172.27
5	2nd torsional	0.356	2.81	17.65	311.41
6	y-direction(NS)	0.239	4.18	26.25	689.08

The natural frequencies and mode shapes resulting from eigenvalue analyses of the computer models and ambient vibration results are compared in Table 5.17, Table 5.18, and Table 5.19. It is seen in Table 5.17 and Table 5.18 that for the first mode in the EW and the NS direction of the translational modes as well as 1st torsional mode in the finite element model the frequencies are lower than the ambient vibration tests while for the second mode in the EW direction and second mode in the NS direction of the translational

modes as well as the second torsional mode the frequency is higher. It is seen in Table 5.19 that for the first and second translational modes in the EW direction and only second mode in the NS direction of the translational modes as well as first torsional mode in the mathematical model the frequencies are lower than the experimental test while for the second mode in the NS direction and the second torsional mode the frequency is higher.

Table 5.17. Comparison between Ambient Vibration Test #1 and Finite Element Model#1 Results.

Mode	Ambient Vibration Test #1		Finite Element Model #1		
	Mode Shape	Frequency (Hz)	Mode Shape	Frequency (Hz)	%Diff.
1	1st translational (EW)	0.66	1st translational (EW)	0.61	7.58
2	1st torsional	0.94	1st torsion	0.89	5.32
3	1st translational (NS)	1.10	1st translational (NS)	1.08	1.82
4	2nd translational (EW)	2.16	2nd translational (EW)	2.17	-0.46
5	2nd torsional	2.90	2nd torsion	2.91	-0.34
6	2nd translational (NS)	3.78	2nd translational (NS)	4.31	-14.02

Table 5.18. Comparison between Ambient Vibration Test#2 and Finite Element Model#2 Results.

Mode	Ambient Vibration Test #2		Finite Element Model #2		
	Mode Shape	Frequency (Hz)	Mode Shape	Frequency (Hz)	%Diff.
1	1st translational (EW)	0.61	1st translational (EW)	0.59	3.28
2	1st torsional	0.87	1st torsion	0.86	1.15
3	1st translational (NS)	1.05	1st translational (NS)	1.04	0.95
4	2nd translational (EW)	2.01	2nd translational (EW)	2.10	-4.48
5	2nd torsional	2.70	2nd torsion	2.82	-4.44
6	2nd translational (NS)	3.70	2nd translational (NS)	4.19	-13.24

Table 5.19. Comparison between Ambient Vibration #3 and Finite Element Model#3 Results.

Mode	Ambient Vibration Test		Finite Element Model#3		
	Mode Shape	**Frequency(Hz)**	**Mode Shape**	**Frequency(Hz)**	**%Diff.**
1	1st translational (EW)	0.62	1st translational (EW)	0.59	4.84
2	1st torsion	0.89	1st torsion	0.85	4.49
3	1st translational (NS)	1.05	1st translational (NS)	1.04	0.95
4	2nd translational (EW)	2.11	2nd translational (EW)	2.09	0.95
5	2nd torsion	2.77	2nd torsion	2.81	-1.44
6	2nd translational (NS)	3.77	2nd translational (NS)	4.18	-10.88

Figure 5.58 and Figure 5.59 display the mode shapes obtained ambient vibration, FDD, and FE model for two construction stages (Case 1 and Case 2). Comparison in identified natural frequencies of the translational modes among ambient vibration, FDD, and FE model is good illustrated that the real dynamic characteristics of the structure is well represented by the virtue of system identification and good agreement among the estimated mode shapes can be observed.

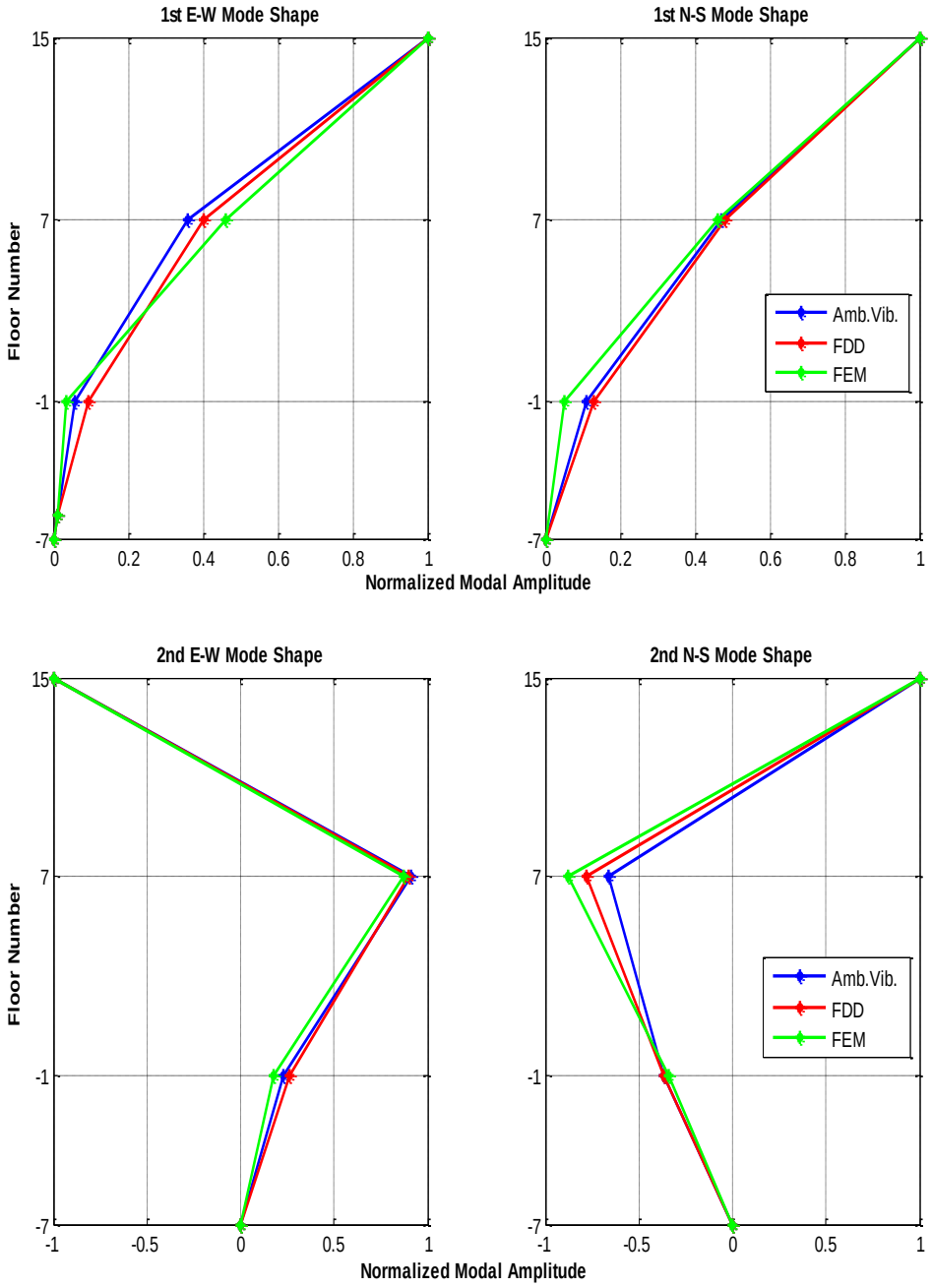

Figure 5.58. Comparison of First Two Mode Shapes obtained data set 27032015(Case 1). Mode shapes are normalized by the roof displacement. Blue line represents the estimated mode shapes using ambient vibration, while red one is the estimated mode shapes obtained FDD technique. The green line shows mode shape using FE analysis, respectively.

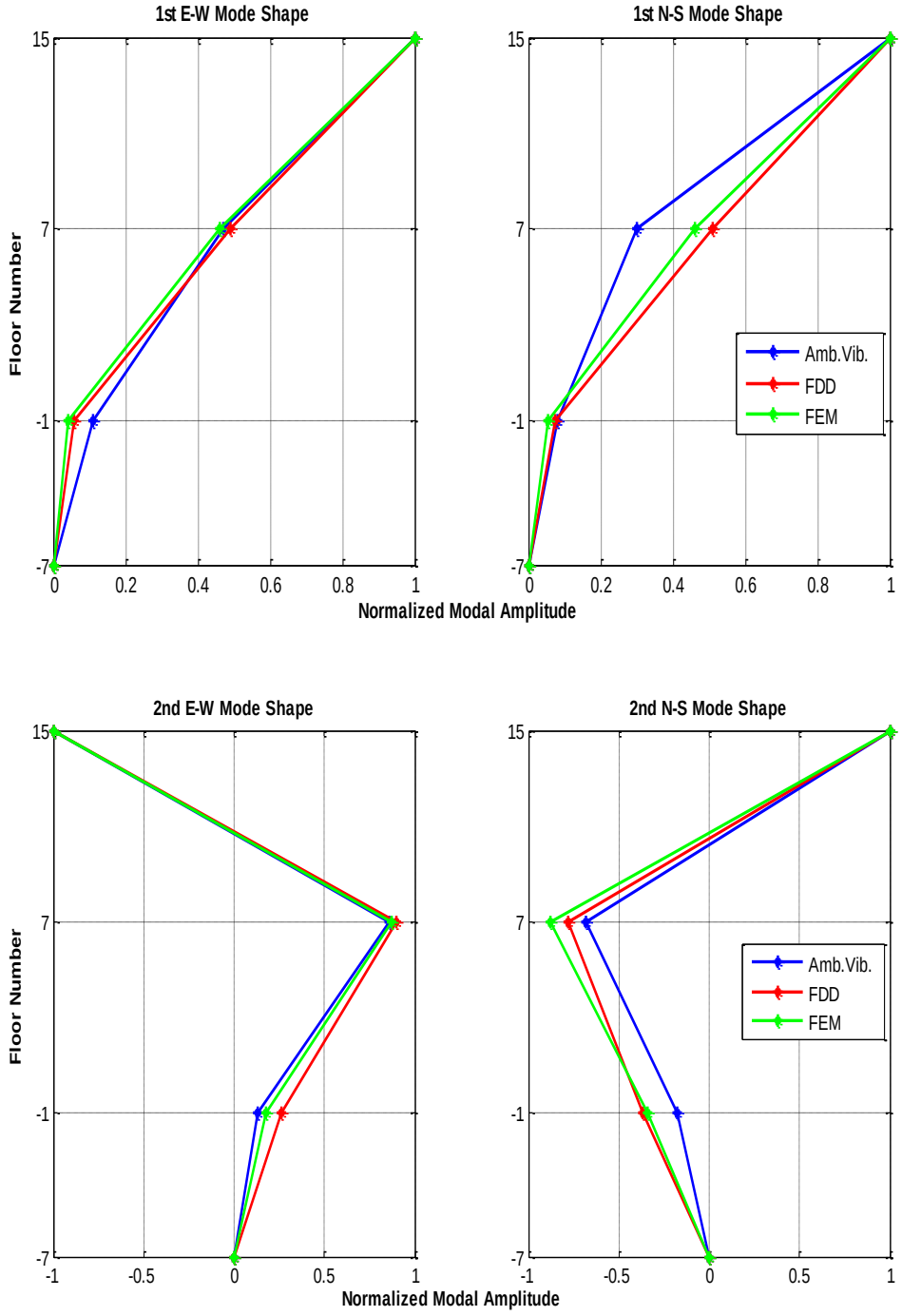

Figure 5.59. Comparison of First Two Mode Shapes obtained data set 13092015(Case 2). Mode shapes are normalized by the roof displacement. Blue line represents the estimated mode shapes using ambient vibration, while red one is the estimated mode shapes obtained FDD technique. The green line shows mode shape using FE analysis, respectively.

6. CONCLUSION

In this study, ambient response measurements of a 23-storey reinforced concrete building at various construction steps were conducted in order to investigate the difference of its dynamic properties with the progress of construction. There are three different cases, namely including only the reinforced concrete structure (Case 1), curtain- wall type façade system installed in addition to the structure (Case 2), and all interior finishes completed (Case 3). Distinguishing the adjustment in the dynamic properties with an extra structural or architectural parts, more correct quantitative assessment of the role of these parts to the mathematical model of the building can be acquired.

Acceleration records were processed using de-trending to remove the linear trend from input data and filtering to remove noise from signals. Velocities and displacements were calculated for three different construction conditions at longitudinal, transverse and vertical directions for each location. Fourier amplitude spectra have been smoothed according to optimum smoothing window length. The ambient tests were successful at identifying six modes of the structure below 5.0 Hz. The results obtained using the three methods. The dynamic characteristics were identified using well-known spectral analyses, FDD (non-parametric) methods and system identification technique (spectral ratio).

Modal parameters identification based on these methods has been presented in comparisons between them as well as with FE model results. Identified natural frequencies and mode shapes from FDD and ambient vibration tests are quite good agreement with the FE results. Due to the lack of additional sensors on floors other than the 15th, mode shapes were not obtained. As to be expected, by adding the glass curtain cladding and other non-structural elements in Case 2, the modal frequencies reduced as the structure increased in mass. It is evident that the changes in the building's fundamental and torsional frequencies occur about 7-7.5%. In Case 3, when the tall building was completed entirely, an increase in the natural frequencies of the building was observed comparing Case 2. The reason is to add steel construction to the gaps of the slabs. The natural frequencies obtained ambient

vibration tests were observed on increase about 1.6% for first fundamental frequencies and on increase about 5% for second fundamental frequencies. The first and second torsional modes also have a translational component in the NS direction.

The results confirmed the overall behavior of the structure, and are a good correlation. The comparison between the ambient vibration data and the finite element model was obtained successfully. The recorded ambient vibrations were used to confirm three different Finite Element Models. The frequencies of Finite Element Models were compared with the results of the ambient vibration tests. The fundamental frequencies are obtained between 0.3% and 14%. As a result, a comparison of the mode shapes obtained from ambient vibration tests, there was no significant difference between the mode shapes obtained for each construction stages (Case 1, Case 2, and Case 3).

An important characteristic of the structural system is the low critical damping percentage. The damping percentages extracted from half-power method using ambient vibration records are quite low (0.62–1.28% for the fundamental modes). The results from analyses of accelerations records from the ambient vibrations are all summarized in Table 6.5. Due to the fact that the damping percentages are very low, it likely contributed to the repetitious, prolonged, and resonating cyclic behavior of the building and the prolonged shaking increases. Prolonged cyclic behavior of the building is important since small amplitudes may be a cause for low-cycle fatigue. The possibility of such low-damping percentages of the structural system was most likely not considered during the design and analyses process.

REFERENCES

1. Akira, M., *Structural Dynamics for Health Monitoring*, Sankeisha Co Ltd., pp.77-96, 2003.

2. Apaydın, N.M., Y., Kaya, E., Şafak, and H., Alçık, "Vibration Characteristics of a Suspension Bridge under Traffic and No Traffic Conditions", *Earthquake Engineering and Structural Dynamics*, Vol. 41, No. 12, pp. 1717-1723, 2012.

3. Bendat, J. S., and A.G., Piersol, "Random Data, Analysis and Measurement Procedures", 2nd Edition, *John Wiley and Sons, Inc.*, New York, USA, 1990.

4. Bindi, D., B., Petrovic, S., Karapetrou, M., Manakou, T., Boxberger, D., Raptakis, K., Pitilakis and S., Parolai, "Seismic response of an 8 story RC building from ambient vibration analysis", *Bulletin of Earthquake Engineering*, Vol.13, No.7, pp. 2095-2120, 2014.

5. Brincker, R., and P., Andersen, "ARMA (Auto Regressive Moving Average) Models in Modal Space", *Proceeding of the 17th International Modal Analysis Conference*, Kissimmee, Florida, 1999.

6. Brincker, R., L., Zhang and P., Andersen, "Modal Identification from Ambient Responses Using Frequency Domain Decomposition", *Proceedings of the 18th International Modal Analysis Conference*, San Antonio, Texas, 2000.

7. Brincker, R., C.E. Ventura, P., Andersen, "Damping Estimation by Frequency Domain Decomposition", *Proceedings of the 19th International Modal Analysis Conference*, pp. 698-703, 2001.

8. Çelebi, M., M., Huang, A., Shakal, J., Hooper, and R., Klemencic, "Ambient Response of a Unique Performance-based Design Tall Building with Dynamic Response

Modification Feature", *Structural Design Tall and Special Buildings*, Vol.22, pp. 816-829, 2013.

9. Çelebi, M., I., Okawa, T., Kashima, S., Koyama, and M., Liba, "Response of a tall building far from the epicenter of the 11 March 2011 M9.0 Great East Japan earthquake and aftershocks", *Structural Design Tall Special Buildings*, Vol. 23, pp. 427-441, 2014.

10. Guillier, B., J. L., Chatelain, D., Machane, M., Farsi, H., Perfettini, E.H., Oubaiche, R., Bensalem, and M., Hellel, "Continuous Monitoring of Ambient Vibration in Building: Time and Space Stability of Dynamic Parameters from CGS Building (Algiers, Algeria)", *Proceedings of the 2nd European Conference on Earthquake Engineering and Seismology*, 25-29 August 2014, Istanbul, Turkey, 2014.

11. Hudson, D., E., "Reading and Interpreting Strong Motion Accelerograms", *Earthquake Engineering Research Institute*, Berkeley, California, U.S.A, 1976.

12. Kaya, Y., "Tools and techniques for real time modal identification", PhD Dissertation, *Earthquake engineering Department*, Boğaziçi University, Istanbul, Turkey, 2009.

13. Kaya, Y., and E., Şafak, "Structural Health Monitoring & Damage Detection", *Proceedings of the 31st IMAC, A Conference and Exposition on Structural Dynamics*, Vol.4, pp.569, 2013.

14. Kaya, Y., and E., Şafak, "Real-time analysis and interpretation of continuous data from structural health monitoring (SHM) systems", *Bulletin of Earthquake Engineering*, Vol.13, No.3, pp. 917-934, 2015.

15. Lamarche, C.P., P., Paultre, J., Proulx, and S., Mousseau, "Assessment of the Frequency Domain Decomposition Technique by Forced-vibration Tests of a Full-scale Structure", *Earthquake Engineering and Structural Dynamics*, Vol. 37, pp. 487-494, 2007.

16. Le, T.H., Y., Tamura, "Modal Identification of Ambient Vibration Structure Using Frequency Domain Decomposition and Wavelet Transform", *The Seventh Asia-Pacific Conference on Wind Engineering*, November 8-12, 2009, Taipei, Taiwan, 2009.

17. Ljung, L., "System Identification: Theory and User", *Prentice hall: Englewood Cliffs*, New Jersey, 1987.

18. Mathworks, "MATLAB-The Language of Technical Computing", *The Math works*, Natick, USA, 2013.

19. Nunez, T.R., and R.L., Boroschek, "Modal Properties of a High Rise Building Under Construction", *Proceedings of the 28th International Operational Modal Analysis Conference on Structural Dynamics*, 1-4 February 2010, Florida, USA, 2010.

20. Petrovic, B., Bindi, D., Pilz, M., Serio, M., Orunbaev, S., Niyazov, J., Hakimov, F., Yasunov, P., Begaliev, U. T., Parolai, S., "Building monitoring in Bishkek and Dushanbe by the use of ambient vibration analysis", *Annals of Geophysics*, Vol. 58, No.1, 2015.

21. Pioldi, F., R., Ferrari, and E., Rizzi, "A Refined FDD Algorithm for Operational Modal Analysis of Buildings under Earthquake Loading", *Proceedings of the 26th International Conference on Noise and Vibration Engineering*, 15-17 September 2014, KU Leuven, Belgium, 2014.

22. Rodgers, J.E., A. K., Sanli, and M., Çelebi, "Seismic Response Analysis of a 13-story Steel Moment-framed Building in Alhambra, California", *U.S. Geological Survey*, 2004.

23. SAP2000, "Integrated Finite Element Analysis and Design of Structures", *Computers and Structures Inc.*, Berkeley, CA, USA, 1998.

24. Soyöz, S., M.Q., Feng, M., Shinozuka, "Structural Reliability Estimation with Vibration-based Identified Parameters", *Journal of Engineering Mechanics*, ASCE, Vol.136, No.1, pp. 100-106, 2010.

25. Şafak, E., "Identification of Linear Structures Using Discrete-Time Filters", *Journal of Structural Engineering*, Vol. 117, No. 10, pp. 3064-3085, 1991.

26. Şafak, E., "Response of a 42-story Steel-frame Building to the Ms=7.1 Loma Prieta Earthquake", *Engineering Structures*, Vol.15, No.6, pp. 403-421, 1993.

27. Şafak, E., "Detection and Identification of Soil-Structure Interaction in Buildings from Vibration Recordings", *Journal of Structural Engineering*, Vol. 22, pp.899-906, 1995.

28. Şafak, E., "Analysis of ambient ground and structural vibration data", *Annual meeting of the seismological society of America*, Incline Village/Lake Tahoe, 2005.

29. Şafak. E., "Detection of Seismic Damage in Structures from Continuous Vibration Records", *Proceedings 9th International Conference on Structural Safety and Reliability*, Rome, Italy, 2005.

30. Şafak, E., "Real-time Structural Monitoring and Damage Detection by Acceleration and GPS Sensors", *8th US National Conference on Earthquake Engineering*, San Francisco, 2006.

31. Şafak, E., E., Çaktı, and Y., Kaya, "Recent Developments on Structural Health Monitoring and Data Analyses", *Earthquake Engineering in Europe, Geotechnical, Geological, and Earthquake Engineering*, Chapter 14, Vol. 17, pp. 331-355, 2010.

32. Şafak, E., E., Durakul, and Y., Kaya, "Structural Health Monitoring of Historical Structures and New Techniques for Data Analysis", *International Operational Modal Analysis Conference*, No.235, Copenhagen, Denmark, 2007.

33. Şafak, E., E., Çaktı, "Simple Techniques to Analyze Vibration Records From Buildings", *Proceedings of the 7th European Workshop on Structural Health Monitoring*, 8-11 July 2014, Nantes, France, 2014.

34. Skolnik, D., L., Ying, Y., Eunjong and J.W., Wallace, "Identification, Model Updating and Response Prediction of an Instrumented 15-Story Steel-Frame Building", *Earthquake Spectra*, Vol. 22, No.3, pp. 781-802, 2006.

35. Turek, M., and C.E., Ventura, "Ambient Vibration Testing and Model Updating of a 44-storey Building in Vancouver, Canada", *Proceedings of the 25th International Operational Modal Analysis Conference*, Orlando, Florida, USA, 2007.

36. *TS-500 Building Code Requirements for Structural Concrete*, Turkish Standards Institute, Ankara.

37. *Turkish Earthquake Code*, Turkish Standards Institute, Ankara, 2007.

38. *Uniform Building Code, International Conference of Building Officials*, Whittier, California, U.S.A, 1997.

39. Ventura, C.E., and N.D., Schuster, "Structural Dynamic Properties of a Reinforced Concrete High-Rise Building during Construction", *Canadian Journal of Civil Engineering*, Vol. 23, No. 4, pp. 950-972, 1996.

40. Ventura, C.E., T., Horyna, "Measured and Calculated Modal Characteristics of the Heritage Court Tower in Vancouver, B.C.", *Proceedings of the 18th International Operational Modal Analysis Conference*, pp. 1070-1074, 2000.

41. Ventura, C.E., J.F., Lord and R.D., Simpson, "Effective Use of Ambient Vibration Measurements for Modal Updating of a 48 Storey Building in Vancouver, Canada", *International Conference on Structural Dynamics Modeling*, Instituto de Engenharia Macânica, Madeira Island, Portugal, 2002.

42. Ventura, C.E., K. M., Thibert, “Dynamic Properties of a 32-storey Building Determined from Different Analysis Methods of Ambient Vibration Test Data”, *Proceedings of the 2nd International Modal Analysis Conference*, pp. 557-564, 2007.

43. Zhang, L., Y., Tamura, A., Yoshida, K., Cho, S., Nakata, and S., Naito, “Ambient Vibration Testing and Modal Identification of an Office Building”, *Proceedings of the 20th International Modal Analysis Conference (IMAC)*, Los Angeles, USA, 2002.,